

January, 2004

## Covariant Light-Front Approach for *s*-wave and *p*-wave Mesons: Its Application to Decay Constants and Form Factors

Hai-Yang Cheng,<sup>1</sup> Chun-Khiang Chua<sup>1</sup> and Chien-Wen Hwang<sup>2</sup>

<sup>1</sup> Institute of Physics, Academia Sinica  
Taipei, Taiwan 115, Republic of China

<sup>2</sup> Department of Physics, National Kaohsiung Normal University  
Kaohsiung, Taiwan 802, Republic of China

### Abstract

We study the decay constants and form factors of the ground-state *s*-wave and low-lying *p*-wave mesons within a covariant light-front approach. Numerical results of the form factors for transitions between a heavy pseudoscalar meson and an *s*-wave or *p*-wave meson and their momentum dependence are presented in detail. In particular, form factors for heavy-to-light and  $B \rightarrow D^{**}$  transitions, where  $D^{**}$  denotes generically a *p*-wave charmed meson, are compared with other model calculations. The experimental measurements of the decays  $B^- \rightarrow D^{**}\pi^-$  and  $B \rightarrow \bar{D}D_s^{**}$  are employed to test the decay constants of  $D_s^{**}$  and the  $B \rightarrow D^{**}$  transition form factors. The heavy quark limit behavior of the decay constants and form factors is examined and it is found that the requirement of heavy quark symmetry is satisfied. The universal Isgur-Wise (IW) functions, one for *s*-wave to *s*-wave and two for *s*-wave to *p*-wave transitions, are obtained. The values of IW functions at zero recoil and their slope parameters can be used to test the Bjorken and Uraltsev sum rules.

## I. INTRODUCTION

Mesonic weak transition form factors and decay constants are two of the most important ingredients in the study of hadronic weak decays of mesons. There exist many different model calculations. The light-front quark model [1, 2] is the only relativistic quark model in which a consistent and fully relativistic treatment of quark spins and the center-of-mass motion can be carried out. This model has many advantages. For example, the light-front wave function is manifestly Lorentz invariant as it is expressed in terms of the momentum fraction variables in analog to the parton distributions in the infinite momentum frame. Moreover, hadron spin can also be correctly constructed using the so-called Melosh rotation. This model is very suitable to study hadronic form factors. Especially, as the recoil momentum increases (corresponding to a decreasing  $q^2$ ), we have to start considering relativistic effects seriously. In particular, at the maximum recoil point  $q^2 = 0$  where the final-state meson could be highly relativistic, there is no reason to expect that the non-relativistic quark model is still applicable.

The relativistic quark model in the light-front approach has been employed to obtain decay constants and weak form factors [3, 4, 5, 6, 7]. There exist, however, some ambiguities and even some inconsistencies in extracting the physical quantities. In the light-front quark model formulation one often picks up a specific Lorentz frame (e.g. the purely longitudinal frame  $q_\perp = 0$ , or the purely transverse frame  $q^+ = q^0 + q^3 = 0$ ) and then calculates a particular component (the “plus” component) of the associated current matrix element. Due to the lack of relativistic covariance, the results may not be unique and may even cause some inconsistencies. For example, it has been pointed out in [7] that in the  $q_\perp = 0$  frame, the so-called  $Z$ -diagram contributions must be incorporated in the form-factor calculations in order to maintain covariance. Another issue is that the usual recipe of taking only the plus component of the current matrix elements will miss the zero-mode contributions and render the matrix element non-covariant. Well known examples are the vector decay constant  $f_V$ , the form factor  $A_1(q^2)$  in the pseudoscalar to vector transition [8] and the electromagnetic form factor  $F_2(q^2)$  of the vector meson (see e.g. [9]). In other words, the familiar expression of  $f_V$ , for example, in the conventional light-front approach [4] is not trustworthy due to the lack of the zero-mode contributions. As a consequence, it is desirable to construct a covariant light-front model that can provide a systematical way of exploring the zero-mode effects. Such a covariant model has been constructed in [10] for heavy mesons within the framework of heavy quark effective theory.

Without appealing to the heavy quark limit, a covariant approach of the light-front model for the usual pseudoscalar and vector mesons has been put forward by Jaus [8]. The starting point of the covariant approach is to consider the corresponding covariant Feynman amplitudes in meson transitions. Then one can pass to the light-front approach by using the light-front decomposition of the internal momentum in covariant Feynman momentum loop integrals and integrating out the  $p^- = p^0 - p^3$  component [11]. At this stage one can then apply some well-studied vertex functions in the conventional light-front approach after  $p^-$  integration. It is pointed out by Jaus that in going from the manifestly covariant Feynman integral to the light-front one, the latter is no longer covariant as it receives additional spurious contributions proportional to the lightlike vector

$\tilde{\omega}^\mu = (1, 0, 0, -1)$ . This spurious contribution is cancelled after correctly performing the integration, namely, by the inclusion of the zero mode contribution [12], so that the result is guaranteed to be covariant.

The main purposes of this work are twofold: First, we wish to extend the covariant analysis of the light-front model in [8] to even-parity,  $p$ -wave mesons. Second, the momentum dependence of the form factors is parametrized in a simple three-parameter form so that the reader is ready to use our numerical results as the analytic expressions of various form factors in the covariant light-front model are usually complicated (see Sec. III). Interest in even-parity charmed mesons has been revived by recent discoveries of two narrow resonances: the  $0^+$  state  $D_{s0}^*(2317)$  [13] and the  $P_1^{1/2}$  state  $D_{s1}(2460)$  [14], and two broad resonances,  $D_0^*(2308)$  and  $D_1(2427)$  [15].<sup>1</sup> Furthermore, the hadronic  $B$  decays such as  $B \rightarrow D^{**}\pi$  and  $B \rightarrow D_s^{**}\bar{D}$  have been recently observed, where  $D^{**}$  denotes a  $p$ -wave charmed meson. A theoretical study of them requires the information of the  $B \rightarrow D^{**}$  form factors and the decay constants of  $D^{**}$  and  $D_s^{**}$ . In the meantime, three body decays of  $B$  mesons have been recently studied at the  $B$  factories: BaBar and Belle. The Dalitz plot analysis allows one to see the structure of exclusive quasi-two-body intermediate states in the three-body signals. The  $p$ -wave resonances observed in three-body decays begin to emerge. Theoretically, the Isgur-Scora-Grinstein-Wise (ISGW) quark model [17] is so far the only model in the literature that can provide a systematical estimate of the transition of a ground-state  $s$ -wave meson to a low-lying  $p$ -wave meson. However, this model and, in fact, many other models in  $P \rightarrow P, V$  ( $P$ : pseudoscalar meson,  $V$ : vector meson) calculations, are based on the non-relativistic constituent quark picture. As noted in passing, the final-state meson at the maximum recoil point  $q^2 = 0$  or in heavy-to-light transitions could be highly relativistic. It is thus important to consider a relativistic approach.

It has been realized that the zero mode contributions can be interpreted as residues of virtual pair creation processes in the  $q^+ \rightarrow 0$  limit [18]. In [8], the calculation of the zero mode contribution is obtained in a frame where the momentum transfer  $q^+$  vanishes. Because of this ( $q^+ = 0$ ) condition, form factors are known only for spacelike momentum transfer  $q^2 = -q_\perp^2 \leq 0$ . One needs to analytically continue them to the timelike region [6], where the physical decay processes are relevant. Recently, it has been shown that within a specific model, form factors obtained directly from the timelike region (with  $q^+ > 0$ ) are identical to those obtained by the analytic continuation from the spacelike region [50].

There are some theoretical constraints implied by heavy quark symmetry (HQS) in the case of heavy-to-heavy transitions and heavy-to-vacuum decays [20]. It is important to check if the calculated form factors and decay constants do satisfy these constraints. Furthermore, under HQS the number of the independent form factors is reduced and they are related to some universal Isgur-Wise (IW) functions. In this work, we shall follow [10] to evaluate the form factors and decay constants in a covariant light-front formulism within the framework of heavy quark effective theory. It is found that the resultant decay constants and form factors do agree with those obtained from

---

<sup>1</sup> We follow the naming scheme of the Particle Data Group [16] to add a superscript “ $**$ ” to the states if the spin-parity is in the “normal” sense,  $J^P = 0^+, 1^-, 2^+, \dots$ .

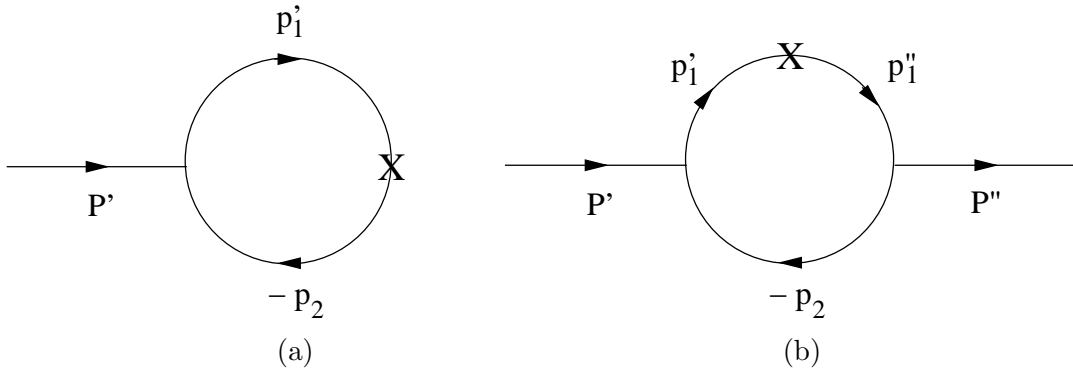


FIG. 1: Feynman diagrams for (a) meson decay and (b) meson transition amplitudes, where  $P'^{(\prime\prime)}$  is the incoming (outgoing) meson momentum,  $p_1'^{(\prime\prime)}$  is the quark momentum,  $p_2$  is the anti-quark momentum and  $X$  denotes the corresponding  $V - A$  current vertex.

the covariant light-front approach and then extended to the heavy quark limit. The relevant IW functions, namely,  $\xi$ ,  $\tau_{1/2}$  and  $\tau_{3/2}$  are obtained. One can then study some properties of these IW functions, including the slopes and sum rules [21, 22].

The paper is organized as follows. In Sec. II, we give the calculations for the decay constants of  $s$ -wave and  $p$ -wave mesons in a covariant light-front model. The calculation for  $s$ -wave meson transitions has been done by Jaus [8]. We extend it to the  $p$ -wave meson case. In Sec. III,  $P \rightarrow P, V, S, A, T$  ( $S, A, T$  standing for scalar, axial-vector and tensor mesons, respectively) transitions are considered. It is interesting to notice that the analytic forms of  $P \rightarrow S, A$  transitions are similar to that of  $P \rightarrow P, V$  transitions, respectively, while the  $P \rightarrow T$  calculation needs formulas beyond [8]. We provide numerical results for  $B$  and  $D$  decay form factors and their  $q^2$  dependence. These results are then compared to the other model calculations. In Sec. IV, properties of the decay constants and form factors in the heavy quark limit are studied. The universal Isgur-Wise functions, one for  $s$ -wave to  $s$ -wave and two for  $s$ -wave to  $p$ -wave transitions, are obtained. Their values at zero recoil and their slope parameters can be used to test the sum rules derived by Bjorken [21] and by Uraltsev [22]. Conclusion is given in Sec V followed by two Appendices devoted to the derivations of conventional light-front vertex functions and some useful formulas.

## II. FORMALISM OF A COVARIANT LIGHT-FRONT MODEL

### A. Formalism

In the conventional light-front framework, the constituent quarks of the meson are required to be on their mass shells (see Appendix A for an introduction) and various physical quantities are extracted from the plus component of the corresponding current matrix elements. However, this procedure will miss the zero-mode effects and render the matrix elements non-covariant. Jaus [8] has proposed a covariant light-front approach that permits a systematical way of dealing with the zero mode contributions. Physical quantities such as the decay constants and form factors can be

calculated in terms of Feynman momentum loop integrals which are manifestly covariant. This of course means that the constituent quarks of the bound state are off-shell. In principle, this covariant approach will be useful if the vertex functions can be determined by solving the QCD bound state equation. In practice, we would have to be contended with the phenomenological vertex functions such as those employed in the conventional light-front model. Therefore, using the light-front decomposition of the Feynman loop momentum, say  $p_\mu$ , and integrating out the minus component of the loop momentum  $p^-$ , one goes from the covariant calculation to the light-front one. Moreover, the antiquark is forced to be on its mass shell after  $p^-$  integration. Consequently, one can replace the covariant vertex functions by the phenomenological light-front ones.

As stated in passing, in going from the manifestly covariant Feynman integral to the light-front one, the latter is no longer covariant as it can receive additional spurious contributions proportional to the lightlike four vector  $\tilde{\omega}$ . The undesired spurious contributions can be eliminated by the inclusion of the zero mode contribution which amounts to performing the  $p^-$  integration in a proper way in this approach. The advantage of this covariant light-front framework is that it allows a systematical way of handling the zero mode contributions and hence permits to obtain covariant matrix elements.

To begin with, we consider decay and transition amplitudes given by one-loop diagrams as shown in Fig. 1 for the decay constants and form factors of ground-state  $s$ -wave mesons and low-lying  $p$ -wave mesons. We follow the approach of [8] and use the same notation. The incoming (outgoing) meson has the momentum  $P'^{(\prime)} = p_1'^{(\prime)} + p_2$ , where  $p_1'^{(\prime)}$  and  $p_2$  are the momenta of the off-shell quark and antiquark, respectively, with masses  $m_1'^{(\prime)}$  and  $m_2$ . These momenta can be expressed in terms of the internal variables  $(x_i, p'_\perp)$ ,

$$p_{1,2}^{\prime+} = x_{1,2} P'^+, \quad p_{1,2\perp}^{\prime\prime} = x_{1,2} P'_\perp \pm p'_\perp, \quad (2.1)$$

with  $x_1 + x_2 = 1$ . Note that we use  $P' = (P'^+, P'^-, P'_\perp)$ , where  $P'^\pm = P'^0 \pm P'^3$ , so that  $P'^2 = P'^+ P'^- - P'^2_\perp$ . In the covariant light-front approach, total four momentum is conserved at each vertex where quarks and antiquarks are off-shell. These differ from the conventional light-front approach (see, for example [4, 7]) where the plus and transverse components of momentum are conserved, and quarks as well as antiquarks are on-shell. It is useful to define some internal quantities analogous to those defined in Appendix A for on-shell quarks:

$$\begin{aligned} M_0'^2 &= (e'_1 + e'_2)^2 = \frac{p_\perp'^2 + m_1'^2}{x_1} + \frac{p_\perp'^2 + m_2^2}{x_2}, & \widetilde{M}_0' &= \sqrt{M_0'^2 - (m_1' - m_2)^2}, \\ e_i^{(\prime)} &= \sqrt{m_i^{(\prime)2} + p_\perp'^2 + p_z'^2}, & p_z' &= \frac{x_2 M_0'}{2} - \frac{m_2^2 + p_\perp'^2}{2x_2 M_0'}. \end{aligned} \quad (2.2)$$

Here  $M_0'^2$  can be interpreted as the kinetic invariant mass squared of the incoming  $q\bar{q}$  system, and  $e_i$  the energy of the quark  $i$ .

It has been shown in [11] that one can pass to the light-front approach by integrating out the  $p^-$  component of the internal momentum in covariant Feynman momentum loop integrals. We need Feynman rules for the meson-quark-antiquark vertices to calculate the amplitudes shown in Fig. 1. These Feynman rules for vertices ( $i\Gamma'_M$ ) of ground-state  $s$ -wave mesons and low-lying  $p$ -wave

mesons are summarized in Table I. As we shall see later, the integration of the minus component of the internal momentum in Fig. 1 will force the antiquark to be on its mass shell. The specific form of the covariant vertex functions for on-shell quarks can be determined by comparing to the conventional vertex functions as shown in Appendix A. Next, we shall use the decay constants as an example to illustrate a typical calculation in the covariant light-front approach.

## B. Decay constants

The decay constants for  $J = 0, 1$  mesons are defined by the matrix elements

$$\begin{aligned} \langle 0 | A_\mu | P(P') \rangle &\equiv \mathcal{A}_\mu^P = i f_P P'_\mu, & \langle 0 | V_\mu | S(P') \rangle &\equiv \mathcal{A}_\mu^S = f_S P'_\mu, \\ \langle 0 | V_\mu | V(P', \varepsilon') \rangle &\equiv \mathcal{A}_\mu^V = M'_V f_V \varepsilon'_\mu, & \langle 0 | A_\mu | {}^3{}^{(1)}A(P', \varepsilon') \rangle &\equiv \mathcal{A}_\mu^{{}^3{}^{(1)}A} = M'_{{}^3{}^{(1)}A} f_{{}^3{}^{(1)}A} \varepsilon'_\mu, \end{aligned} \quad (2.3)$$

where the  ${}^{2S+1}L_J = {}^1S_0, {}^3P_0, {}^3S_1, {}^3P_1, {}^1P_1$  and  ${}^3P_2$  states of  $q'_1 \bar{q}_2$  mesons are denoted by  $P, S, V, {}^3A, {}^1A$  and  $T$ , respectively. Note that a  ${}^3P_2$  state cannot be produced by a current. It is useful to note that in the SU(N)-flavor limit ( $m'_1 = m_2$ ) we should have vanishing  $f_S$  and  $f_{{}^1A}$ . The former can be seen by applying equations of motion to the matrix element of the scalar resonance in Eq. (2.3) to obtain

$$m_S^2 f_S = i(m'_1 - m_2) \langle 0 | \bar{q}_1 q_2 | S \rangle. \quad (2.4)$$

The latter is based on the argument that the light  ${}^3P_1$  and  ${}^1P_1$  states transfer under charge conjugation as

$$M_a^b({}^3P_1) \rightarrow M_b^a({}^3P_1), \quad M_a^b({}^1P_1) \rightarrow -M_b^a({}^1P_1), \quad (a = 1, 2, 3), \quad (2.5)$$

where the light axial-vector mesons are represented by a  $3 \times 3$  matrix. Since the weak axial-vector current transfers as  $(A_\mu)_a^b \rightarrow (A_\mu)_a^b$  under charge conjugation, it is clear that the decay constant of the  ${}^1P_1$  meson vanishes in the SU(3) limit [23]. This argument can be generalized to

TABLE I: Feynman rules for the vertices ( $i\Gamma'_M$ ) of the incoming mesons-quark-antiquark, where  $p'_1$  and  $p_2$  are the quark and antiquark momenta, respectively. Under the contour integrals to be discussed below,  $H'_M$  and  $W'_M$  are reduced to  $h'_M$  and  $w'_M$ , respectively, whose expressions are given by Eq. (2.11). Note that for outgoing mesons, we shall use  $i(\gamma_0 \Gamma_M^\dagger \gamma_0)$  for the corresponding vertices.

$M({}^{2S+1}L_J)$	$i\Gamma'_M$
pseudoscalar ( ${}^1S_0$ )	$H'_P \gamma_5$
vector ( ${}^3S_1$ )	$iH'_V [\gamma_\mu - \frac{1}{W'_V} (p'_1 - p_2)_\mu]$
scalar ( ${}^3P_0$ )	$-iH'_S$
axial ( ${}^3P_1$ )	$-iH'_A [\gamma_\mu + \frac{1}{W'_A} (p'_1 - p_2)_\mu] \gamma_5$
axial ( ${}^1P_1$ )	$-iH'_{1A} [\frac{1}{W'_{1A}} (p'_1 - p_2)_\mu] \gamma_5$
tensor ( ${}^3P_2$ )	$i\frac{1}{2}H'_T [\gamma_\mu - \frac{1}{W'_V} (p'_1 - p_2)_\mu] (p'_1 - p_2)_\nu$

heavy axial-vector mesons. In fact, under similar charge conjugation argument  $[(V_\mu)_a^b \rightarrow -(V_\mu)_b^a, M_a^b(^3P_0) \rightarrow M_b^a(^3P_0)]$  one can also prove the vanishing of  $f_S$  in the SU(N) limit.

Furthermore, in the heavy quark limit ( $m'_1 \rightarrow \infty$ ), the heavy quark spin  $s_Q$  decouples from the other degrees of freedom so that  $s_Q$  and the total angular momentum of the light antiquark  $j$  are separately good quantum numbers. Hence, it is more convenient to use the  $L_J^j = P_2^{3/2}, P_1^{3/2}, P_1^{1/2}$  and  $P_0^{1/2}$  basis. It is obvious that the first and the last of these states are  ${}^3P_2$  and  ${}^3P_0$ , respectively, while [24]

$$|P_1^{3/2}\rangle = \sqrt{\frac{2}{3}} |{}^1P_1\rangle + \frac{1}{\sqrt{3}} |{}^3P_1\rangle, \quad |P_1^{1/2}\rangle = \frac{1}{\sqrt{3}} |{}^1P_1\rangle - \sqrt{\frac{2}{3}} |{}^3P_1\rangle. \quad (2.6)$$

Heavy quark symmetry (HQS) requires (see Sec. IV) [20, 25]

$$f_V = f_P, \quad f_{A^{1/2}} = f_S, \quad f_{A^{3/2}} = 0, \quad (2.7)$$

where we have denoted the  $P_1^{1/2}$  and  $P_1^{3/2}$  states by  $A^{1/2}$  and  $A^{3/2}$ , respectively. These relations in the above equation can be understood from the fact that  $(S_0^{1/2}, S_1^{1/2})$ ,  $(P_0^{1/2}, P_1^{1/2})$  and  $(P_1^{3/2}, P_2^{3/2})$  form three doublets in the HQ limit and that the tensor meson cannot be induced from the  $V - A$  current. It is important to check if the calculated decay constants satisfy the non-trivial SU(N)-flavor and HQS relations.

We now follow [8] to evaluate meson decay constants. The matrix element for the annihilation of a pseudoscalar state via axial currents can be easily written down and it has the expression

$$\mathcal{A}_\mu^P = -i^2 \frac{N_c}{(2\pi)^4} \int d^4 p'_1 \frac{H'_P}{N'_1 N'_2} s_\mu^P, \quad (2.8)$$

where

$$\begin{aligned} s_\mu^P &\equiv \text{Tr}[\gamma_\mu \gamma_5 (\not{p}'_1 + m'_1) \gamma_5 (-\not{p}_2 + m_2)] \\ &= -4[m_2 P'_\mu + (m'_1 - m_2) p'_{1\mu}], \end{aligned} \quad (2.9)$$

$N'_1 = p'^2_1 - m'^2_1 + i\epsilon$  and  $N_2 = p^2_2 - m^2_2 + i\epsilon$ . We need to integrate out  $p'^{-}_1$  in  $\mathcal{A}_\mu^P$ . As stressed in [8], if it is assumed that the vertex function  $H'$  has no pole in the upper complex  $p'^{-}_1$  plane, then the covariant calculation of meson properties and the calculation of the light-front formulism will give identical results at the one-loop level. Therefore, by closing the contour in the upper complex  $p'^{-}_1$  plane and assuming that  $H'_P$  is analytic within the contour, the integration picks up a residue at  $p_2 = \hat{p}_2$ , where  $\hat{p}_2^2 = m_2^2$ . The other momentum is given by momentum conservation,  $\hat{p}'_1 = P' - \hat{p}_2$ . Consequently, one has the following replacements:

$$\begin{aligned} N'_1 &\rightarrow \hat{N}'_1 = \hat{p}'^2_1 - m'^2_1 = x_1(M'^2 - M_0'^2), \\ H'_M &\rightarrow \hat{H}'_M = H'_M(\hat{p}'^2_1, \hat{p}_2^2) \equiv h'_M, \\ W'_M &\rightarrow \hat{W}'_M = W'_M(\hat{p}'^2_1, \hat{p}_2^2) \equiv w'_M, \\ \int \frac{d^4 p'_1}{N'_1 N'_2} H'_M s^M &\rightarrow -i\pi \int \frac{dx_2 d^2 p'_\perp}{x_2 \hat{N}'_1} h'_M \hat{s}^M, \end{aligned} \quad (2.10)$$

in a generic one-loop vacuum to particle  $M$  amplitude  $\mathcal{A}_\mu^M$ . In this work the explicit forms of  $h'_M$  and  $w'_M$  are given by (see Appendix A)

$$h'_P = h'_V = (M'^2 - M_0'^2) \sqrt{\frac{x_1 x_2}{N_c}} \frac{1}{\sqrt{2} \widetilde{M'_0}} \varphi',$$

$$\begin{aligned}
h'_S &= \sqrt{\frac{2}{3}} h'_{3A} = (M'^2 - M_0'^2) \sqrt{\frac{x_1 x_2}{N_c}} \frac{1}{\sqrt{2} \widetilde{M}_0'} \frac{\widetilde{M}_0'^2}{2\sqrt{3} M_0'} \varphi'_p, \\
h'_{1A} &= h'_T = (M'^2 - M_0'^2) \sqrt{\frac{x_1 x_2}{N_c}} \frac{1}{\sqrt{2} \widetilde{M}_0'} \varphi'_p, \\
w'_V &= M'_0 + m'_1 + m_2, \quad w'_{3A} = \frac{\widetilde{M}_0'^2}{m'_1 - m_2}, \quad w'_{1A} = 2,
\end{aligned} \tag{2.11}$$

where  $\varphi'$  and  $\varphi'_p$  are the light-front momentum distribution amplitudes for  $s$ -wave and  $p$ -wave mesons, respectively. There are several popular phenomenological light-front wave functions that have been employed to describe various hadronic structures in the literature. In the present work, we shall use the Gaussian-type wave function [26]

$$\begin{aligned}
\varphi' &= \varphi'(x_2, p'_\perp) = 4 \left( \frac{\pi}{\beta'^2} \right)^{\frac{3}{4}} \sqrt{\frac{dp'_z}{dx_2}} \exp \left( -\frac{p_z'^2 + p_\perp'^2}{2\beta'^2} \right), \\
\varphi'_p &= \varphi'_p(x_2, p'_\perp) = \sqrt{\frac{2}{\beta'^2}} \varphi', \quad \frac{dp'_z}{dx_2} = \frac{e'_1 e_2}{x_1 x_2 M'_0}.
\end{aligned} \tag{2.12}$$

The parameter  $\beta'$  is expected to be of order  $\Lambda_{\text{QCD}}$ . The derivation of these vertex functions is shown in Appendix A.

The matrix element  $\mathcal{A}_\mu^P$  can be evaluated readily by using above equations. However,  $\mathcal{A}_\mu^P$  obtained in this way contains a spurious contribution proportional to  $\tilde{\omega}^\mu = (\tilde{\omega}^-, \tilde{\omega}^+, \tilde{\omega}_\perp) = (2, 0, 0_\perp)$ . It arises from the momentum decomposition of  $\hat{p}_1'^\mu$

$$\begin{aligned}
\hat{p}_1'^\mu &= (P' - \hat{p}_2)^\mu \\
&= x_1 P'^\mu + (0, 0, \hat{p}'_\perp)^\mu + \frac{1}{2} \left( x_2 P'^- - \frac{\hat{p}_2^2 + m_2^2}{x_2 P'^+} \right) \tilde{\omega}^\mu.
\end{aligned} \tag{2.13}$$

In fact, after the integration,  $p'_1$  can be expressed in terms of two external vectors,  $P'$  and  $\tilde{\omega}$ . Therefore, in the integrand of  $\mathcal{A}_\mu^M$ , one has

$$\begin{aligned}
p'_{1\mu} &\doteq \frac{\tilde{\omega} \cdot p'_1}{\tilde{\omega} \cdot P'} P'_\mu + \frac{1}{\tilde{\omega} \cdot P'} \tilde{\omega}_\mu \left( P' \cdot p'_1 - \frac{\tilde{\omega} \cdot p'_1}{\tilde{\omega} \cdot P'} P'^2 \right) \\
&\doteq x_1 P'_\mu + \frac{1}{2 \tilde{\omega} \cdot P'} \tilde{\omega}_\mu [-N_2 + N'_1 + m_1'^2 - m_2^2 + (1 - 2x_1) M'^2].
\end{aligned} \tag{2.14}$$

The symbol  $\doteq$  in the above equation reminds us that it is true only in the  $\mathcal{A}^M$  integration. There is one missing piece in the contour integration, namely, the contribution of the zero mode from the  $p_1'^+ = 0$  region [12]. The appearance of  $N_2$  in the numerator as shown in the above equation (2.8) also prompts an extra care in performing the  $p_1'^-$  contour integration. It is interesting that this zero mode contribution provides a cue for the spurious term in  $\mathcal{A}_\mu^M$ . As shown in [8], the inclusion of the zero mode contribution in  $\mathcal{A}_\mu^M$  matrix elements in practice amounts to the replacements

$$\hat{p}'_1 \rightarrow x_1 P', \quad \hat{N}_2 \rightarrow \hat{N}'_1 + m_1'^2 - m_2^2 + (1 - 2x_1) M'^2, \tag{2.15}$$

in the  $\hat{S}^M$  under the integration. By virtue of Eqs. (2.3), (2.10) and (2.15), we obtain [8]

$$f_P = \frac{N_c}{16\pi^3} \int dx_2 d^2 p'_\perp \frac{h'_P}{x_1 x_2 (M'^2 - M_0'^2)} 4(m'_1 x_2 + m_2 x_1). \tag{2.16}$$

It should be stressed that  $f_P$  itself is free of zero mode contributions as its derivation does not involve the replacement of  $\hat{N}_2$  (see also Sec. III.B). With the explicit form of  $h'_P$  shown in Eq. (2.11), the familiar expression of  $f_P$  in the conventional light-front approach [4, 7], namely,

$$f_P = 2 \frac{\sqrt{2N_c}}{16\pi^3} \int dx_2 d^2 p'_\perp \frac{1}{\sqrt{x_1 x_2} \tilde{M}'_0} (m'_1 x_2 + m_2 x_1) \varphi'(x_2, p'_\perp), \quad (2.17)$$

is reproduced.

The decay constant of a scalar meson can be obtained in a similar manner. By using the corresponding Feynman rules shown in Table I, we have

$$\mathcal{A}_\mu^S = -i^2 \frac{N_c}{(2\pi)^4} \int d^4 p'_1 \frac{H'_S}{N'_1 N'_2} \text{Tr}[\gamma_\mu(\not{p}'_1 + m'_1)(-i)(-\not{p}_2 + m_2)]. \quad (2.18)$$

Note that the trace ( $\equiv s_\mu^S$ ) in the above equation is related to  $s_\mu^P$  in Eq. (2.8) by the replacement of  $m_2 \rightarrow -m_2$  and by adding an overall factor of  $-i$ . Likewise, by using Eqs. (2.3), (2.10) and (2.15), it follows that

$$f_S = \frac{N_c}{16\pi^3} \int dx_2 d^2 p'_\perp \frac{h'_S}{x_1 x_2 (M'^2 - M'_0)^2} 4(m'_1 x_2 - m_2 x_1). \quad (2.19)$$

For  $m'_1 = m_2$ , the meson wave function is symmetric with respect to  $x_1$  and  $x_2$ , and hence  $f_S = 0$ , as it should be.

We now turn to the decay constants of vector and axial-vector mesons. The decay amplitude for a vector meson is given by

$$\mathcal{A}_\mu^V = -i^2 \frac{N_c}{(2\pi)^4} \int d^4 p'_1 \frac{i H'_V}{N'_1 N'_2} \text{Tr} \left\{ \gamma_\mu(\not{p}'_1 + m'_1) \left[ \gamma_\nu - \frac{(p'_1 - p_2)_\nu}{W'_V} \right] (-\not{p}_2 + m_2) \right\} \varepsilon'^\nu. \quad (2.20)$$

We consider the case with the transverse polarization

$$\varepsilon(\pm) = \left( \frac{2}{P'^+} \varepsilon_\perp \cdot \not{P}'_\perp, 0, \varepsilon_\perp \right), \quad \varepsilon_\perp = \mp \frac{1}{\sqrt{2}} (1, \pm i). \quad (2.21)$$

Contracting  $\mathcal{A}_\mu^V$  with  $\varepsilon^*(\pm)$  and applying Eqs. (2.3), (2.10) and (2.15) lead to [8]<sup>2</sup>

$$\begin{aligned} f_V = & \frac{N_c}{4\pi^3 M'} \int dx_2 d^2 p'_\perp \frac{h'_V}{x_1 x_2 (M'^2 - M'_0)^2} \\ & \times \left[ x_1 M'_0 - m'_1 (m'_1 - m_2) - p'^2_\perp + \frac{m'_1 + m_2}{w'_V} p'^2_\perp \right]. \end{aligned} \quad (2.22)$$

We wish to stress that the vector decay constant obtained in the conventional light-front model [4] does not coincide with the above result (2.22) owing to the missing zero mode contribution,

---

<sup>2</sup> When  $\mathcal{A}_\mu^V$  is contracted with the longitudinal polarization vector  $\varepsilon^\mu(0)$ ,  $f_V$  will receive additional contributions characterized by the  $B$  functions defined in Appendix B (see Eq. (3.5) of [27]) which give about 10% corrections to  $f_V$  for the vertex function  $h'_V$  used in Eq. (2.11). It is not clear to us why the result of  $f_V$  depends on the polarization vector. Note that the new residual contributions are absent in the approach of [28] in which a different scheme has been developed to identify the zero mode contributions to the decay constants and form factors.

whose presence is evidenced by its involvement of  $\hat{N}_2$  [8, 27]. Since  $\mathcal{A}_\mu^{3A}$  ( $\mathcal{A}_\mu^{1A}$ ) is related to  $\mathcal{A}_\mu^V$  by a suitable replacement of  $H'_V \rightarrow -H'_{3A(1A)}$  and  $m_2 \rightarrow -m_2$ ,  $W'_V \rightarrow -W'_{3A(1A)}$  in the trace (only the  $1/W'$  terms being kept in the  $1A$  case), this allows us to readily obtain

$$\begin{aligned} f_{3A} &= -\frac{N_c}{4\pi^3 M'} \int dx_2 d^2 p'_\perp \frac{h'_{3A}}{x_1 x_2 (M'^2 - M_0'^2)} \\ &\quad \times \left[ x_1 M_0'^2 - m'_1 (m'_1 + m_2) - p'_\perp^2 - \frac{m'_1 - m_2}{w'_{3A}} p'_\perp^2 \right], \\ f_{1A} &= \frac{N_c}{4\pi^3 M'} \int dx_2 d^2 p'_\perp \frac{h'_{1A}}{x_1 x_2 (M'^2 - M_0'^2)} \left( \frac{m'_1 - m_2}{w'_{1A}} p'_\perp^2 \right). \end{aligned} \quad (2.23)$$

It is clear that  $f_{1A} = 0$  for  $m'_1 = m_2$ . The SU(N)-flavor constraints on  $f_S$  and  $f_{1A}$  are thus satisfied. The HQS relations on decay constants will be discussed in Section IV.

In order to have a numerical study for decay constants, we need to specify the constituent quark masses and the parameter  $\beta$  appearing in the Gaussian-type wave function (2.12). For constituent quark masses we use [6, 7, 8, 29]

$$m_{u,d} = 0.26 \text{ GeV}, \quad m_s = 0.37 \text{ GeV}, \quad m_c = 1.40 \text{ GeV}, \quad m_b = 4.64 \text{ GeV}. \quad (2.24)$$

As we shall see in Sec. III, the masses of strange and charmed quarks are constrained from the measured form-factor ratios in semileptonic  $D \rightarrow K^* \ell \bar{\nu}$  decays. Shown in Tables II and III are the input parameter  $\beta$  and decay constants, respectively. In Table III the decay constants in parentheses are used to determine  $\beta$ . For the purpose of an estimation, for  $p$ -wave mesons in  $D$ ,  $D_s$  and  $B$  systems we shall use the  $\beta$  parameters obtained in the ISGW2 model [30], the improved version of the ISGW model, up to some simple scaling. Several remarks are in order: (i) The values of the parameter  $\beta_V$  presented in Table II are slightly smaller than the ones obtained in the earlier literature. For example,  $\beta_\rho = 0.26$ ,  $\beta_{K^*} = 0.27$  and  $\beta_{D^*} = 0.38$  are obtained here using the Gaussian-type wave function, while the corresponding values are 0.30, 0.31, 0.46 in [7]. This is because we have utilized the correct light-front expression for the vector decay constant  $f_V$  [cf. Eq. (2.22)]. It is interesting to notice that  $\beta_V$  in the ISGW2 model also has a similar reduction due to hyperfine interactions, which have been neglected in the original ISGW model in the mass spectrum calculation. (ii) The  $\beta$  parameters for  $p$ -wave states of  $D$ ,  $D_s$  and  $B$  systems are the smallest when compared to  $\beta_{P,V}$ . (iii) The decay constants of  ${}^3P_1$  and  ${}^3P_1^{3/2}$  states have opposite signs to that of  ${}^1P_1$  or  ${}^1P_1^{1/2}$  as can be easily seen from Eq. (2.6).

TABLE II: The input parameter  $\beta$  (in units of GeV) in the Gaussian-type wave function (2.12).

$2S+1L_J$	$\beta_{u\bar{d}}$	$\beta_{s\bar{u}}$	$\beta_{c\bar{u}}$	$\beta_{c\bar{s}}$	$\beta_{b\bar{u}}$
${}^1S_0$	0.3102	0.3864	0.4496	0.4945	0.5329
${}^3S_1$	0.2632	0.2727	0.3814	0.3932	0.4764
${}^3P_0$	$\beta_{a_1}$	$\beta_{K({}^3P_1)}$	0.3305	0.3376	0.4253
${}^3P_1$	0.2983	0.303	0.3305	0.3376	0.4253
${}^1P_1$	$\beta_{a_1}$	$\beta_{K({}^3P_1)}$	0.3305	0.3376	0.4253

TABLE III: Mesonic decay constants (in units of MeV) obtained by using Eqs. (2.16), (2.19), (2.22) and (2.23). Those in parentheses are taken as inputs to determine the corresponding  $\beta$ 's shown in Table II. The decay constant  $f_{K_1(1270)} = 175$  MeV is also used as an input (see the text for detail).

$2S+1L_J$	$f_{u\bar{d}}$	$f_{s\bar{u}}$	$f_{c\bar{u}}$	$f_{c\bar{s}}$	$f_{b\bar{u}}$
$^1S_0$	(131)	(160)	(200)	(230)	(180)
$^3S_1$	(216)	(210)	(220)	(230)	(180)
$^3P_0$	0	21	86	71	112
$^3P_1$	(−203)	−186	−127	−121	−123
$^1P_1$	0	11	45	38	68
$P_1^{1/2}$	−	−	130	122	140
$P_1^{3/2}$	−	−	−36	−38	−15

In principle, the parameter  $\beta$  for  $p$ -wave mesons can be determined from the study of the meson spectroscopy. Although we have not explored this issue in this work, it is important to keep in mind that  $\beta$ 's are closely related to meson masses. In Table III we have employed  $|f_{a_1}| = 203$  MeV and  $f_{D_s^*} = f_{D_s}$  as inputs. It is generally argued that  $a_1(1260)$  should have a similar decay constant as the  $\rho$  meson. Presumably,  $f_{a_1}$  can be extracted from the decay  $\tau \rightarrow a_1(1260)\nu_\tau$ . Though this decay is not shown in the Particle Data Group (PDG) [16], an experimental value of  $|f_{a_1}| = 203 \pm 18$  MeV is nevertheless quoted in [31].<sup>3</sup> Contrary to the non-strange charmed meson case where  $D^*$  has a slightly larger decay constant than  $D$ , the recent measurements of  $B \rightarrow D_s^{(*)} D^{(*)}$  [16, 32] indicate that the decay constants of  $D_s^*$  and  $D_s$  are similar. Hence we shall take  $f_{D_s^*} = f_{D_s}$ . As for the decay constant of  $B^*$ , a recent lattice calculation yields  $f_{B^*}/f_B = 1.01 \pm 0.01^{+0.04}_{-0.01}$  [33]. Therefore we will set  $f_{B^*} = f_B$  in Table III.

It is clear from Eq. (2.4) that the decay constant of light scalar resonances is largely suppressed relative to that of the pseudoscalar mesons owing to the small mass difference between the constituent quark masses. However, as shown in Table III, this suppression becomes less restrictive for heavy scalar mesons because of heavy and light quark mass imbalance. Note that what is the underlying quark structure of light scalar resonances is still controversial. While it has been widely advocated that the light scalar nonet formed by  $\sigma(600)$ ,  $\kappa(800)$ ,  $f_0(980)$  and  $a_0(980)$  can be identified primarily as four-quark states, it is generally believed that the nonet states  $f_0(1370)$ ,  $a_0(1450)$ ,  $K_0^*(1430)$  and  $f_0(1500)/f_0(1710)$  are the conventional  $q\bar{q}'$  states (for a review, see e.g. [34]). Therefore, the prediction of  $f_S = 21$  MeV for the scalar meson in the  $s\bar{u}$  content (see Table III) is most likely designated for the  $K_0^*(1430)$  state. Notice that this prediction is slightly smaller than the result of 42 MeV obtained in [35] based on the finite-energy sum rules, and far less than the estimate of  $(70 \pm 10)$  MeV in [36]. It is worth remarking that even if the light scalar mesons are

<sup>3</sup> The decay constant of  $a_1$  can be tested in the decay  $B^+ \rightarrow \bar{D}^0 a_1^+$  which receives the main contribution from the color-allowed amplitude proportional to  $f_{a_1} F^{BD}(m_{a_1}^2)$ .

made from 4 quarks, the decay constants of the neutral scalars  $\sigma(600)$ ,  $f_0(980)$  and  $a_0^0(980)$  must vanish owing to charge conjugation invariance.

In principle, the decay constant of the scalar strange charmed meson  $D_{s0}^*$  can be determined from the hadronic decay  $B \rightarrow \bar{D}D_{s0}^*$  since it proceeds only via external  $W$ -emission. Indeed, a recent measurement of the  $D\bar{D}_{s0}^*$  production in  $B$  decays by Belle [37] indicates a  $f_{D_{s0}^*}$  of order 60 MeV [38] which is close to the expectation of 71 MeV (see Table III). In Sec. III.E we will discuss more about  $\bar{D}D_s^{**}$  productions in  $B$  decays. The smallness of the decay constant  $f_{D_{s0}^*}$  relative to  $f_{D_s}$  can be seen from Eqs. (2.16) and (2.19) that

$$f_{D_s(D_{s0}^*)} \propto \int dx_2 \cdots [m_c x_2 \pm m_s(1 - x_2)]. \quad (2.25)$$

Since the momentum fraction  $x_2$  of the strange quark in the  $D_s(D_{s0}^*)$  meson is small, its effect being constructive in  $D_s$  case and destructive in  $D_{s0}^*$  is sizable and explains why  $f_{D_{s0}^*}/f_{D_s} \sim 0.3$ .

Except for  $a_1$  and  $b_1$  mesons which cannot have mixing because of the opposite  $C$ -parities, physical strange axial-vector mesons are the mixture of  ${}^3P_1$  and  ${}^1P_1$  states, while the heavy axial-vector resonances are the mixture of  $P_1^{1/2}$  and  $P_1^{3/2}$ . For example,  $K_1(1270)$  and  $K_1(1400)$  are the mixture of  $K_3P_1$  and  $K_1P_1$  (denoted by  $K_{1A}$  and  $K_{1B}$ , respectively, by PDG [16]) owing to the mass difference of the strange and non-strange light quarks:

$$\begin{aligned} K_1(1270) &= K_{3P_1} \sin \theta + K_{1P_1} \cos \theta, \\ K_1(1400) &= K_{3P_1} \cos \theta - K_{1P_1} \sin \theta, \end{aligned} \quad (2.26)$$

with  $\theta \approx -58^\circ$  as implied from the study of  $D \rightarrow K_1(1270)\pi$ ,  $K_1(1400)\pi$  decays [45]. We use  $f_{K_1(1270)} = 175$  MeV [45] to fix  $\beta_{K(3P_1)} \simeq \beta_{K(1P_1)} = 0.303$  GeV and obtain  $f_{K_1(1400)} = -87$  MeV. Note that these  $\beta_{K(3P_1)}$ ,  $\beta_{K(1P_1)}$  are close to  $\beta_{K^*}$ . For the masses of  $K_{1P_1}$  and  $K_{3P_1}$ , we follow [23] to determine them from the mass relations  $2m_{K_{1P_1}}^2 = m_{b_1(1232)}^2 + m_{h_1(1380)}^2$  and  $m_{K_{3P_1}}^2 = m_{K_1(1270)}^2 + m_{K_1(1400)}^2 - m_{K_{1P_1}}^2$ . For  $D$  and  $B$  systems, it is clear from Table III that  $|f_{A^{3/2}}| \ll f_S < f_{A^{1/2}}$ , in accordance with the expectation from HQS [cf. Eq. (2.7)].

### III. COVARIANT MODEL ANALYSIS OF FORM FACTORS

In this section we first review the analysis of the form factors for  $s$ -wave mesons within the framework of the covariant light-front quark model [8] and then extend it to the  $p$ -wave meson case followed by numerical results and discussion.

#### A. Form factors

Form factors for  $P \rightarrow P, V$  transitions are defined by

$$\begin{aligned} \langle P(P'') | V_\mu | P(P') \rangle &= P_\mu f_+(q^2) + q_\mu f_-(q^2), \\ \langle V(P'', \varepsilon'') | V_\mu | P(P') \rangle &= \epsilon_{\mu\nu\alpha\beta} \varepsilon''^{\nu\alpha} P^\alpha q^\beta g(q^2), \\ \langle V(P'', \varepsilon'') | A_\mu | P(P') \rangle &= -i \left\{ \varepsilon''^\mu f(q^2) + \varepsilon''^\mu \cdot P \left[ P_\mu a_+(q^2) + q_\mu a_-(q^2) \right] \right\}, \end{aligned} \quad (3.1)$$

where  $P = P' + P''$ ,  $q = P' - P''$  and the convention  $\epsilon_{0123} = 1$  is adopted. These form factors are related to the commonly used Bauer-Stech-Wirbel (BSW) form factors [46] via

$$\begin{aligned} F_1^{PP}(q^2) &= f_+(q^2), \quad F_0^{PP}(q^2) = f_+(q^2) + \frac{q^2}{q \cdot P} f_-(q^2), \\ V^{PV}(q^2) &= -(M' + M'') g(q^2), \quad A_1^{PV}(q^2) = -\frac{f(q^2)}{M' + M''}, \\ A_2^{PV}(q^2) &= (M' + M'') a_+(q^2), \quad A_3^{PV}(q^2) - A_0^{PV}(q^2) = \frac{q^2}{2M''} a_-(q^2), \end{aligned} \quad (3.2)$$

where the latter form factors are defined by [46]

$$\begin{aligned} \langle P(P'') | V_\mu | P(P') \rangle &= \left( P_\mu - \frac{M'^2 - M''^2}{q^2} q_\mu \right) F_1^{PP}(q^2) + \frac{M'^2 - M''^2}{q^2} q_\mu F_0^{PP}(q^2), \\ \langle V(P'', \varepsilon'') | V_\mu | P(P') \rangle &= -\frac{1}{M' + M''} \epsilon_{\mu\nu\alpha\beta} \varepsilon''^{\nu\alpha} P^\alpha q^\beta V^{PV}(q^2), \\ \langle V(P'', \varepsilon'') | A_\mu | P(P') \rangle &= i \left\{ (M' + M'') \varepsilon''^{\mu\nu} A_1^{PV}(q^2) - \frac{\varepsilon''^{\mu\nu} \cdot P}{M' + M''} P_\mu A_2^{PV}(q^2) \right. \\ &\quad \left. - 2M'' \frac{\varepsilon''^{\mu\nu} \cdot P}{q^2} q_\mu [A_3^{PV}(q^2) - A_0^{PV}(q^2)] \right\}, \end{aligned} \quad (3.3)$$

with  $F_1^{PP}(0) = F_0^{PP}(0)$ ,  $A_3^{PV}(0) = A_0^{PV}(0)$ , and

$$A_3^{PV}(q^2) = \frac{M' + M''}{2M''} A_1^{PV}(q^2) - \frac{M' - M''}{2M''} A_2^{PV}(q^2). \quad (3.4)$$

The general expressions for  $P$  to low-lying  $p$ -wave meson transitions are given by [17]

$$\begin{aligned} \langle S(P'') | A_\mu | P(P') \rangle &= i \left[ u_+(q^2) P_\mu + u_-(q^2) q_\mu \right], \\ \langle A^{1/2}(P'', \varepsilon'') | V_\mu | P(P') \rangle &= i \left\{ \ell_{1/2}(q^2) \varepsilon''^{\mu\nu} + \varepsilon''^{\mu\nu} \cdot P [P_\mu c_+^{1/2}(q^2) + q_\mu c_-^{1/2}(q^2)] \right\}, \\ \langle A^{1/2}(P'', \varepsilon'') | A_\mu | P(P') \rangle &= -q_{1/2}(q^2) \epsilon_{\mu\nu\alpha\beta} \varepsilon''^{\nu\alpha} P^\alpha q^\beta, \\ \langle A^{3/2}(P'', \varepsilon'') | V_\mu | P(P') \rangle &= i \left\{ \ell_{3/2}(q^2) \varepsilon''^{\mu\nu} + \varepsilon''^{\mu\nu} \cdot P [P_\mu c_+^{3/2}(q^2) + q_\mu c_-^{3/2}(q^2)] \right\}, \\ \langle A^{3/2}(P'', \varepsilon'') | A_\mu | P(P') \rangle &= -q_{3/2}(q^2) \epsilon_{\mu\nu\alpha\beta} \varepsilon''^{\nu\alpha} P^\alpha q^\beta, \\ \langle T(P'', \varepsilon'') | V_\mu | P(P') \rangle &= h(q^2) \epsilon_{\mu\nu\alpha\beta} \varepsilon''^{\nu\alpha} P_\lambda P^\alpha q^\beta, \\ \langle T(P'', \varepsilon'') | A_\mu | P(P') \rangle &= -i \left\{ k(q^2) \varepsilon''^{\mu\nu} P^\nu + \varepsilon''^{\mu\nu} \cdot P^\alpha P^\beta [P_\mu b_+(q^2) + q_\mu b_-(q^2)] \right\}. \end{aligned} \quad (3.5)$$

The form factors  $\ell_{1/2(3/2)}$ ,  $c_+^{1/2(3/2)}$ ,  $c_-^{1/2(3/2)}$  and  $q_{1/2(3/2)}$  are defined for the transitions to the heavy  $P_1^{1/2}$  ( $P_1^{3/2}$ ) state. For transitions to light axial-vector mesons, it is more appropriate to employ the  $L - S$  coupled states  ${}^1P_1$  and  ${}^3P_1$  denoted by the particles  ${}^1A$  and  ${}^3A$  in our notation. The relation between  $P_1^{1/2}$ ,  $P_1^{3/2}$  and  ${}^1P_1$ ,  ${}^3P_1$  states is given by Eq. (2.6). The corresponding form factors  $\ell_{1A({}^3A)}$ ,  $c_+^{1A({}^3A)}$ ,  $c_-^{1A({}^3A)}$  and  $q_{1A({}^3A)}$  for  $P \rightarrow {}^1A$  ( ${}^3A$ ) transitions can be defined in an analogous way.<sup>4</sup>

<sup>4</sup> The form factors  $\ell_{1A({}^3A)}$ ,  $c_+^{1A({}^3A)}$ ,  $c_-^{1A({}^3A)}$  and  $q_{1A({}^3A)}$  are dubbed as  $\ell(v)$ ,  $c_+(s_+)$ ,  $c_-(s_-)$  and  $q(r)$ , respectively, in the ISGW model [17].

Note that only the form factors  $u_+(q^2)$ ,  $u_-(q^2)$  and  $k(q^2)$  in the above parametrization are dimensionless. It is thus convenient to define dimensionless form factors by<sup>5</sup>

$$\begin{aligned}\langle S(P'')|A_\mu|P(P')\rangle &= -i \left[ \left( P_\mu - \frac{M'^2 - M''^2}{q^2} q_\mu \right) F_1^{PS}(q^2) + \frac{M'^2 - M''^2}{q^2} q_\mu F_0^{PS}(q^2) \right], \\ \langle A(P'', \varepsilon'')|V_\mu|P(P')\rangle &= -i \left\{ (m_P - m_A) \varepsilon_\mu^* V_1^{PA}(q^2) - \frac{\varepsilon^* \cdot P'}{m_P - m_A} P_\mu V_2^{PA}(q^2) \right. \\ &\quad \left. - 2m_A \frac{\varepsilon^* \cdot P'}{q^2} q_\mu [V_3^{PA}(q^2) - V_0^{PA}(q^2)] \right\}, \\ \langle A(P'', \varepsilon'')|A_\mu|P(P')\rangle &= -\frac{1}{m_P - m_A} \epsilon_{\mu\nu\rho\sigma} \varepsilon^{*\nu} P^\rho q^\sigma A^{PA}(q^2),\end{aligned}\tag{3.6}$$

with

$$V_3^{PA}(q^2) = \frac{m_P - m_A}{2m_A} V_1^{PA}(q^2) - \frac{m_P + m_A}{2m_A} V_2^{PA}(q^2),\tag{3.7}$$

and  $V_3^{PA}(0) = V_0^{PA}(0)$ . They are related to the form factors in (3.3) via

$$\begin{aligned}F_1^{PS}(q^2) &= -u_+(q^2), \quad F_0^{PS}(q^2) = -u_+(q^2) - \frac{q^2}{q \cdot P} u_-(q^2), \\ A^{PA}(q^2) &= -(M' - M'') q(q^2), \quad V_1^{PA}(q^2) = -\frac{\ell(q^2)}{M' - M''}, \\ V_2^{PA}(q^2) &= (M' - M'') c_+(q^2), \quad V_3^{PA}(q^2) - V_0^{PA}(q^2) = \frac{q^2}{2M''} c_-(q^2).\end{aligned}\tag{3.8}$$

In above equations, the axial-vector meson  $A$  stands for  $A^{1/2}$  or  $A^{3/2}$ . Besides the dimensionless form factors, this parametrization has the advantage that the  $q^2$  dependence of the form factors is governed by the resonances of the same spin, for instance, the momentum dependence of  $F_0(q^2)$  is determined by scalar resonances.

To obtain the  $P \rightarrow M$  transition form factors with  $M$  being a ground-state  $s$ -wave meson or a low-lying  $p$ -wave meson, we shall consider the matrix elements

$$\langle M(P'')|V_\mu - A_\mu|P(P')\rangle \equiv \mathcal{B}_\mu^{PM},\tag{3.9}$$

where the corresponding Feynman diagram is shown in Fig. 1(b). We follow [8] to obtain  $P \rightarrow P, V$  form factors before extending the formalism to the  $p$ -wave meson case. As we shall see, the  $P \rightarrow S(A)$  transition form factors can be easily obtained by some suitable modifications on  $P \rightarrow P(V)$  ones, and we need some extension of the analysis in [8] to the  $P \rightarrow T$  case.

For the case of  $M = P$ , it is straightforward to obtain

$$\mathcal{B}_\mu^{PP} = -i^3 \frac{N_c}{(2\pi)^4} \int d^4 p'_1 \frac{H'_P H''_P}{N'_1 N''_1 N_2} S_{V\mu}^{PP},\tag{3.10}$$

---

<sup>5</sup> The definition here for dimensionless  $P \rightarrow A$  transition form factors differs than Eq. (3.17) of [38] where the coefficients  $(m_P \pm m_A)$  are replaced by  $(m_P \mp m_A)$ . It will become clear in Sec. IV that this definition will lead to HQS relations for  $B \rightarrow D_0^*, D_1$  transitions [cf. Eq. (4.7)] similar to that for  $B \rightarrow D, D^*$  ones.

where

$$S_{V\mu}^{PP} = \text{Tr}[\gamma_5(\not{p}_1'' + m_1'')\gamma_\mu(\not{p}_1' + m_1')\gamma_5(-\not{p}_2 + m_2)], \quad (3.11)$$

$N_1'' = p_1''^2 - m_1''^2 + i\epsilon$  and the subscript of  $S_V$  stands for the transition vector current. As noted in the Introduction we consider the  $q^+ = 0$  frame [8]. As in the  $\mathcal{A}_\mu^P$  case, the  $p_1'^-$  integration picks up the residue  $p_2 = \hat{p}_2$  and leads to

$$\begin{aligned} N_1'^{(\prime\prime)} &\rightarrow \hat{N}_1'^{(\prime\prime)} = x_1(M'^{(\prime\prime)2} - M_0'^{(\prime\prime)2}), \\ H_M'^{(\prime\prime)} &\rightarrow h_M'^{(\prime\prime)}, \\ W_M'' &\rightarrow w_M'', \\ \int \frac{d^4 p_1'}{N_1' N_1'' N_2} H_P' H_M'' S^{PM} &\rightarrow -i\pi \int \frac{dx_2 d^2 p_\perp'}{x_2 \hat{N}_1' \hat{N}_1''} h_P' h_M'' \hat{S}^{PM}, \end{aligned} \quad (3.12)$$

where

$$M_0''^2 = \frac{p_\perp''^2 + m_1''^2}{x_1} + \frac{p_\perp''^2 + m_2^2}{x_2}, \quad (3.13)$$

with  $p_\perp'' = p_\perp' - x_2 q_\perp$ . In general, after the integration in  $\mathcal{B}^{PM}$ ,  $\hat{p}_1'$  can be expressed in terms of three external vectors,  $P'$ ,  $q$  and  $\tilde{\omega}$ . Furthermore, the inclusion of the zero mode contribution cancels away the  $\tilde{\omega}$  dependence and in practice for  $\hat{p}_1'$  and  $\hat{N}_2$  in  $\hat{S}^{PM}$  under the integration, we have [8]

$$\begin{aligned} \hat{p}_{1\mu}' &\doteq P_\mu A_1^{(1)} + q_\mu A_2^{(1)}, \\ \hat{p}_{1\mu}' \hat{p}_{1\nu}' &\doteq g_{\mu\nu} A_1^{(2)} + P_\mu P_\nu A_2^{(2)} + (P_\mu q_\nu + q_\mu P_\nu) A_3^{(2)} + q_\mu q_\nu A_4^{(2)}, \\ \hat{p}_{1\mu}' \hat{p}_{1\nu}' \hat{p}_{1\alpha}' &\doteq (g_{\mu\nu} P_\alpha + g_{\mu\alpha} P_\nu + g_{\nu\alpha} P_\mu) A_1^{(3)} + (g_{\mu\nu} q_\alpha + g_{\mu\alpha} q_\nu + g_{\nu\alpha} q_\mu) A_2^{(3)} \\ &\quad + P_\mu P_\nu P_\alpha A_3^{(3)} + (P_\mu P_\nu q_\alpha + P_\mu q_\nu P_\alpha + q_\mu P_\nu P_\alpha) A_4^{(3)} \\ &\quad + (q_\mu q_\nu P_\alpha + q_\mu P_\nu q_\alpha + P_\mu q_\nu q_\alpha) A_5^{(3)} + q_\mu q_\nu q_\alpha A_6^{(3)}, \\ \hat{N}_2 &\rightarrow Z_2, \quad x_1 \hat{N}_2 \rightarrow 0, \\ \hat{p}_{1\mu}' \hat{N}_2 &\rightarrow q_\mu \left[ A_2^{(1)} Z_2 + \frac{q \cdot P}{q^2} A_1^{(2)} \right], \\ \hat{p}_{1\mu}' \hat{p}_{1\nu}' \hat{N}_2 &\rightarrow g_{\mu\nu} A_1^{(2)} Z_2 + q_\mu q_\nu \left[ A_4^{(2)} Z_2 + 2 \frac{q \cdot P}{q^2} A_2^{(1)} A_1^{(2)} \right], \\ \hat{p}_{1\mu}' \hat{p}_{1\nu}' \hat{p}_{1\alpha}' \hat{N}_2 &\rightarrow (g_{\mu\nu} q_\alpha + g_{\mu\alpha} q_\nu + g_{\nu\alpha} q_\mu) \left[ A_2^{(3)} Z_2 + \frac{q \cdot P}{3q^2} (A_1^{(2)})^2 \right] \\ &\quad + q_\mu q_\nu q_\alpha \left\{ A_6^{(3)} Z_2 + 3 \frac{q \cdot P}{q^2} \left[ A_2^{(1)} A_2^{(3)} - \frac{1}{3q^2} (A_1^{(2)})^2 \right] \right\}, \end{aligned} \quad (3.14)$$

where  $A_j^{(i)}$ ,  $Z_2$  are functions of  $x_{1,2}$ ,  $p_\perp'^2$ ,  $p_\perp' \cdot q_\perp$  and  $q^2$ , and their explicit expressions are given in [8]. We do not show the spurious contributions in the above equation since they vanish either after applying the above rules or after integration. The last rule on  $\hat{p}_{1\mu}' \hat{p}_{1\nu}' \hat{p}_{1\alpha}' \hat{N}_2$  in the above equation, which is needed in the  $P \rightarrow T$  calculation, is extended in this work. One needs to consider the product of four  $\hat{p}_1'$ 's. For completeness, the formulas for the product of four  $\hat{p}_1'$ 's and the expressions for  $A_j^{(i)}$ ,  $Z_2$  can be found in Appendix B.

From Eqs. (3.10)–(3.14) one can obtain the form factors  $f_{\pm}(q^2)$  for  $q^2 = -q_{\perp}^2 \leq 0$  [see Eq. (B3)]. We will return to the issue of the momentum dependence of form factors in the next sub-section. The explicit expressions for  $f_{\pm}$  can be evaluated readily by using the explicit representations of  $\hat{N}_1^{(\prime\prime)}$ ,  $h^{(\prime\prime)}$  given in Eqs. (3.12) and (2.11). At  $q^2 = 0$ , the form factor  $f_{+}(0)$  is reduced to the familiar form [3, 47]

$$f_{+}(0) = \frac{1}{16\pi^3} \int dx d^2 p'_{\perp} \varphi''^*(x, p'_{\perp}) \varphi'(x, p'_{\perp}) \frac{\mathcal{A}' \mathcal{A}'' + p'^2_{\perp}}{\sqrt{\mathcal{A}'^2 + p'^2_{\perp}} \sqrt{\mathcal{A}''^2 + p'^2_{\perp}}}, \quad (3.15)$$

where

$$\mathcal{A}' = m'_1 x + m_2(1 - x), \quad \mathcal{A}'' = m''_1 x + m_2(1 - x), \quad (3.16)$$

with  $x \equiv x_2$ .

For the  $P \rightarrow S$  transition amplitude, we have

$$\mathcal{B}_{\mu}^{PS} = -i^3 \frac{N_c}{(2\pi)^4} \int d^4 p'_1 \frac{H'_P H''_S}{N'_1 N''_1 N_2} S_{A\mu}^{PS}, \quad (3.17)$$

with

$$\begin{aligned} S_{A\mu}^{PS} &= \text{Tr}[(-i)(p''_1 + m''_1) \gamma_{\mu} \gamma_5 (p'_1 + m'_1) \gamma_5 (-p'_2 + m_2)] \\ &= -i S_{V\mu}^{PP}(m''_1 \rightarrow -m''_1). \end{aligned} \quad (3.18)$$

Thus, the  $P \rightarrow S$  transition form factors are related to  $f_{\pm}$  by

$$u_{\pm} = -f_{\pm}(m''_1 \rightarrow -m''_1, h''_P \rightarrow h''_S). \quad (3.19)$$

To be specific, we give the explicit forms of  $u_{\pm}(q^2)$  obtained in the covariant light-front model

$$\begin{aligned} u_{+}(q^2) &= \frac{N_c}{16\pi^3} \int dx_2 d^2 p'_{\perp} \frac{h'_P h''_S}{x_2 \hat{N}'_1 \hat{N}''_1} \left[ -x_1(M_0'^2 + M_0''^2) - x_2 q^2 \right. \\ &\quad \left. + x_2(m'_1 + m''_1)^2 + x_1(m'_1 - m_2)^2 + x_1(m''_1 + m_2)^2 \right], \\ u_{-}(q^2) &= \frac{N_c}{16\pi^3} \int dx_2 d^2 p'_{\perp} \frac{2h'_P h''_S}{x_2 \hat{N}'_1 \hat{N}''_1} \left\{ x_1 x_2 M'^2 + p'^2_{\perp} + m'_1 m_2 + (m''_1 + m_2)(x_2 m'_1 + x_1 m_2) \right. \\ &\quad \left. - 2 \frac{q \cdot P}{q^2} \left( p'^2_{\perp} + 2 \frac{(p'_{\perp} \cdot q_{\perp})^2}{q^2} \right) - 2 \frac{(p'_{\perp} \cdot q_{\perp})^2}{q^2} + \frac{p'_{\perp} \cdot q_{\perp}}{q^2} [M''^2 - x_2(q^2 + q \cdot P) \right. \\ &\quad \left. - (x_2 - x_1)M'^2 + 2x_1 M_0'^2 - 2(m'_1 - m_2)(m'_1 - m''_1)] \right\}. \end{aligned} \quad (3.20)$$

It is ready to evaluate these form factors by using the explicit expressions of  $\hat{N}$  and  $h$ . Numerical study of these form factors will be given in the next sub-section.

We next turn to the  $P \rightarrow V, A$  transition form factors. For the  $P \rightarrow V$  transition, we have

$$\mathcal{B}_{\mu}^{PV} = -i^3 \frac{N_c}{(2\pi)^4} \int d^4 p'_1 \frac{H'_P (iH''_V)}{N'_1 N''_1 N_2} S_{\mu\nu}^{PV} \varepsilon''^{\nu}, \quad (3.21)$$

where

$$\begin{aligned} S_{\mu\nu}^{PV} &= (S_V^{PV} - S_A^{PV})_{\mu\nu} \\ &= \text{Tr} \left[ \left( \gamma_{\nu} - \frac{1}{W_V''} (p''_1 - p_2)_{\nu} \right) (p''_1 + m''_1) (\gamma_{\mu} - \gamma_{\mu} \gamma_5) (p''_1 + m'_1) \gamma_5 (-p'_2 + m_2) \right]. \end{aligned} \quad (3.22)$$

As will be seen later, this expression of  $S$  is also useful for the  $P \rightarrow T$  calculation, and hence its explicit representation is included in Appendix B. By the aid of Eqs. (3.12) and (3.14), it is straightforward to obtain the  $P \rightarrow V$  form factors,  $g(q^2)$ ,  $f(q^2)$ ,  $a_{\pm}(q^2)$  [8]. For reader's convenience, the explicit forms of these form factors are summarized in Appendix B. Note that the vector form factor  $V(q^2 = 0) = -(M' + M'')g(q^2 = 0)$  is consistent with that in [7, 47] obtained by a Taylor expansion of the  $h''_V/\hat{N}_1''$  term in  $g(q^2)$  [see Eq. (B4)] with respect to  $p''_{\perp 2}$ . To show this, we write

$$\frac{h''_V}{\hat{N}_1''} = \frac{h''_V}{\hat{N}_1''} \Big|_{p''_{\perp 2} \rightarrow p''_{\perp 2}} - 2x_2 p'_{\perp} \cdot q_{\perp} \left( \frac{d}{dp''_{\perp 2}} \frac{h''_V}{\hat{N}_1''} \right)_{p''_{\perp 2} \rightarrow p''_{\perp 2}} + \mathcal{O}(x_2^2 q^2), \quad (3.23)$$

and see that the second term on the right-hand side is needed when considering the  $q_{\perp} \rightarrow 0$  limit of the  $p' \cdot q_{\perp}/q^2$  term in the integrand of  $g(q^2)$ , while  $\mathcal{O}(x_2^2 q^2)$  terms in the above equation vanish in the same limit. We perform the angular integration in the  $\vec{p}'_{\perp}$  plane before taking the  $q^2 \rightarrow 0$  limit. After these steps, we obtain the same expression of  $V(q^2 = 0)$  as in [7, 47].

The extension to  $P \rightarrow A$  transitions is straightforward and, as we shall see shortly, the resulting form factors have very similar expressions as that in the above case. For the  $P \rightarrow {}^3A$ ,  ${}^1A$  transitions, we have

$$\begin{aligned} \mathcal{B}_\mu^{P^3A} &= -i^3 \frac{N_c}{(2\pi)^4} \int d^4 p'_1 \frac{H'_P(-iH''_3A)}{N'_1 N''_1 N_2} S_{\mu\nu}^{P^3A} \varepsilon''^{*\nu}, \\ \mathcal{B}_\mu^{P^1A} &= -i^3 \frac{N_c}{(2\pi)^4} \int d^4 p'_1 \frac{H'_P(-iH''_1A)}{N'_1 N''_1 N_2} S_{\mu\nu}^{P^1A} \varepsilon''^{*\nu}, \end{aligned} \quad (3.24)$$

where

$$\begin{aligned} S_{\mu\nu}^{P^3A} &= (S_V^{P^3A} - S_A^{P^3A})_{\mu\nu} \\ &= \text{Tr} \left[ \left( \gamma_{\nu} - \frac{1}{W''_{3A}} (p''_1 - p_2)_{\nu} \right) \gamma_5 (\not{p}_1'' + m''_1) (\gamma_{\mu} - \gamma_{\mu} \gamma_5) (\not{p}_1' + m'_1) \gamma_5 (-\not{p}_2 + m_2) \right] \\ &= \text{Tr} \left[ \left( \gamma_{\nu} - \frac{1}{W''_{3A}} (p''_1 - p_2)_{\nu} \right) (\not{p}_1'' - m''_1) (\gamma_{\mu} \gamma_5 - \gamma_{\mu}) (\not{p}_1' + m'_1) \gamma_5 (-\not{p}_2 + m_2) \right], \\ S_{\mu\nu}^{P^1A} &= (S_V^{P^1A} - S_A^{P^1A})_{\mu\nu} \\ &= \text{Tr} \left[ \left( -\frac{1}{W''_{1A}} (p''_1 - p_2)_{\nu} \right) \gamma_5 (\not{p}_1'' + m''_1) (\gamma_{\mu} - \gamma_{\mu} \gamma_5) (\not{p}_1' + m'_1) \gamma_5 (-\not{p}_2 + m_2) \right] \\ &= \text{Tr} \left[ \left( -\frac{1}{W''_{1A}} (p''_1 - p_2)_{\nu} \right) (\not{p}_1'' - m''_1) (\gamma_{\mu} \gamma_5 - \gamma_{\mu}) (\not{p}_1' + m'_1) \gamma_5 (-\not{p}_2 + m_2) \right]. \end{aligned} \quad (3.25)$$

We therefore have  $S_{V(A)}^{P^3A, P^1A} = S_{A(V)}^{PV}$  with the replacement  $m''_1 \rightarrow -m''_1$ ,  $W''_V \rightarrow W''_{3A, 1A}$ . Note that only the  $1/W''$  terms are kept in  $S^{P^1A}$ . Consequently,

$$\begin{aligned} \ell^{3A, 1A}(q^2) &= f(q^2) \text{ with } (m''_1 \rightarrow -m''_1, h''_V \rightarrow h''_{3A, 1A}, w''_V \rightarrow w''_{3A, 1A}), \\ q^{3A, 1A}(q^2) &= g(q^2) \text{ with } (m''_1 \rightarrow -m''_1, h''_V \rightarrow h''_{3A, 1A}, w''_V \rightarrow w''_{3A, 1A}), \\ c_+^{3A, 1A}(q^2) &= a_+(q^2) \text{ with } (m''_1 \rightarrow -m''_1, h''_V \rightarrow h''_{3A, 1A}, w''_V \rightarrow w''_{3A, 1A}), \\ c_-^{3A, 1A}(q^2) &= a_-(q^2) \text{ with } (m''_1 \rightarrow -m''_1, h''_V \rightarrow h''_{3A, 1A}, w''_V \rightarrow w''_{3A, 1A}), \end{aligned} \quad (3.26)$$

where only the  $1/W''$  terms in  $P \rightarrow {}^1A$  form factors are kept. It should be cautious that the replacement of  $m_1'' \rightarrow -m_1''$  should not be applied to  $m_1''$  in  $w''$  and  $h''$ . These form factors can be expressed in the  $P_1^{3/2}$  and  $P_1^{1/2}$  basis by using Eq. (2.6).

Finally we turn to the  $P \rightarrow T$  transition given by

$$\mathcal{B}_\mu^{PT} = -i^3 \frac{N_c}{(2\pi)^4} \int d^4 p'_1 \frac{H'_P(iH''_T)}{N'_1 N''_1 N_2} S_{\mu\nu\lambda}^{PT} \varepsilon''^{\nu\lambda}, \quad (3.27)$$

where

$$S_{\mu\nu\lambda}^{PT} = S_{\mu\nu}^{PV}(-q + p'_1)_\lambda. \quad (3.28)$$

The contribution from the  $S_{\mu\nu}^{PV}(-q)_\lambda$  part is trivial, since  $q_\lambda$  can be taken out from the integration, which is already done in the  $P \rightarrow V$  case. Contributions from the  $\hat{S}_{\mu\nu}^{PV} \hat{p}'_{1\lambda}$  part can be worked out by using Eq. (3.14). In particular, the calculation of  $k(q^2)$  and  $b_-(q^2)$  needs to use the  $\hat{p}'_1 \hat{p}'_1 \hat{p}'_1 \hat{N}_2$  formula. Putting all these together leads to

$$\begin{aligned} h(q^2) &= -g(q^2) \Big|_{h''_V \rightarrow h''_T} + \frac{N_c}{16\pi^3} \int dx_2 d^2 p'_\perp \frac{2h'_P h''_T}{x_2 \hat{N}'_1 \hat{N}''_1} \left[ (m'_1 - m''_1)(A_3^{(2)} + A_4^{(2)}) \right. \\ &\quad \left. + (m''_1 + m'_1 - 2m_2)(A_2^{(2)} + A_3^{(2)}) - m'_1(A_1^{(1)} + A_2^{(1)}) + \frac{2}{w''_V}(2A_1^{(3)} + 2A_2^{(3)} - A_1^{(2)}) \right], \\ k(q^2) &= -f(q^2) \Big|_{h''_V \rightarrow h''_T} + \frac{N_c}{16\pi^3} \int dx_2 d^2 p'_\perp \frac{h'_P h''_T}{x_2 \hat{N}'_1 \hat{N}''_1} \left\{ 2(A_1^{(1)} + A_2^{(1)})[m_2(q^2 - \hat{N}'_1 - \hat{N}''_1 - m'^2_1 - m''^2_1) \right. \\ &\quad - m'_1(M'^2 - \hat{N}''_1 - m'^2_1 - m^2_2) - m''_1(M'^2 - \hat{N}'_1 - m'^2_1 - m^2_2) - 2m'_1 m''_1 m_2] \\ &\quad + 2(m'_1 + m''_1) \left( A_2^{(1)} Z_2 + \frac{q \cdot P}{q^2} A_1^{(2)} \right) + 16(m_2 - m'_1)(A_1^{(3)} + A_2^{(3)}) + 4(2m'_1 - m''_1 - m_2)A_1^{(2)} \\ &\quad + \frac{4}{w''_V} \left( [M'^2 + M''^2 - q^2 + 2(m'_1 - m_2)(m''_1 + m_2)](2A_1^{(3)} + 2A_2^{(3)} - A_1^{(2)}) \right. \\ &\quad \left. - 4 \left[ A_2^{(3)} Z_2 + \frac{q \cdot P}{3q^2} (A_1^{(2)})^2 \right] + 2A_1^{(2)} Z_2 \right\}, \\ b_+(q^2) &= -a_+(q^2) \Big|_{h''_V \rightarrow h''_T} + \frac{N_c}{16\pi^3} \int dx_2 d^2 p'_\perp \frac{h'_P h''_T}{x_2 \hat{N}'_1 \hat{N}''_1} \left\{ 8(m_2 - m'_1)(A_3^{(3)} + 2A_4^{(3)} + A_5^{(3)}) \right. \\ &\quad - 2m'_1(A_1^{(1)} + A_2^{(1)}) + 4(2m'_1 - m''_1 - m_2)(A_2^{(2)} + A_3^{(2)}) + 2(m'_1 + m''_1)(A_2^{(2)} + 2A_3^{(2)} + A_4^{(2)}) \\ &\quad + \frac{2}{w''_V} \left[ 2[M'^2 + M''^2 - q^2 + 2(m'_1 - m_2)(m''_1 + m_2)](A_3^{(3)} + 2A_4^{(3)} + A_5^{(3)} - A_2^{(2)} - A_3^{(2)}) \right. \\ &\quad \left. + [q^2 - \hat{N}'_1 - \hat{N}''_1 - (m'_1 + m''_1)^2](A_2^{(2)} + 2A_3^{(2)} + A_4^{(2)} - A_1^{(1)} - A_2^{(1)}) \right] \Big\}, \\ b_-(q^2) &= -a_-(q^2) \Big|_{h''_V \rightarrow h''_T} + \frac{N_c}{16\pi^3} \int dx_2 d^2 p'_\perp \frac{h'_P h''_T}{x_2 \hat{N}'_1 \hat{N}''_1} \left\{ 8(m_2 - m'_1)(A_4^{(3)} + 2A_5^{(3)} + A_6^{(3)}) \right. \\ &\quad - 6m'_1(A_1^{(1)} + A_2^{(1)}) + 4(2m'_1 - m''_1 - m_2)(A_3^{(2)} + A_4^{(2)}) \\ &\quad + 2(3m'_1 + m''_1 - 2m_2)(A_2^{(2)} + 2A_3^{(2)} + A_4^{(2)}) \\ &\quad + \frac{2}{w''_V} \left[ 2[M'^2 + M''^2 - q^2 + 2(m'_1 - m_2)(m''_1 + m_2)](A_4^{(3)} + 2A_5^{(3)} + A_6^{(3)} - A_3^{(2)} - A_4^{(2)}) \right. \\ &\quad \left. + [q^2 - \hat{N}'_1 - \hat{N}''_1 - (m'_1 + m''_1)^2](A_2^{(2)} + 2A_3^{(2)} + A_4^{(2)} - A_1^{(1)} - A_2^{(1)}) \right] \Big\}, \end{aligned}$$

$$\begin{aligned}
& +2Z_2(3A_4^{(2)}-2A_6^{(3)}-A_2^{(1)})+2\frac{q\cdot P}{q^2}\left(6A_2^{(1)}A_1^{(2)}-6A_2^{(1)}A_2^{(3)}+\frac{2}{q^2}(A_1^{(2)})^2-A_1^{(2)}\right) \\
& +[q^2-2M'^2+\hat{N}'_1-\hat{N}''_1-(m'_1+m''_1)^2+2(m'_1-m_2)^2] \\
& \times(A_2^{(2)}+2A_3^{(2)}+A_4^{(2)}-A_1^{(1)}-A_2^{(1)})\Bigg]\Bigg\}. \tag{3.29}
\end{aligned}$$

To summarize, equipped with the explicit expressions of the form factors  $f_+(q^2), f_-(q^2)$  [Eq. (B3)] for  $P \rightarrow P$  transitions,  $u_+(q^2), u_-(q^2)$  [Eq. (3.20)] for  $P \rightarrow S$  transitions,  $g(q^2), f(q^2), a_+(q^2), a_-(q^2)$  [Eq. (B4)] for  $P \rightarrow V$  transitions,  $\ell(q^2), q(q^2), c_+(q^2), c_-(q^2)$  [Eq. (3.26)] for  $P \rightarrow A$  transition and  $h(q^2), k(q^2), b_+(q^2), b_-(q^2)$  [Eq. (3.29)] for  $P \rightarrow T$  transitions, we are ready to perform numerical studies of them. The  $P \rightarrow S, A, T$  transition form factors are the main new results in this work.

## B. Comments on zero-mode effects

In the present paper we have followed and extended the work of Jaus [8] to the  $p$ -wave meson case. As stressed by Jaus, there are two classes of form factors and decay constants. There is one class of form factors like  $F_1(q^2)$  for transitions between pseudoscalar mesons,  $V(q^2)$  and  $A_2(q^2)$  for transitions between pseudoscalar and vector mesons, and the pseudoscalar decay constant  $f_P$  that are free of zero mode contributions. Another class of form factors like  $A_1(q^2)$  (or  $f(q^2)$ ) and the vector decay constant  $f_V$  are associated with zero modes. Jaus employed a simple multipole ansatz for the meson vertex function

$$H_M(p_1^2, p_2^2) = \frac{g}{(p_1^2 - \Lambda^2 + i\epsilon)^n} \tag{3.30}$$

as the starting point of his simple covariant toy model. Then the zero mode contributions can be systematically calculated in this toy model.

Note that the vertex function (3.30) is not symmetric in the four momenta of the constituent quarks and hence can hardly be considered a realistic approximation of the meson vertex. To remedy this difficulty, Bakker, Choi and Ji (BCJ) [9] proposed to replace the point gauge-boson vertex  $\gamma_\mu(1 - \gamma_5)$  by

$$\gamma_\mu(1 - \gamma_5) \rightarrow \frac{\Lambda_1^2}{p_1^2 - \Lambda_1^2 + i\epsilon} \gamma_\mu(1 - \gamma_5) \frac{\Lambda_2^2}{p_2^2 - \Lambda_2^2 + i\epsilon}. \tag{3.31}$$

It is easily seen that the two methods due to Jaus and BCJ should give the same result for form factors, but may lead to different results for decay constants. Contrary to the conclusion made by Jaus, BCJ claimed that in the symmetric gauge-boson vertex method, both the decay constant  $f_V$  and the form factor  $f(q^2)$  are free of zero mode contributions [9, 50]. Since  $f(q^2)$  is identical in both methods, it appears to us that the controversy about the role played by the zero mode lies in the fact Jaus and BCJ have a different approach for zero-mode effects. In the covariant light-front approach of Jaus [8], the decomposition of the current-induced matrix element into 4-vectors will require to introduce a lightlike 4-vector  $\tilde{\omega}$  which is not covariant. Zero modes are required to eliminate the spurious  $\tilde{\omega}$  dependence. BCJ decompose the propagator into on-shell and

instantaneous (not on-shell) parts and argue that only the latter part can be the origin of a zero mode contribution.

The covariant toy model cannot be generalized beyond the simple meson vertex given by (3.30), namely, there are some possible residual  $\tilde{\omega}$  contributions. In [27] Jaus has developed a method that permits the calculation of the contribution of zero modes associated with the current-induced matrix element. Through the study of the angular condition imposed on helicity amplitudes, several consistency conditions can be derived under some plausible assumptions and used to determine the zero mode contributions. Within this approach, both  $f_V$  and  $f(q^2)$  receive additional residual contributions (see Eqs. (3.16) and (3.9) of [27], respectively) which can be expressed in terms of  $B_n^{(m)}$  and  $C_n^{(m)}$  functions defined in Appendix B.<sup>6</sup> These functions depend on  $p_1^-$  and behavior like  $(p_1'^-)^i(p_1'^+)^j$ . Jaus then gave a counting rule for detecting zero modes [27]: For the  $B$  functions  $i \leq j$ , there is no zero mode contribution and the value of  $B_n^{(m)}$  can be calculated unambiguously at the spectator quark pole. For the  $C$  functions  $i \geq j+1$  and the value of  $C_n^{(m)}$  is the sum of a spectator quark pole term and an unknown zero mode contribution. These  $B$  and  $C$  functions vanish in the covariant toy model, as it should be. Beyond the toy model, the  $C$  functions contain unknown zero-mode contributions. Jaus used some consistency conditions to fix some of the  $C$  functions. Under this approach, Jaus has worked out a general expression for the decay constant  $f_V$ . Since the requirement that the vertex function has no poles in the upper complex  $p_1^-$  plane is not satisfied in the BCJ calculation of  $f_V$ , it is not clear if the BCJ result for  $f_V$  is a special case of the general result of Jaus [27] and hence a direct comparison between them cannot be made.

Several remarks are in order. (i) Our meson light-front vertex functions (2.11) are symmetric in quark momenta. However,  $B$  and  $C$  functions do not appear in  $f_V$  [Eq. (2.22)] and  $f(q^2)$  [Eq. (B4)] for two reasons. First of all, we have  $C_1^{(1)} \doteq 0$  from Eqs. (3.14) and (B9). Second, we contract  $\mathcal{A}_\mu^V$  [see Eq. (2.20)] and  $S_{\mu\nu}^{PV}$  [Eq. (3.22)] with the transverse polarization vector  $\epsilon^\mu(\pm)$ . We have checked explicitly that for the vertex functions given in (2.11), the coefficients  $B_j^{(i)}$  under integration (see Appendix B) are numerically almost vanishing and the form factor  $f(q^2)$  is affected at most at one percent level. For our purposes, we can therefore neglect all the residual contributions to the form factors. (ii) The derivation of the decay constant  $f_P$  and the form factors  $f_+(q^2), g(q^2), a_+(q^2), u_+(q^2), q(q^2), c_+(q^2)$ , and  $h(q^2), b_+(q^2)$  does not depend on  $\hat{N}_2$  and those relations connected to  $\hat{N}_2$  (see Eq. (3.14) and recall that  $\hat{N}_2 = Z_2 - C_1^{(1)}$ ). These form factors are free of zero mode effects and can be obtained using the conventional light-front approach. (iii) Zero mode effects vanish in the heavy quark limit (see Sec. IV). For example, the HQS relation  $f_P = f_V$  indicates that  $f_V$  is immune to the zero mode contribution.

---

<sup>6</sup> The remaining spurious  $\tilde{\omega}$  contribution to the form factor  $a_-(q^2)$  cannot be determined in the same manner.

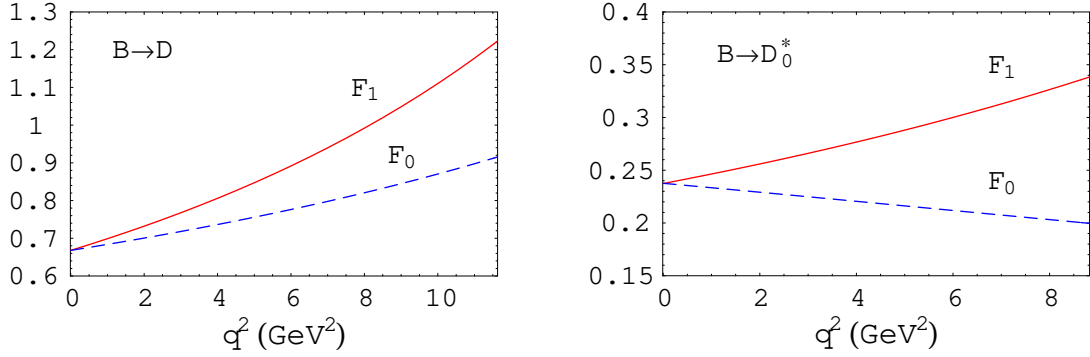


FIG. 2: Form factors  $F_1(q^2)$  and  $F_0(q^2)$  for  $B \rightarrow D$  and  $B \rightarrow D_0^*$  transitions.

### C. Form-factor momentum dependence and numerical results

Because of the condition  $q^+ = 0$  we have imposed during the course of calculation, form factors are known only for spacelike momentum transfer  $q^2 = -q_\perp^2 \leq 0$ , whereas only the timelike form factors are relevant for the physical decay processes. It has been proposed in [6] to recast the form factors as explicit functions of  $q^2$  in the spacelike region and then analytically continue them to the timelike region. Another approach is to construct a double spectral representation for form factors at  $q^2 < 0$  and then analytically continue it to  $q^2 > 0$  region [48]. It has been shown recently that, within a specific model, form factors obtained directly from the timelike region (with  $q^+ > 0$ ) are identical to the ones obtained by the analytic continuation from the spacelike region [50].

TABLE IV: Form factors of  $D \rightarrow \pi, \rho, a_0(1450), a_1(1260), b_1(1235), a_2(1320)$  transitions obtained in the covariant light-front model are fitted to the 3-parameter form Eq. (3.32) except for the form factor  $V_2$  denoted by \* for which the fit formula Eq. (3.33) is used. All the form factors are dimensionless except for  $h, b_+, b_-$  with dimensions  $\text{GeV}^{-2}$ . For the parameter  $\beta_T$  appearing in the tensor-meson wave function, we assume that it is the same as the  $\beta$  parameter of  $p$ -wave meson with the same quark content.

$F$	$F(0)$	$F(q_{\max}^2)$	$a$	$b$	$F$	$F(0)$	$F(q_{\max}^2)$	$a$	$b$
$F_1^{D\pi}$	0.67	2.71	1.19	0.36	$F_0^{D\pi}$	0.67	1.16	0.50	0.01
$V^{D\rho}$	0.86	1.36	1.24	0.48	$A_0^{D\rho}$	0.64	0.93	1.07	0.54
$A_1^{D\rho}$	0.58	0.71	0.51	0.03	$A_2^{D\rho}$	0.48	0.68	0.95	0.30
$F_1^{Da_0}$	0.52	0.54	1.07	0.26	$F_0^{Da_0}$	0.52	0.52	-0.08	0.03
$A^{Da_1}$	0.20	0.22	0.98	0.20	$V_0^{Da_1}$	0.31	0.34	0.85	0.49
$V_1^{Da_1}$	1.54	1.53	-0.05	0.05	$V_2^{Da_1}$	0.06	0.06	0.12	0.10
$A^{Db_1}$	0.11	0.13	1.08	0.54	$V_0^{Db_1}$	0.49	0.54	0.89	0.28
$V_1^{Db_1}$	1.37	1.45	0.46	0.05	$V_2^{Db_1}$	-0.10*	-0.11*	0.21*	0.67*
$h$	0.188	0.208	1.21	1.09	$k$	0.340	0.338	-0.07	0.12
$b_+$	-0.084	-0.091	0.97	0.58	$b_-$	0.120	0.133	1.15	0.66

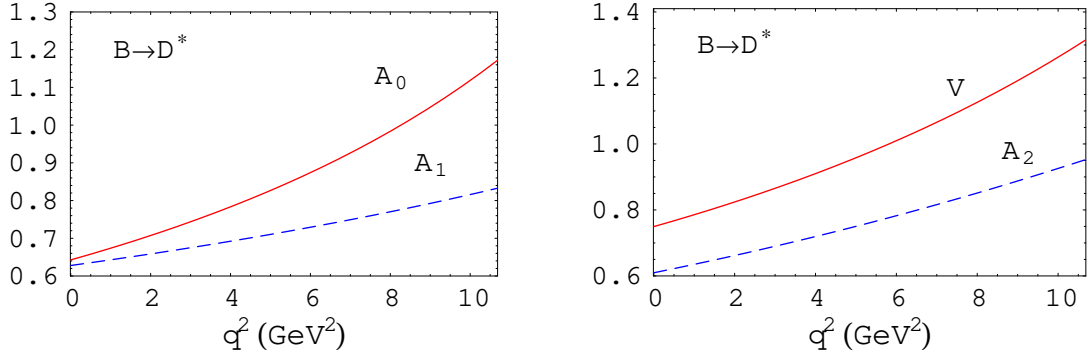


FIG. 3: Form factors  $V(q^2)$ ,  $A_0(q^2)$ ,  $A_1(q^2)$  and  $A_2(q^2)$  for  $B \rightarrow D^*$  transitions.

In principle, form factors at  $q^2 > 0$  can be evaluated directly in the frame where the momentum transfer is purely longitudinal, i.e.,  $q_\perp = 0$ , so that  $q^2 = q^+ q^-$  covers the entire range of momentum transfer [7]. The price one has to pay is that, besides the conventional valence-quark contribution, one must also consider the non-valence configuration (or the so-called  $Z$ -graph) arising from quark-pair creation from the vacuum. However, a reliable way of estimating the  $Z$ -graph contribution is still lacking unless one works in a specific model, for example, the one advocated in [50]. Fortunately, this additional non-valence contribution vanishes in the frame where the momentum transfer is purely transverse i.e.,  $q^+ = 0$ .

To proceed we find that except for the form factor  $V_2$  to be discussed below, the momentum dependence of form factors in the spacelike region can be well parameterized and reproduced in the three-parameter form:

$$F(q^2) = \frac{F(0)}{1 - a(q^2/m_{B(D)}^2) + b(q^2/m_{B(D)}^2)^2}, \quad (3.32)$$

for  $B(D) \rightarrow M$  transitions. The parameters  $a$ ,  $b$  and  $F(0)$  are first determined in the spacelike

TABLE V: Same as Table IV except for  $D \rightarrow K, K^*, K_0^*(1430), K_{1P_1}, K_{3P_1}, K_2^*(1430)$  transitions.

$F$	$F(0)$	$F(q_{\max}^2)$	$a$	$b$	$F$	$F(0)$	$F(q_{\max}^2)$	$a$	$b$
$F_1^{DK}$	0.78	1.57	1.05	0.23	$F_0^{DK}$	0.78	0.99	0.38	0.00
$V^{DK^*}$	0.94	1.33	1.17	0.42	$A_0^{DK^*}$	0.69	0.92	1.04	0.44
$A_1^{DK^*}$	0.65	0.75	0.50	0.02	$A_2^{DK^*}$	0.57	0.75	0.94	0.27
$F_1^{DK_0^*}$	0.48	0.51	1.01	0.24	$F_0^{DK_0^*}$	0.48	0.50	-0.11	0.02
$A^{DK_{1P_1}}$	0.10	0.11	1.03	0.48	$V_0^{DK_{1P_1}}$	0.44	0.47	0.80	0.27
$V_1^{DK_{1P_1}}$	1.53	1.58	0.39	0.05	$V_2^{DK_{1P_1}}$	-0.09*	-0.09*	-0.16*	0.51*
$A^{DK_{3P_1}}$	0.98	1.05	0.92	0.17	$V_0^{DK_{3P_1}}$	0.34	0.38	1.44	0.15
$V_1^{DK_{3P_1}}$	2.02	2.02	-0.01	0.03	$V_2^{DK_{3P_1}}$	0.03	0.03	-0.18	0.10
$h$	0.192	0.205	1.17	0.99	$k$	0.368	0.367	-0.04	0.11
$b_+$	-0.096	-0.102	1.05	0.58	$b_-$	0.137	0.147	1.17	0.69

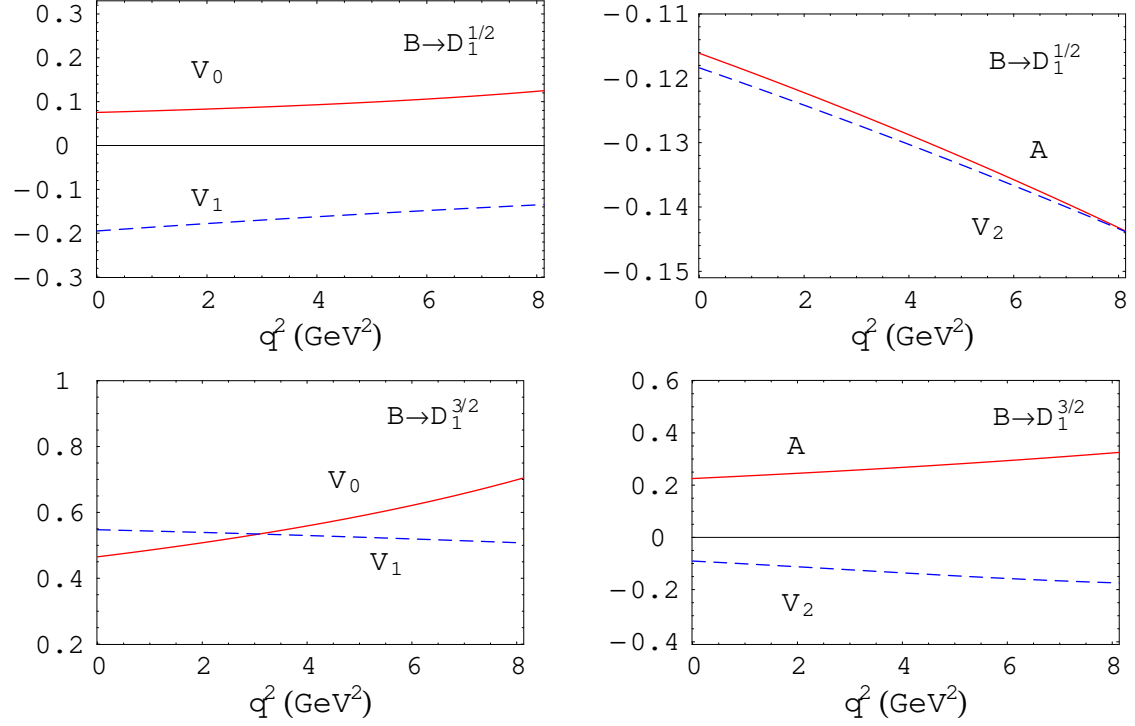


FIG. 4: Form factors  $A(q^2)$ ,  $V_0(q^2)$ ,  $V_1(q^2)$  and  $V_2(q^2)$  for  $B \rightarrow D_1^{1/2,3/2}$  transitions.

region. We then employ this parametrization to determine the physical form factors at  $q^2 \geq 0$ . In practice, the parameters  $a, b$  and  $F(0)$  are obtained by performing a 3-parameter fit to the form factors in the range  $-20 \text{ GeV}^2 \leq q^2 \leq 0$  for  $B$  decays and  $-10 \text{ GeV}^2 \leq q^2 \leq 0$  for  $D$  decays. These parameters are generally insensitive to the  $q^2$  range to be fitted except for the form factor  $V_2(q^2)$  in  $B(D) \rightarrow {}^1P_1, {}^3P_1^{3/2}$  transitions. The corresponding parameters  $a$  and  $b$  are rather sensitive to the

TABLE VI: Same as Table IV except for  $B \rightarrow \pi, \rho, a_0(1450), a_1(1260), b_1(1235), a_2(1320)$  transitions.

$F$	$F(0)$	$F(q^2_{\max})$	$a$	$b$	$F$	$F(0)$	$F(q^2_{\max})$	$a$	$b$
$F_1^{B\pi}$	0.25	1.16	1.73	0.95	$F_0^{B\pi}$	0.25	0.86	0.84	0.10
$V^{B\rho}$	0.27	0.79	1.84	1.28	$A_0^{B\rho}$	0.28	0.76	1.73	1.20
$A_1^{B\rho}$	0.22	0.53	0.95	0.21	$A_2^{B\rho}$	0.20	0.57	1.65	1.05
$F_1^{Ba_0}$	0.26	0.68	1.57	0.70	$F_0^{Ba_0}$	0.26	0.35	0.55	0.03
$A^{Ba_1}$	0.25	0.76	1.51	0.64	$V_0^{Ba_1}$	0.13	0.32	1.71	1.23
$V_1^{Ba_1}$	0.37	0.42	0.29	0.14	$V_2^{Ba_1}$	0.18	0.36	1.14	0.49
$A^{Bb_1}$	0.10	0.23	1.92	1.62	$V_0^{Bb_1}$	0.39	0.98	1.41	0.66
$V_1^{Bb_1}$	0.18	0.36	1.03	0.32	$V_2^{Bb_1}$	-0.03*	-0.15*	2.13*	2.39*
$h$	0.008	0.015	2.20	2.30	$k$	0.031	0.010	-2.47	2.47
$b_+$	-0.005	-0.011	1.95	1.80	$b_-$	0.0016	0.0011	-0.23	1.18

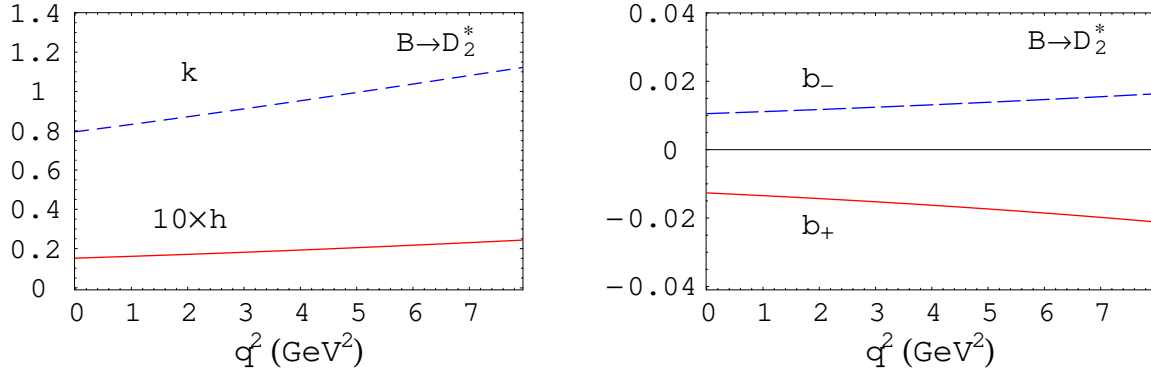


FIG. 5: Form factors  $k(q^2)$ ,  $h(q^2)$ ,  $b_+(q^2)$  and  $b_-(q^2)$  for  $B \rightarrow D_2^*$  transitions. Except for the dimensionless  $k(q^2)$ , all other form factors are in units of  $\text{GeV}^{-2}$ .

TABLE VII: Same as Table IV except for  $B \rightarrow K, K^*, K_0^*(1430), K_{1P_1}, K_{3P_1}, K_2^*(1430)$  transitions.

$F$	$F(0)$	$F(q_{\max}^2)$	$a$	$b$	$F$	$F(0)$	$F(q_{\max}^2)$	$a$	$b$
$F_1^{BK}$	0.35	2.17	1.58	0.68	$F_0^{BK}$	0.35	0.80	0.71	0.04
$V^{BK^*}$	0.31	0.96	1.79	1.18	$A_0^{BK^*}$	0.31	0.87	1.68	1.08
$A_1^{BK^*}$	0.26	0.58	0.93	0.19	$A_2^{BK^*}$	0.24	0.70	1.63	0.98
$F_1^{BK_0^*}$	0.26	0.70	1.52	0.64	$F_0^{BK_0^*}$	0.26	0.33	0.44	0.05
$A^{BK_{3P_1}}$	0.26	0.69	1.47	0.59	$V_0^{BK_{3P_1}}$	0.14	0.31	1.62	1.14
$V_1^{BK_{3P_1}}$	0.39	0.42	0.21	0.16	$V_2^{BK_{3P_1}}$	0.17	0.30	1.02	0.45
$A^{BK_{1P_1}}$	0.11	0.25	1.88	1.53	$V_0^{BK_{1P_1}}$	0.41	0.99	1.40	0.64
$V_1^{BK_{1P_1}}$	0.19	0.35	0.96	0.30	$V_2^{BK_{1P_1}}$	-0.05*	-0.16*	1.78*	2.12*
$h$	0.008	0.018	2.17	2.22	$k$	0.015	0.004	-3.70	1.78
$b_+$	-0.006	-0.013	1.96	1.79	$b_-$	0.002	0.002	0.38	0.92

chosen range for  $q^2$ . This sensitivity is attributed to the fact that the form factor  $V_2(q^2)$  approaches to zero at very large  $-|q^2|$  where the three-parameter parametrization (3.32) becomes questionable. To overcome this difficulty, we will fit this form factor to the form

$$F(q^2) = \frac{F(0)}{(1 - q^2/m_{B(D)}^2)[1 - a(q^2/m_{B(D)}^2) + b(q^2/m_{B(D)}^2)^2]} \quad (3.33)$$

and achieve a substantial improvement. For example, we have  $a = 2.18$  and  $b = 6.08$  when  $V_2^{BK_{1P_1}}$  is fitted to Eq. (3.32) and they become  $a = 1.78$  and  $b = 2.12$  (see Table VII) when the fit formula Eq. (3.33) is employed.

In Tables IV–VIII we show the form factors and their  $q^2$  dependence for the transitions  $B(D) \rightarrow \pi, \rho, a_0(1450), a_1(1260), b_1(1235), a_2(1320)$ ,  $B(D) \rightarrow K, K^*, K_0^*(1430), K_{1P_1}, K_{3P_1}, K_2^*(1430)$  and  $B \rightarrow D, D^*, D_0^*(2308), D_1^{1/2}, D_1^{3/2}, D_2^*(2460)$ . The  $b \rightarrow c$  transition form factors are plotted in Figs. 2–5. Because the quark contents of the  $f_0, f_1, f_2$  mesons lying in the mass region of  $1.3 - 1.7$  GeV are not well established, we will not consider them in this work. In calculations, we have taken

TABLE VIII: Same as Table IV except for  $B \rightarrow D, D^*, D_0^*, D_1^{1/2}, D_1^{3/2}, D_2^*$  transitions. For the purpose of comparing with heavy quark symmetry, the form factors  $u_{\pm}, c_{\pm}, \ell, q$  are also shown.

$F$	$F(0)$	$F(q_{\max}^2)$	$a$	$b$	$F$	$F(0)$	$F(q_{\max}^2)$	$a$	$b$
$F_1^{BD}$	0.67	1.22	1.25	0.39	$F_0^{BD}$	0.67	0.92	0.65	0.00
$V^{BD*}$	0.75	1.32	1.29	0.45	$A_0^{BD*}$	0.64	1.17	1.30	0.31
$A_1^{BD*}$	0.63	0.83	0.65	0.02	$A_2^{BD*}$	0.61	0.95	1.14	0.52
$F_1^{BD_0^*}$	0.24	0.34	1.03	0.27	$F_0^{BD_0^*}$	0.24	0.20	-0.49	0.35
$A^{BD_1^{1/2}}$	-0.12	-0.14	0.71	0.18	$V_0^{BD_1^{1/2}}$	0.08	0.13	1.28	-0.29
$V_1^{BD_1^{1/2}}$	-0.19	-0.13	-1.25	0.97	$V_2^{BD_1^{1/2}}$	-0.12	-0.14	0.67	0.20
$A^{BD_1^{3/2}}$	0.23	0.33	1.17	0.39	$V_0^{BD_1^{3/2}}$	0.47	0.70	1.17	0.03
$V_1^{BD_1^{3/2}}$	0.55	0.51	-0.19	0.27	$V_2^{BD_1^{3/2}}$	-0.09*	-0.17*	2.14*	4.21*
$u_+$	-0.24	-0.34	1.03	0.27	$u_-$	0.31	0.42	0.86	0.20
$\ell_{1/2}$	0.56	0.38	-1.25	0.97	$q_{1/2}$	0.041	0.050	0.71	0.18
$c_+^{1/2}$	-0.042	-0.050	0.67	0.20	$c_-^{1/2}$	0.045	0.055	0.71	0.20
$\ell_{3/2}$	-1.56	-1.45	-0.19	0.27	$q_{3/2}$	-0.079	-0.114	1.17	0.39
$c_+^{3/2}$	-0.032*	-0.061*	2.14*	4.21*	$c_-^{3/2}$	-0.027	-0.026	0.03	0.45
$h$	0.015	0.024	1.67	1.20	$k$	0.79	1.12	1.29	0.93
$b_+$	-0.013	-0.021	1.68	0.98	$b_-$	0.011	0.016	1.50	0.91

the meson masses from [16]. The masses of  $D_0^*$  and  $D_1$  have been measured recently by Belle to be  $2308 \pm 17 \pm 15 \pm 28$  MeV and  $2427 \pm 26 \pm 20 \pm 15$  MeV, respectively [15]. Since  $D_1(2427)$  and  $D'_1(2420)$  are almost degenerate, we shall take  $m_{D_1^{1/2}} \approx m_{D_1^{3/2}} \approx 2427$  MeV.

Several remarks are in order:

1. Many form factors contain terms like  $(p'_\perp \cdot q_\perp)/q^2$  in their integrands. At first sight, it appears that linear  $p'_\perp$  terms will not make contributions after integrating over  $p'_\perp$ . But this is not the case. As noted before, a Taylor expansion of the  $h''_M/\hat{N}_1''$  term with respect to  $p''_\perp^2$  will generate a term proportional to  $p'_\perp \cdot q_\perp$  [cf. Eq. (3.23)]. When combined with the  $(p'_\perp \cdot q_\perp)/q^2$  term in the integrand of transition form factors, this leads to

$$\int d^2 p'_\perp \frac{(p'_\perp \cdot q_\perp)^2}{q^2} = -\frac{1}{2} \int d^2 p'_\perp p''_\perp^2 \quad (3.34)$$

in the  $q^+ = 0$  frame. In analytic studies, however, it is more convenient to utilize the identity obtained in [8]

$$\int dx_2 d^2 p'_\perp \frac{h'_P h''_M}{x_2 \hat{N}'_1 \hat{N}''_1} 2B_1^{(2)} = \int dx_2 d^2 p'_\perp \frac{h'_P h''_M}{x_2 \hat{N}'_1 \hat{N}''_1} (x_1 Z_2 - 2A_1^{(2)}) = 0. \quad (3.35)$$

Using the expressions of  $Z_2$  and  $A_1^{(2)}$  given in Eq. (B9), it is easily seen that the  $(p'_\perp \cdot q_\perp)/q^2$  term under integration can be related to other  $q$ -independent quantities. The above identity allows us to integrate out the  $p'_\perp \cdot q_\perp$  term without explicitly performing the Taylor expansion

of  $h''_M/\hat{N}_1''$ . Instead of using Eq. (3.34) or (3.35) we have taken into account such effects in numerical calculations by substituting the relation  $p''_\perp = p'_\perp - x_2 q_\perp$  into  $h''_M/\hat{N}_1''$ .

- Owing to the less energy release, form factors for  $D \rightarrow \pi, \rho, \dots$  and  $D \rightarrow K, K^*, K^{**}$  transitions are more sensitive to the masses of charmed and light quarks. For this we can utilize the form-factor ratios  $r_V \equiv V^{DK^*}(0)/A_1^{DK^*}(0)$  and  $r_2 \equiv A_2^{DK^*}(0)/A_1^{DK^*}(0)$  measured in  $D \rightarrow K^* \ell \bar{\nu}$  decays to constrain the quark masses. The most recent and most precise measurement by FOCUS yields [49]

$$r_V = 1.504 \pm 0.057 \pm 0.039, \quad r_2 = 0.875 \pm 0.049 \pm 0.064. \quad (3.36)$$

The best quark masses  $m_u, m_s$  and  $m_c$  obtained in this manner are listed in Eq. (2.24).

- In the absence of any information for the parameter  $\beta_T$  appearing in the wave function of tensor mesons, we have taken  $\beta_T$  to be the same as the  $\beta$  parameter of the  $p$ -wave meson with the same quark content, for example,  $\beta(D_2^*) = \beta(D_0^*) = 0.331$ . Note that among the four  $P \rightarrow T$  transition form factors, the one  $k(q^2)$  is particularly sensitive to  $\beta_T$ . It is not clear to us if the complicated analytic expression for  $k(q^2)$  in Eq. (3.29) is not complete. To overcome this difficulty, we apply the heavy quark symmetry relations in Eq. (4.4) below to obtain  $k(q^2)$  for  $B \rightarrow D_2^*$  transition

$$k(q^2) = m_B m_{D_2^*} \left( 1 + \frac{m_B^2 + m_{D_2^*}^2 - q^2}{2m_B m_{D_2^*}} \right) \left[ h(q^2) - \frac{1}{2} b_+(q^2) + \frac{1}{2} b_-(q^2) \right]. \quad (3.37)$$

This can be tested in  $B^- \rightarrow D_2^{*0} \pi^-$  decays to be discussed below in Sec. III.E.

- For heavy-to-heavy transitions such as  $B \rightarrow D, D^*, D^{**}$ , the sign of various form factors can be checked by heavy quark symmetry. In the heavy quark limit, heavy quark symmetry requires that the form factors  $u_-, \ell_{1/2}, q_{1/2}, c_-^{1/2}, h, k$  and  $b_-$  be positive, while  $u_+, \ell_{3/2}, q_{3/2}, c_+^{1/2}, c_+^{3/2}, c_-^{3/2}$  and  $b_+$  be negative [see Eqs. (4.3)–(4.5)]. Our results are indeed in accordance with HQS (see Table VIII).
- For  $P \rightarrow A$  transitions, the form factor  $V_0$  is always positive, while the sign of other form factors  $A, V_1, V_2$  depends on the process under consideration, for example, they are all positive in  $B(D) \rightarrow a_1, K_{3P_1}$  transitions and negative in  $B \rightarrow D_1$  transitions.
- The form factors of  $B$  to light axial-vector meson transitions obey the relations  $V_0^{Ba_1} < A_0^{B\rho} < V_0^{Bb_1}$  and  $V_0^{BK_{3P_1}} < A_0^{BK^*} < V_0^{BK_{1P_1}}$ .
- It is pointed out in [7] that for  $B \rightarrow D, D^*$  transitions, the form factors  $F_1, A_0, A_2, V$  exhibit a dipole behavior, while  $F_0$  and  $A_1$  show a monopole dependence. According to the three-parameter parametrization (3.32), the dipole behavior corresponds to  $b = (a/2)^2$ , while  $b = 0$  and  $a \neq 0$  induces a monopole dependence. An inspection of Tables IV–VIII indicates that form factors  $F_0^{BD}, A_1^{BD^*}, F_0^{BK}, F_0^{Ba_0}$  and  $F_0^{DK(\pi)}$  have a monopole behavior, while  $F_1^{BD}, V^{BD^*}, A^{BD_1^{3/2}}, F_1^{B(D)K}, A^{B(D)K_{3P_1}}, V_0^{BK_{1P_1}}, F_1^{B(D)a_0}$  and  $F_1^{DK_0^*}$  have a dipole dependence.

TABLE IX: Form factors of  $D \rightarrow \pi, \rho, K, K^*$  transitions at  $q^2 = 0$  in various models.

Model	$F_{1,0}^{D\pi}(0)$	$A_0^{D\rho}(0)$	$A_1^{D\rho}(0)$	$A_2^{D\rho}(0)$	$V^{D\rho}(0)$	$F_{1,0}^{DK}(0)$	$A_0^{DK^*}(0)$	$A_1^{DK^*}(0)$	$A_2^{DK^*}(0)$	$V^{DK^*}(0)$
This work	0.67	0.64	0.58	0.48	0.86	0.78	0.69	0.65	0.57	0.94
MS [51]	0.69	0.66	0.59	0.49	0.90	0.78	0.76	0.66	0.49	1.03
QSR [53]	0.5	0.6	0.5	0.4	1.0	0.6	0.4	0.5	0.6	1.1
BSW [46]	0.69	0.67	0.78	0.92	1.23	0.76	0.73	0.88	1.15	1.23

8. In the heavy quark limit,  $F_1^{BD_0^*}(q^2) = F_0^{BD_0^*}/[1 - q^2/(m_B - m_{D_0^*})^2]$ , while  $F_1^{BD}(q^2) = F_0^{BD}/[1 - q^2/(m_B + m_D)^2]$  (see Eqs. (4.6) and (4.7)). This explains why  $F_1$  and  $F_0$  in the  $B \rightarrow D_0^*$  transition deviate at large  $q^2$  faster than that in the  $B \rightarrow D$  case (Fig. 2).
9. Unlike the form factor  $F_0$  in  $P \rightarrow a_0, K_0^*$  transitions which is almost flat in its  $q^2$  behavior,  $F_0^{BD_0^*}$  is decreasing with  $q^2$  as it must approach to zero at the maximum  $q^2$  when  $m_Q \rightarrow \infty$  [see Eq. (4.7)]. In general, form factors for  $P \rightarrow S$  transitions increase slowly with  $q^2$  compared to that for  $P \rightarrow P$  ones. For example,  $F^{Ba_0}(0) \sim F^{B\pi}(0)$  at  $q^2 = 0$ , while at zero recoil  $F^{Ba_0}(q_{\max}^2) \ll F^{B\pi}(q_{\max}^2)$ . Note that the form factors of  $B \rightarrow a_0$  or  $B \rightarrow K_0^*$  are similar to that of  $B \rightarrow \pi$  or  $B \rightarrow K$  at  $q^2 = 0$ , while  $F_{1,0}^{BD_0^*}(0) \ll F_{1,0}^{BD}(0)$ . This can be understood from the fact that  $P \rightarrow S$  form factors are the same as  $P \rightarrow P$  ones except for the replacement of  $m_1'' \rightarrow -m_1''$  and  $h_P'' \rightarrow -h_S''$  [see Eq. (3.20)]. Consequently, the  $\mathcal{A}''$  term in Eq. (3.16) is subject to more suppression in heavy-to-heavy transitions than in heavy-to-light ones. We shall see in Sec. III.E that the suppression of the  $B \rightarrow D_0^*$  form factor relative to the  $B \rightarrow D$  one is supported by experiment.
10. To determine the physical form factors for  $B(D) \rightarrow K_1(1270), K_1(1400)$ ,  $B \rightarrow D_1(2427), D_1(2420), D_{s1}(2460), D_{s1}(2536)$  transitions, one needs to know the mixing angles of  ${}^1P_1 - {}^3P_1$  [see Eq. (2.26)] and  $D_1^{1/2} - D_1^{3/2}$ . As noted in passing, the mixing angle for  $K_1$  systems is about  $-58^\circ$  as implied from the study of  $D \rightarrow K_1(1270)\pi$ .  $K_1(1400)\pi$  decays [45]. A mixing angle  $\theta_{D_1} = (5.7 \pm 2.4)^\circ$  is obtained by Belle through a detailed  $B \rightarrow D^*\pi\pi$  analysis [15], while  $\theta_{D_{s1}} \approx 7^\circ$  is determined from the quark potential model [38] as the present upper limits on the widths of  $D_{s1}(2460)$  and  $D'_{s1}(2536)$  do not provide any constraints on the  $D_{s1}^{1/2} - D_{s1}^{3/2}$  mixing angle.

#### D. Comparison with other model calculations

It is useful to compare our results based on the covariant light-front model with other theoretical calculations. Except for the Isgur-Scora-Grinstein-Wise (ISGW) quark model [17], all the existing studies on mesonic form factors focus mainly on the ground-state  $s$ -wave to  $s$ -wave transitions. For  $P \rightarrow P, V$  form factors we choose the BSW model [46], the Melikhov-Stech (MS) model [51] and light-cone sum rules [52] for comparison. Shown in Tables IX–XI are  $(D, B) \rightarrow \pi, \rho, K, K^*, D, D^*$  transition form factors calculated in various models. We see that the covariant light-front model

TABLE X: Form factors of  $B \rightarrow \pi, \rho, K, K^*$  transitions at  $q^2 = 0$  in various models.

Model	$F_{1,0}^{B\pi}(0)$	$A_0^{B\rho}(0)$	$A_1^{B\rho}(0)$	$A_2^{B\rho}(0)$	$V^{B\rho}(0)$	$F_{1,0}^{BK}(0)$	$A_0^{BK^*}(0)$	$A_1^{BK^*}(0)$	$A_2^{BK^*}(0)$	$V^{BK^*}(0)$
This work	0.25	0.28	0.22	0.20	0.27	0.35	0.31	0.26	0.24	0.31
MS [51]	0.29	0.29	0.26	0.24	0.31	0.36	0.45	0.36	0.32	0.44
LCSR [52]	0.26	0.37	0.26	0.22	0.34	0.34	0.47	0.34	0.28	0.46
BSW [46]	0.33	0.28	0.28	0.28	0.33	0.38	0.32	0.33	0.33	0.37

 TABLE XI: Form factors of  $B \rightarrow D, D^*$  transitions at  $q^2 = 0$  in various models.

Model	$F_{1,0}^{BD}(0)$	$A_0^{BD^*}(0)$	$A_1^{BD^*}(0)$	$A_2^{BD^*}(0)$	$V^{BD^*}(0)$
This work	0.67	0.64	0.63	0.62	0.75
MS [51]	0.67	0.69	0.66	0.62	0.76
BSW [46]	0.69	0.62	0.65	0.69	0.71

predictions are most close to that of the MS model except for  $B \rightarrow K^*$  transitions.

*ISGW model :*

Before our work, the ISGW quark model [17] is the only model that can provide a systematical estimate of the transition of a ground-state  $s$ -wave meson to a low-lying  $p$ -wave meson. However, this model is based on the non-relativistic constituent quark picture. In general, the form factors evaluated in the original version of the ISGW model are reliable only at  $q^2 = q_m^2$ , the maximum

 TABLE XII: Form factors of  $B \rightarrow D^{**}$  transitions calculated in the ISGW2 model.

$F$	$F(0)$	$F(q_{\max}^2)$	$a$	$b$	$F$	$F(0)$	$F(q_{\max}^2)$	$a$	$b$
$F_1^{BD_0^*}$	0.18	0.24	0.28	0.25	$F_0^{BD_0^*}$	0.18	-0.008	-	-
$A_0^{BD_1^{1/2}}$	-0.16	-0.21	0.87	0.24	$V_0^{BD_1^{1/2}}$	0.18	0.23	0.89	0.25
$V_1^{BD_1^{1/2}}$	-0.19	0.006	-	-	$V_2^{BD_1^{1/2}}$	-0.18	-0.24	0.87	0.24
$A_0^{BD_1^{3/2}}$	0.16	0.19	0.46	0.065	$V_0^{BD_1^{3/2}}$	0.43	0.51	0.54	0.074
$V_1^{BD_1^{3/2}}$	0.40	0.32	-0.60	1.15	$V_2^{BD_1^{3/2}}$	-0.12	-0.19	1.45	0.83
$u_+$	-0.18	-0.24	0.88	0.25	$u_-$	0.46	0.62	0.87	0.25
$\ell_{1/2}$	0.54	-0.016	-	-	$q_{1/2}$	0.057	0.074	0.87	0.24
$c_+^{1/2}$	-0.064	-0.083	0.87	0.24	$c_-^{1/2}$	0.068	0.088	0.87	0.24
$\ell_{3/2}$	-1.15	-0.90	-0.60	1.15	$q_{3/2}$	-0.057	-0.066	0.46	0.065
$c_+^{3/2}$	-0.043	-0.066	1.45	0.83	$c_-^{3/2}$	-0.018	-0.013	0.23	5.38
$h$	0.011	0.014	0.86	0.23	$k$	0.60	0.68	0.40	0.68
$b_+$	-0.010	-0.013	0.86	0.23	$b_-$	0.010	0.013	0.86	0.23

momentum transfer. The reason is that the form-factor  $q^2$  dependence in the ISGW model is proportional to  $\exp[-(q_m^2 - q^2)]$  and hence the form factor decreases exponentially as a function of  $(q_m^2 - q^2)$ . This has been improved in the ISGW2 model [30] in which the form factor has a more realistic behavior at large  $(q_m^2 - q^2)$  which is expressed in terms of a certain polynomial term. In addition to the form-factor momentum dependence, the ISGW2 model incorporates a number of improvements, such as the constraints imposed by heavy quark symmetry, hyperfine distortions of wave functions,  $\dots$ , etc. [30].

The ISGW2 model predictions for  $B \rightarrow D^{**}$  transition form factors are shown in Table XII. Note that form factors  $F_0^{BD_0^*}(q^2)$ ,  $V_1^{BD_1^{1/2}}(q^2)$  (or  $\ell_{1/2}(q^2)$ ) cannot be parameterized in the form of (3.32) or (3.33) since they vanish at certain  $q^2$ , e.g. around  $q^2 \approx 8 \text{ GeV}^2$  for  $V_1^{BD_1^{1/2}}(q^2)$ . We see from the comparison of Table XII with Table VIII that (i) the form factors at small  $q^2$  obtained in the covariant light-front and ISGW2 models agree within 40%, and (ii) as  $q^2$  increases,  $F_1^{BD_0^*}(q^2)$ ,  $A^{BD_1^{3/2}}(q^2)$ ,  $V_0^{BD_1^{3/2}}(q^2)$ ,  $h(q^2)$ ,  $|b_+(q^2)|$  and  $b_-(q^2)$  increase more rapidly in the LF model than those in the ISGW2 model, whereas  $F_0^{BD_0^*}(q^2)$  and  $|V_1^{BD_1^{1/2}}(q^2)|$  decrease more sharply in the latter model so that they even flip a sign near the zero recoil point.

The fact that both LF and ISGW2 models have similar  $B \rightarrow D^{**}$  form factors at small  $q^2$  implies that relativistic effects could be mild in  $B \rightarrow D^{**}$  transitions. Nevertheless, relativistic effects may manifest in heavy-to-light transitions, especially at the maximum recoil. An example is provided shortly below.

*Others :*

Based on the light-cone sum rules, Chernyak [36] has estimated the  $B \rightarrow a_0(1450)$  transition form factor and obtained  $F_{1,0}^{Ba_0}(0) = 0.46$ , while our result is 0.26 and is similar to the  $B \rightarrow \pi$  form factor at  $q^2 = 0$ . For  $B \rightarrow a_1(1260)$  form factors, there are two existing calculations: one in a quark-meson model (CQM) [54] and the other based on the QCD sum rule (QSR) [55]. The results are quite different, for example,  $V_0^{Ba_1}(0)$  obtained in the quark-meson model, 1.20, is larger than the sum-rule prediction,  $-0.23 \pm 0.05$ , by a factor of five apart from a sign difference. Predictions in various models are summarized in Table XIII. If  $a_1(1260)$  behaves as the scalar partner of the  $\rho$  meson, it is expected that  $V_0^{Ba_1}$  is similar to  $A_0^{B\rho}$ . Therefore, it appears to us that a magnitude of

TABLE XIII:  $B \rightarrow a_1(1260)$  transition form factors at  $q^2 = 0$  in various models. The results of CQM and QSR have been rescaled according to the form-factor definition in Eq. (3.6).

Model	$A^{Ba_1}(0)$	$V_0^{Ba_1}(0)$	$V_1^{Ba_1}(0)$	$V_2^{Ba_1}(0)$
This work	0.25	0.13	0.37	0.18
ISGW2 [30]	0.21	1.01	0.54	-0.05
CQM [54]	0.09	1.20	1.32	0.34
QSR [55]	$-0.41 \pm 0.06$	$-0.23 \pm 0.05$	$-0.68 \pm 0.08$	$-0.33 \pm 0.03$

order unity for  $V_0^{Ba_1}(0)$  as predicted by the ISGW2 model and CQM is very unlikely. Notice that the sign of the form factors predicted by QSR is opposite to ours. In hadronic  $B \rightarrow a_1 P$  decays, the relevant form factors are  $V_0^{Ba_1}$  and  $F_1^{BP}$  under the factorization approximation. Presumably, the measurement of  $\bar{B}^0 \rightarrow a_1^+ \pi^-$  will enable us to test  $V_0^{Ba_1}$ .

### E. Comparison with experiment

There are several experimentally measured decay modes, namely,  $B \rightarrow \bar{D}D_s^{**}$  and  $B^- \rightarrow D^{**}\pi^-$  decays, which allow to test our model calculations of decay constants and form factors for  $p$ -wave charmed mesons  $D^{**}$  and  $D_s^{**}$ .

For  $\bar{B} \rightarrow \bar{D}D_s^{**}$  decays, they proceed only via external  $W$ -emission and hence can be used to determine the decay constant of  $D_s^{**}$ . More precisely, their factorizable amplitudes are simply given by

$$A(\bar{B} \rightarrow \bar{D}D_s^{**}) = \frac{G_F}{\sqrt{2}} V_{cb} V_{cs}^* a_1 \langle \bar{D}_s^{**} | (\bar{s}c) | 0 \rangle \langle D | (\bar{c}b) | \bar{B} \rangle, \quad (3.38)$$

where  $(\bar{q}_1 q_2) \equiv \bar{q}_1 \gamma_\mu (1 - \gamma_5) q_2$  and  $a_1$  is a parameter of order unity. The recent Belle measurements read [37]

$$\begin{aligned} \mathcal{B}[B \rightarrow \bar{D}D_{s0}^*(2317)] \mathcal{B}[D_{s0}^*(2317) \rightarrow D_s \pi^0] &= (8.5_{-1.9}^{+2.1} \pm 2.6) \times 10^{-4}, \\ \mathcal{B}[B \rightarrow \bar{D}D_{s1}(2460)] \mathcal{B}[D_{s1}(2460) \rightarrow D_s^* \pi^0] &= (17.8_{-3.9}^{+4.5} \pm 5.3) \times 10^{-4}. \end{aligned} \quad (3.39)$$

The  $D_{s0}^*(2317)$  width is dominated by its hadronic decay to  $D_s \pi^0$  as the upper limit on the ratio  $\Gamma(D_{s0}^* \rightarrow D_s^* \gamma) / \Gamma(D_{s0}^* \rightarrow D_s \pi^0)$  was set to be 0.059 recently by CLEO [14]. Therefore,  $0.94 \lesssim \mathcal{B}[D_{s0}^*(2317) \rightarrow D_s \pi^0] \lesssim 1.0$ . It follows from Eqs. (3.39) and (3.38) that (see [38] for detail)

$$f_{D_{s0}^*} \approx 47 - 73 \text{ MeV}, \quad (3.40)$$

for  $a_1 = 1.07$ . To estimate the branching ratios of  $D_s^* \pi^0$  in the  $D_{s1}(2460)$  decay, we need some experimental and theoretical inputs. There are two different measurements of the radiative mode by Belle: a value of  $0.38 \pm 0.11 \pm 0.04$  for the ratio  $D_s \gamma / D_s^* \pi^0$  is determined from  $B \rightarrow \bar{D}D_{s1}$  decays [37], while the result of  $0.55 \pm 0.13 \pm 0.08$  is obtained from the charm fragmentation of  $e^+ e^- \rightarrow c \bar{c}$  [39]. These two measurements are consistent with each other, though the central values are somewhat different. We shall take the averaged value of  $0.44 \pm 0.09$  for  $D_s \gamma / D_s^* \pi^0$ . The ratio  $D_s \pi^+ \pi^- / D_s^* \pi^0$  is measured to be  $0.14 \pm 0.04 \pm 0.02$  by Belle [39]. As for  $D_s^* \gamma / D_s^* \pi^0$ , it is found to be less than 0.22, 0.31 and 0.16, respectively, by BaBar [40], Belle [39] and CLEO [14]. Theoretically, the  $M1$  transition  $D_{s1} \rightarrow D_{s0}^* \gamma$  turns out to be quite small [41]. Assuming that the  $D_{s1}(2460)$  decay is saturated by  $D_s^* \pi^0$ ,  $D_s \gamma$ ,  $D_s^* \gamma$  and  $D_s \pi \pi$ , we are led to

$$0.53 \lesssim \mathcal{B}(D_{s1}(2460) \rightarrow D_s^* \pi^0) \lesssim 0.68. \quad (3.41)$$

This in turn implies  $\mathcal{B}[B \rightarrow \bar{D}D_{s1}(2460)] = (1.6 \sim 4.6) \times 10^{-3}$ . As a result, the decay constant of  $D_{s1}(2460)$  is found to be

$$f_{D_{s1}(2460)} \approx 110 - 190 \text{ MeV}. \quad (3.42)$$

Our predictions  $f_{D_{s0}^*} = 71$  MeV and  $f_{D_{s1}} = 117$  MeV with the latter being obtained from the relation

$$f_{D_{s1}} = f_{D_{s1}^{1/2}} \cos \theta_s + f_{D_{s1}^{3/2}} \sin \theta_s \quad (3.43)$$

with  $\theta_s \approx 7^\circ$  inferred from the potential model [38], are in agreement with experiment.

Ideally, the neutral  $B$  decays  $\overline{B}^0 \rightarrow D^{**+} \pi^-$  that receive only color-allowed contributions can be used to extract  $B \rightarrow D^{**}$  transition form factors. Unfortunately, such decays have not yet been measured. Nevertheless, the decays  $B^- \rightarrow D^{*0} \pi^-$  that receive both contributions from color-allowed and color-suppressed diagrams provide a nice ground for testing the  $B \rightarrow D^{**}$  form factors and the  $D^{**}$  decay constants. Following [38], we show the predicted branching ratios in Table XIV. The experimental results are taken from Belle [15], BaBar [42] and PDG [16]. For  $B^- \rightarrow D_2^{*0} \pi^-$  we combine the Belle and BaBar measurements

$$\begin{aligned} \mathcal{B}(B^- \rightarrow D_2^{*0} \pi^-) \mathcal{B}(D_2^{*0} \rightarrow D^+ \pi^-) &= (3.1 \pm 0.4) \times 10^{-4}, \\ \mathcal{B}(B^- \rightarrow D_2^{*0} \pi^-) \mathcal{B}(D_2^{*0} \rightarrow D^{*+} \pi^-) &= (1.8 \pm 0.4) \times 10^{-4}, \end{aligned} \quad (3.44)$$

to arrive at

$$\mathcal{B}(B^- \rightarrow D_2^{*0} \pi^-) \mathcal{B}(D_2^{*0} \rightarrow D^+ \pi^-, D^{*+} \pi^-) = (4.9 \pm 0.6) \times 10^{-4}. \quad (3.45)$$

Using  $\mathcal{B}(D_2^{*0} \rightarrow D^+ \pi^-, D^{*+} \pi^-) = 2/3$  following from the assumption that the  $D_2^{*0}$  width is saturated by  $D\pi$  and  $D^*\pi$ , we are led to  $\mathcal{B}(B^- \rightarrow D_2^{*0} \pi^-) = (7.4 \pm 0.8) \times 10^{-4}$ . We see from the Table XIV that the agreement between theory and experiment is generally good. In particular, the suppression of the  $D_0^{*0} \pi^-$  production relative to the  $D^0 \pi^-$  one (the branching ratio for the latter being  $(5.3 \pm 0.5) \times 10^{-3}$  [16]) clearly indicates a smaller  $B \rightarrow D_0^*$  form factor relative to  $B \rightarrow D$  one. For comparison, we also show the ISGW2 predictions in the same Table. Since the decay constants of  $p$ -wave charmed mesons are not provided in the ISGW2 model, we employ the decay constants in this work and the ISGW2 form factors to obtain the ISGW2 results quoted in Table XIV. Predictions in the other models are summarized in [38].

TABLE XIV: The predicted branching ratios for  $B^- \rightarrow D^{*0} \pi^-$  decays in the covariant light-front (CLF) and ISGW2 models. Since the decay constants of  $p$ -wave charmed mesons are not provided in the latter model, we employ the CLF decay constants and the ISGW2 form factors for the ISGW2 results quoted below. Experimental results are taken from Belle [15], BaBar [42] and PDG [16]. The axial-vector meson mixing angle is taken to be  $\theta = 12^\circ$  [38] and the parameters  $a_{1,2}$  are given by  $a_1 = 1.07$  and  $a_2 = 0.27$ .

Decay	This work	ISGW2	Expt
$B^- \rightarrow D_0^*(2308)^0 \pi^-$	$7.3 \times 10^{-4}$	$4.8 \times 10^{-4}$	$(9.2 \pm 2.9) \times 10^{-4}$ [15]
$B^- \rightarrow D_1(2427)^0 \pi^-$	$4.6 \times 10^{-4}$	$9.4 \times 10^{-4}$	$(7.5 \pm 1.7) \times 10^{-4}$ [15]
$B^- \rightarrow D'_1(2420)^0 \pi^-$	$1.1 \times 10^{-3}$	$8.2 \times 10^{-4}$	$(9.3 \pm 1.4) \times 10^{-4}$ [15, 42]
			$(1.5 \pm 0.6) \times 10^{-3}$ [16]
$B^- \rightarrow D_2^*(2460)^0 \pi^-$	$1.0 \times 10^{-3}$	$5.7 \times 10^{-4}$	$(7.4 \pm 0.8) \times 10^{-4}$ [15, 42]

Since the tensor meson cannot be produced from the  $V - A$  current, the decay  $B^- \rightarrow D_2^{*0} \pi^-$  can be used to determine the form factor combination  $\eta(q^2) \equiv k(q^2) + b_+(q^2)(m_B^2 - m_{D_2^*}^2) + b_-(q^2)q^2$  at  $q^2 = m_\pi^2$ . The measured rate implies that  $\eta(m_\pi^2) = 0.43 \pm 0.02$ , to be compared with the predictions of 0.52 and 0.38 in the covariant LF and ISGW2 models, respectively.

It is worth mentioning that the ratio

$$R = \frac{\mathcal{B}(B^- \rightarrow D_2^{*0}(2460)^0 \pi^-)}{\mathcal{B}(B^- \rightarrow D_1'(2420)^0 \pi^-)} \quad (3.46)$$

is measured to be  $0.80 \pm 0.07 \pm 0.16$  by BaBar [42],  $0.77 \pm 0.15$  by Belle [15] and  $1.8 \pm 0.8$  by CLEO [43]. The early prediction by Neubert [44] yields a value of 0.35. The predictions of  $R = 0.91$  in the covariant light-front model and 0.67 in the ISGW2 model are in accordance with the data.

#### IV. HEAVY QUARK LIMIT

In the heavy quark limit, heavy quark symmetry (HQS) [20] provides model-independent constraints on the decay constants and form factors. For example, pseudoscalar and vector mesons would have the same decay constants and all the heavy-to-heavy mesonic decay form factors are reduced to some universal Isgur-Wise functions. Therefore, it is important to study the heavy quark limit behavior of these physical quantities to check the consistency of calculations. Since the analysis of heavy hadron structures and their dynamics in the infinite quark mass limit has been tremendously simplified by heavy quark symmetry and heavy quark effective theory (HQET) developed from QCD in terms of  $1/m_Q$  expansion [56], it would be much simpler to study the decay constants and form factors directly within the framework of a covariant light-front model of heavy mesons fully based on HQS and HQET. Indeed, we have constructed such a model in [10] which can be viewed as the heavy quark limit of the covariant light-front approach discussed in Sec. II. We shall show explicitly that the decay constants and form factors obtained in the covariant light-front model and then extended to the heavy quark limit do agree with those derived directly in the light-front model based on HQET.

Before proceeding, it is worth making a few remarks: (i) Just as in the conventional light-front model, it is assumed in [10] that the valance quarks of the meson are on their mass shell in the covariant light-front model based on HQET. However, this is not in contradiction to the covariant light-front approach discussed in Sec. II. As stressed before, the antiquark is on its mass shell after  $p^-$  integration in the covariant light-front calculation. Moreover, the off shellness of the heavy quark vanishes in the strict heavy quark limit. Therefore, the calculation based on the light-front model in [10] is covariant. (ii) Since the heavy quark-pair creation is forbidden in the  $m_Q \rightarrow \infty$  limit, the  $Z$ -graph is no longer a problem in the reference frame where  $q^+ \geq 0$ . This allows us to compute the Isgur-Wise functions directly in the timelike region.

In this work, we will adopt two different approaches to elaborate on the heavy quark limit behavior of physical quantities: one from top to bottom and the other from bottom to top. In the top-to-bottom approach, we will derive the decay constants and form factors in the covariant light-front model within HQET and obtain model-independent HQS relations. In the bottom-to-top approach, we study the heavy quark limit behavior of the decay constants and transition form

factors of heavy mesons obtained in Secs. II and III and show that they do match the covariant model results based on HQET.

### A. Heavy quark symmetry relations

In the infinite quark mass limit, the decay constants of heavy mesons must satisfy the HQS relations given by Eq. (2.7), while all the heavy-to-heavy mesonic decay form factors are reduced to three universal Isgur-Wise (IW) functions,  $\xi$  for  $s$ -wave to  $s$ -wave and  $\tau_{1/2}$  as well as  $\tau_{3/2}$  for  $s$ -wave to  $p$ -wave transitions. Specifically,  $B \rightarrow D, D^*$  form factors are related to the IW function  $\xi(\omega)$  by [20]

$$\begin{aligned}\xi(\omega) &= \frac{1}{2\sqrt{m_B m_D}} \left[ (m_B + m_D)f_+(q^2) + (m_B - m_D)f_-(q^2) \right] \\ &= -\frac{1}{\sqrt{m_B m_{D^*}}} \frac{f(q^2)}{1 + \omega} = -2\sqrt{m_B m_{D^*}} g(q^2) \\ &= \sqrt{m_B m_{D^*}} \left( a_+(q^2) - a_-(q^2) \right),\end{aligned}\quad (4.1)$$

and obey two additional HQS relations

$$a_+(q^2) + a_-(q^2) = 0, \quad (m_B - m_D)f_+(q^2) + (m_B + m_D)f_-(q^2) = 0, \quad (4.2)$$

where  $\omega = (m_B^2 + m_{D^{(*)}}^2 - q^2)/(2m_B m_{D^{(*)}})$ . The  $B \rightarrow D_0^*$  and  $B \rightarrow D_1^{1/2}$  form factors in the heavy quark limit are related to  $\tau_{1/2}(\omega)$  via [24]

$$\begin{aligned}\tau_{1/2}(\omega) &= \frac{1}{4\sqrt{m_B m_{D_0^*}}} \left[ (m_B - m_{D_0^*})u_+(q^2) + (m_B + m_{D_0^*})u_-(q^2) \right] \\ &= \frac{1}{2\sqrt{m_B m_{D_1^{1/2}}}} \frac{\ell_{1/2}(q^2)}{\omega - 1} = \sqrt{m_B m_{D_1^{1/2}}} q_{1/2}(q^2) \\ &= -\frac{\sqrt{m_B m_{D_1^{1/2}}}}{2} \left( c_+^{1/2}(q^2) - c_-^{1/2}(q^2) \right),\end{aligned}\quad (4.3)$$

while  $B \rightarrow D_1^{3/2}$  and  $B \rightarrow D_2^*$  transition form factors are related to  $\tau_{3/2}(\omega)$  by

$$\begin{aligned}\tau_{3/2}(\omega) &= -\sqrt{\frac{2}{m_B m_{D_1^{3/2}}}} \frac{\ell_{3/2}(q^2)}{\omega^2 - 1} = -\frac{1}{3} \sqrt{\frac{2m_B^3}{m_{D_1^{3/2}}}} \left( c_+^{3/2}(q^2) + c_-^{3/2}(q^2) \right) \\ &= \sqrt{\frac{2m_B^3}{m_{D_1^{3/2}}}} \frac{c_+^{3/2}(q^2) - c_-^{3/2}(q^2)}{\omega - 2} = 2\sqrt{\frac{m_B^3 m_{D_2^*}}{3}} h(q^2) \\ &= \sqrt{\frac{m_B}{3m_{D_2^*}}} \frac{k(q^2)}{1 + \omega} = -\frac{2\sqrt{2}}{1 + \omega} \sqrt{m_B m_{D_1^{3/2}}} q_{3/2}(q^2) \\ &= -\sqrt{\frac{m_B^3 m_{D_2^*}}{3}} \left( b_+(q^2) - b_-(q^2) \right),\end{aligned}\quad (4.4)$$

and subject to the HQS relations

$$\begin{aligned}b_+(q^2) + b_-(q^2) &= 0, & c_+^{1/2}(q^2) + c_-^{1/2}(q^2) &= 0, \\ (m_B + m_{D_0^*})u_+(q^2) + (m_B - m_{D_0^*})u_-(q^2) &= 0.\end{aligned}\quad (4.5)$$

In terms of the dimensionless form factors defined in (3.2) and (3.6), Eqs. (4.1) and (4.2) can be recast to

$$\begin{aligned}
\xi(\omega) &= \frac{2\sqrt{m_B m_D}}{m_B + m_D} F_1^{BD}(q^2) = \frac{2\sqrt{m_B m_D}}{m_B + m_D} \frac{F_0^{BD}(q^2)}{\left[1 - \frac{q^2}{(m_B + m_D)^2}\right]} \\
&= \frac{2\sqrt{m_B m_{D^*}}}{m_B + m_{D^*}} V^{BD^*}(q^2) = \frac{2\sqrt{m_B m_{D^*}}}{m_B + m_{D^*}} A_0^{BD^*}(q^2) \\
&= \frac{2\sqrt{m_B m_{D^*}}}{m_B + m_{D^*}} A_2^{BD^*}(q^2) = \frac{2\sqrt{m_B m_{D^*}}}{m_B + m_{D^*}} \frac{A_1^{BD^*}(q^2)}{\left[1 - \frac{q^2}{(m_B + m_{D^*})^2}\right]}.
\end{aligned} \tag{4.6}$$

Likewise, Eqs. (4.3) and (4.5) can be rewritten as

$$\begin{aligned}
\tau_{1/2}(\omega) &= \frac{\sqrt{m_B m_{D_0^*}}}{m_B - m_{D_0^*}} F_1^{BD_0^*}(q^2) = \frac{\sqrt{m_B m_{D_0^*}}}{m_B - m_{D_0^*}} \frac{F_0^{BD_0^*}(q^2)}{\left[1 - \frac{q^2}{(m_B - m_{D_0^*})^2}\right]} \\
&= -\frac{\sqrt{m_B m_{D_1^{1/2}}}}{m_B - m_{D_1^{1/2}}} A^{BD_1^{1/2}}(q^2) = \frac{\sqrt{m_B m_{D_1^{1/2}}}}{m_B - m_{D_1^{1/2}}} V_0^{BD_1^{1/2}}(q^2) \\
&= -\frac{\sqrt{m_B m_{D_1^{1/2}}}}{m_B - m_{D_1^{1/2}}} V_2^{BD_1^{1/2}}(q^2) = -\frac{\sqrt{m_B m_{D_1^{1/2}}}}{m_B - m_{D_1^{1/2}}} \frac{V_1^{BD_1^{1/2}}(q^2)}{\left[1 - \frac{q^2}{(m_B - m_{D_1^{1/2}})^2}\right]}.
\end{aligned} \tag{4.7}$$

In next subsections we will derive the above HQS relations for form factors and IW functions using the covariant light-front model based on HQET.

We see from Table VIII that HQS relations (4.5) for form factors  $b_{\pm}$  and  $c_{\pm}^{1/2}$  are respected even for finite heavy quark masses. From the numerical results of  $\tau_{1/2}(\omega = 1) = 0.31$  and  $\tau_{3/2}(\omega = 1) = 0.61$  to be presented below in Sec. VI.F, one can check the HQS relations (4.7) and (4.4) at the zero-recoil point. It turns out that, among the fourteen  $B \rightarrow D^{**}$  form factors, the covariant light-front model predictions for  $A^{BD_1^{1/2(3/2)}}, V_0^{BD_1^{1/2}}, V_2^{BD_1^{1/2}}, h, b_+, b_-$  are in good agreement with those in the heavy quark limit, while the agreement is fair for  $c_+^{3/2}$  and  $c_-^{3/2}$ . However, the predictions for  $F_{1,0}^{BD_0^*}, V_1^{BD_1^{1/2(3/2)}}$  and  $k$  at zero recoil show a large deviation from the HQS expectation. Indeed, Eqs. (4.7) and (4.4) indicate that except for  $F_1^{BD_0^*}$ , these form factors should approach to zero when  $q^2$  reaches its maximum value, a feature not borne out in the covariant light-front calculations for finite quark masses. This may signal that  $\Lambda_{\text{QCD}}/m_Q$  corrections are particularly important in this case. Phenomenologically, it is thus dangerous to determine all the form factors directly from the IW functions and HQS relations since  $1/m_Q$  corrections may play an essential role for some of them and the choice of the  $\beta$  parameters for  $s$ -wave and  $p$ -wave wave functions will affect the IW functions.

## B. Covariant light-front model within HQET

To begin with, we rescale the bound state of a heavy meson by  $|P_H^+, P_{H\perp}, J, J_z\rangle = \sqrt{M_H} |H(v, J, J_z)\rangle$ . It is well known that in the heavy quark limit, the heavy quark propagator can

be replaced by

$$\frac{i}{\not{p}_Q - m_Q + i\epsilon} \rightarrow \frac{i(1+\not{v})}{2v \cdot k + i\epsilon}, \quad (4.8)$$

where  $p_Q = m_Q v + k$  and  $k$  is the residual momentum of the heavy quark. One can then redo all the calculations in Sec. II by using the above propagator for  $q'_1$  and  $q''_1$  and perform the contour integral as before. Since the contour integral forces the antiquark to be on its mass shell, it is equivalent to using the so-called on-shell Feynman rules [10] in calculations. The zero mode effect arises from the  $p_1'^+ = p_1''+ = 0$  region and it can be interpreted as virtual pair creation processes [18]. In the infinite quark mass limit, both quarks are close to their mass shell and far from the  $p_1'^+ = p_1''+ = 0$  region. Consequently, the pair creation is forbidden and the zero mode contribution vanishes in the heavy quark limit. Hence, we do not need to stick to the  $q^+ = 0$  frame and are able to study form factors directly in the timelike region.

To extract the on-shell Feynman rules, we use the calculation of the pseudoscalar meson annihilation [c.f. Fig. 1(a)] as an illustration. By virtue of Eq. (4.8), the matrix element of Eq. (2.8) can be rewritten as

$$\langle 0 | A_\mu | P(v) \rangle = \frac{\mathcal{A}_\mu^P}{\sqrt{M_H}} = -i^2 \frac{N_c}{(2\pi)^4} \int d^4 p_q \frac{H'_P}{2v \cdot k N_2 \sqrt{M_H}} \text{Tr}[\gamma_\mu \gamma_5 (1+\not{v}) \gamma_5 (-\not{p}_q + m_q)], \quad (4.9)$$

where we have used  $p'_1 = p_Q$ ,  $p_2 = p_q$ ,  $m_2 = m_q$ ,  $N_2 = p_q^2 - m_q^2 + i\epsilon$  and  $k = -p_q + (M_H - m_Q)v$  from 4-momentum conservation. As in Sec. II, we need to perform the contour integral by closing the upper complex  $p_1'^-$ -plane, or equivalently, the lower complex  $p_q^-$ -plane. The integration forces  $p_q^2 = m_q^2$  and consequently,

$$\langle 0 | A_\mu | P(v) \rangle = -i^2 \frac{N_c}{(2\pi)^4} \int d^4 p_q (-2\pi i) \delta(p_q^2 - m_q^2) \frac{h'_P}{2v \cdot k \sqrt{M_H}} \text{Tr}[\gamma_\mu \gamma_5 (1+\not{v}) \gamma_5 (-\not{p}_q + m_q)]. \quad (4.10)$$

Since  $x_2$  is of order  $\Lambda_{\text{QCD}}/m_Q$  in the heavy quark limit, it is useful to define  $X \equiv m_Q x_2$ , which is of order  $\Lambda_{\text{QCD}}$  even if  $m_Q \rightarrow \infty$ . For on-shell  $p_q$  we have  $p_q^- = (p_{q\perp}^2 + m_q^2)/p_q^+$  and

$$v \cdot p_q = \frac{1}{2X} (p_{q\perp}^2 + m_q^2 + X^2). \quad (4.11)$$

It is then straightforward to obtain

$$\frac{h'_P}{2v \cdot k \sqrt{M_H}} \rightarrow \frac{1}{2\sqrt{N_c}} \frac{1}{\sqrt{v \cdot p_q + m_q}} \Phi'(X, p_{q\perp}^2), \quad (4.12)$$

with the aid of Eqs. (2.2), (2.11) and the replacements

$$\begin{aligned} \widetilde{M}_0 &\rightarrow \sqrt{2(v \cdot p_q + m_q)m_Q}, \\ \varphi(x, p_{q\perp}^2) &\rightarrow \sqrt{\frac{m_Q}{X}} \Phi(X, p_{q\perp}^2). \end{aligned} \quad (4.13)$$

An important feature of the covariant model is the requirement that the light-front wave function must be a function of  $v \cdot p_q$  [10]:

$$\Phi(X, p_{q\perp}^2) \longrightarrow \Phi(v \cdot p_q). \quad (4.14)$$

As we will see later, the widely used Gaussian-type wave functions have such a structure in the heavy quark limit, while the BSW wave function does not have one. The normalization condition of  $\Phi(v \cdot p_q)$  can be recast in a covariant form:

$$\int \frac{d^4 p_q}{(2\pi)^4} (2\pi) \delta(p_q^2 - m_q^2) |\Phi(v \cdot p_q)|^2 = 1, \quad (4.15)$$

or

$$\int_0^\infty \frac{dX}{X} \int \frac{d^2 p_\perp}{2(2\pi)^3} |\Phi(X, p_\perp^2)|^2 = 1. \quad (4.16)$$

Putting everything together we have

$$\begin{aligned} \langle 0 | A_\mu | P(v) \rangle &= -i^2 \frac{N_c}{(2\pi)^4} \int d^4 p_q (-2\pi i) \delta(p_q^2 - m_q^2) \\ &\times \frac{1}{2\sqrt{N_c}} \frac{1}{\sqrt{v \cdot p_q + m_q}} \Phi(v \cdot p_q) \text{Tr}[\gamma_\mu \gamma_5 (1 + \not{v}) \gamma_5 (-\not{p}_q + m_q)]. \end{aligned} \quad (4.17)$$

In practice, we can use the following on-shell Feynman rules to obtain the above and other amplitudes. The diagrammatic rule is given as follows [10]:

(i) The heavy meson bound state in the heavy quark limit gives a vertex (wave function) as follows:

$$\text{---} \bullet : \frac{1}{\sqrt{N_c}} \sqrt{\frac{1}{v \cdot p_q + m_q}} \Phi(v \cdot p_q) i\Gamma_H, \quad (4.18)$$

$$\bullet \text{---} : \frac{1}{\sqrt{N_c}} \sqrt{\frac{1}{v \cdot p_q + m_q}} \Phi^*(v \cdot p_q) i\bar{\Gamma}_H, \quad (4.19)$$

with  $\bar{\Gamma}_H = \gamma^0 \Gamma_H^\dagger \gamma^0$ . For  $p$ -wave mesons, we denote the covariant wave function by  $\Phi_p(v \cdot p_q)$ .

(ii) The internal line attached to the bound state gives an on-mass-shell propagator,

$$\text{---} \quad : \quad i \left( \frac{1 + \not{v}}{2} \right) \quad (\text{for heavy quarks}), \quad (4.20)$$

$$\text{---} \quad : \quad i(-\not{p}_q + m_q) \quad (\text{for light antiquarks}), \quad (4.21)$$

where  $v^2 = 1$  and  $p_q^2 = m_q^2$ .

(iii) For the internal antiquark line attached to the bound state, sum over helicity and integrate the internal momentum using

$$N_c \int \frac{d^4 p_q}{(2\pi)^4} (-2\pi i) \delta(p_q^2 - m_q^2), \quad (4.22)$$

where the delta function comes from the on-mass-shell condition and  $N_c$  comes from the color summation.

(iv) For all other lines and vertices that do not attach to the bound states, the diagrammatic rules are the same as the Feynman rules in the conventional field theory.

These are the basic rules for the subsequent evaluations in the covariant model. The vertex  $\Gamma_H$  for the incoming heavy meson can be read from Table I or from Eqs. (A11) and (A19) by applying Eq. (4.13). Hence, the vertex functions in the heavy quark limit have the expressions:

$$\begin{aligned}
^1S_0 : & -i\gamma_5 \\
^3S_1 : & \not{v} \\
^3P_0 : & -\frac{1}{\sqrt{3}}(v \cdot p_q + m_q) \\
^1P_1 : & \varepsilon \cdot p_q \gamma_5 \\
^3P_1 : & -\frac{1}{\sqrt{2}} \left[ (v \cdot p_q + m_q) \left( \not{v} - \frac{\varepsilon \cdot p_q}{v \cdot p_q + m_q} \right) \right] \gamma_5 \\
^3P_2 : & -\varepsilon_{\mu\nu} \gamma^\mu p_q^\nu.
\end{aligned} \tag{4.23}$$

In terms of the  $P_1^{1/2}$  and  $P_1^{3/2}$  states, the relevant vertex functions read

$$\begin{aligned}
P_1^{1/2} : & \frac{1}{\sqrt{3}}(v \cdot p_q + m_q) \not{v} \gamma_5 \\
P_1^{3/2} : & -\frac{1}{\sqrt{6}}[(v \cdot p_q + m_q) \not{v} - 3\varepsilon \cdot p_q] \gamma_5.
\end{aligned} \tag{4.24}$$

### C. Decay constants

In the infinite quark mass limit, the decay constants are defined by

$$\begin{aligned}
\langle 0 | \bar{q} \gamma^\mu \gamma_5 h_v | P(v) \rangle &= i F_P v^\mu, \quad \langle 0 | \bar{q} \gamma^\mu h_v | P^*(v, \varepsilon) \rangle = F_V \varepsilon^\mu, \\
\langle 0 | \bar{q} \gamma^\mu h_v | S(v, \varepsilon) \rangle &= F_S v^\mu, \quad \langle 0 | \bar{q} \gamma^\mu \gamma_5 h_v | A^{1/2}(v, \varepsilon) \rangle = F_{A^{1/2}} \varepsilon^\mu, \\
\langle 0 | \bar{q} \gamma^\mu \gamma_5 h_v | A^{3/2}(v, \varepsilon) \rangle &= F_{A^{3/2}} \varepsilon^\mu,
\end{aligned} \tag{4.25}$$

where the decay constant  $F_H$  is related to the usual one  $f_H$  by  $F_H = \sqrt{M_H} f_H$ . Note that the tensor meson cannot be created from the  $V - A$  current. HQS demands that [20, 25]

$$F_V = F_P, \quad F_{A^{1/2}} = F_S, \quad F_{A^{3/2}} = 0. \tag{4.26}$$

Using the Feynman rules shown above, it is ready to evaluate the one-body matrix elements for heavy scalar and axial-vector mesons:

$$\begin{aligned}
\langle 0 | \bar{q} \gamma^\mu h_v | S(v) \rangle &= -\frac{1}{\sqrt{3}} \text{Tr} \left\{ \gamma^\mu \frac{1+\not{v}}{2} \mathcal{M}_1 \right\}, \\
\langle 0 | \bar{q} \gamma^\mu \gamma_5 h_v | A^{1/2}(v, \varepsilon) \rangle &= \frac{1}{\sqrt{3}} \text{Tr} \left\{ \gamma^\mu \gamma_5 \frac{1+\not{v}}{2} \not{v} \gamma_5 \mathcal{M}_1 \right\},
\end{aligned} \tag{4.27}$$

where

$$\mathcal{M}_1 = \sqrt{N_c} \int \frac{d^4 p_q}{(2\pi)^4} (2\pi) \delta(p_q^2 - m_q^2) \frac{\Phi_p(v \cdot p_q)}{\sqrt{v \cdot p_q + m_q}} (m_q - \not{p}_q) (v \cdot p_q + m_q). \tag{4.28}$$

Letting  $\mathcal{M}_1 = a_1 + b_1 \not{v}$ , we obtain

$$\begin{aligned}
a_1 &= \sqrt{N_c} \int \frac{d^4 p_q}{(2\pi)^4} (2\pi) \delta(p_q^2 - m_q^2) \Phi_p(v \cdot p_q) m_q \sqrt{v \cdot p_q + m_q}, \\
b_1 &= -\sqrt{N_c} \int \frac{d^4 p_q}{(2\pi)^4} (2\pi) \delta(p_q^2 - m_q^2) \Phi_p(v \cdot p_q) (v \cdot p_q) \sqrt{v \cdot p_q + m_q}.
\end{aligned} \tag{4.29}$$

Thus,

$$\begin{aligned}
F_S &= F_{A^{1/2}} = -\frac{2}{\sqrt{3}}(a_1 + b_1) \\
&= 2\sqrt{\frac{N_c}{3}} \int \frac{d^4 p_q}{(2\pi)^4} (2\pi) \delta(p_q^2 - m_q^2) \Phi_p(v \cdot p_q) \sqrt{v \cdot p_q + m_q} (v \cdot p_q - m_q) \\
&= 2\sqrt{\frac{N_c}{3}} \int \frac{dX d^2 p_\perp}{2(2\pi)^3 X} \Phi_p(X, p_\perp^2) \sqrt{\frac{p_\perp^2 + (m_q + X)^2}{2X}} \frac{p_\perp^2 + (m_q - X)^2}{2X}.
\end{aligned} \tag{4.30}$$

Likewise, for the axial-vector  $P_1^{3/2}$  meson

$$\langle 0 | \bar{q} \gamma^\mu \gamma_5 h_v | A^{3/2}(v, \varepsilon) \rangle = -\frac{1}{\sqrt{6}} \text{Tr} \left\{ \gamma^\mu \gamma_5 \frac{1 + \not{v}}{2} [\not{v}(\gamma_\alpha + v_\alpha) - 3\varepsilon_\alpha] \gamma_5 \mathcal{M}_2^\alpha \right\}, \tag{4.31}$$

with

$$\mathcal{M}_2^\alpha = \sqrt{N_c} \int \frac{d^4 p_q}{(2\pi)^4} (2\pi) \delta(p_q^2 - m_q^2) \frac{\Phi_p(v \cdot p_q)}{\sqrt{v \cdot p_q + m_q}} (m_q - \not{p}_q) p_q^\alpha. \tag{4.32}$$

The general expression of  $\mathcal{M}_2^\alpha$  is

$$\mathcal{M}_2^\alpha = a_2 v^\alpha + b_2 \gamma^\alpha + c_2 \not{v} v^\alpha + d_2 \not{v} \gamma^\alpha. \tag{4.33}$$

Since  $\varepsilon \cdot v = 0$  and the contraction of  $\gamma_\mu$  with the spin 3/2 field vanishes, namely,

$$(1 + \not{v}) [\not{v}(\gamma_\alpha + v_\alpha) - 3\varepsilon_\alpha] \gamma^\alpha = 0, \tag{4.34}$$

we are led to  $F_{A^{3/2}} = 0$  in the heavy quark limit.

For completeness, the decay constants of the  $s$ -wave heavy mesons are included here [10]

$$\begin{aligned}
F_P &= F_V \\
&= 2\sqrt{N_c} \int \frac{dX d^2 p_\perp}{2(2\pi)^3 X} \Phi(X, p_\perp^2) \sqrt{\frac{(X + m_q)^2 + p_\perp^2}{2X}}.
\end{aligned} \tag{4.35}$$

We now show that the decay constants obtained in the covariant light-front model in Sec. II do respect the heavy quark symmetry relations given in (2.7) or (4.26) in the infinite quark mass limit and have expressions in agreement with Eqs. (4.30) and (4.35). To illustrate this, we consider the decay constants of pseudoscalar and vector mesons. In the  $m'_1 = m_Q \rightarrow \infty$  limit, Eqs. (2.17) and (2.22) are reduced to

$$\begin{aligned}
\sqrt{m_Q} f_P &\rightarrow 4\sqrt{\frac{N_c}{2}} \int \frac{dX d^2 p_\perp}{2(2\pi)^3 \sqrt{X}} \Phi(X, p_\perp^2) \frac{X + m_q}{\sqrt{(X + m_q)^2 + p_\perp^2}}, \\
\sqrt{m_Q} f_V &\rightarrow 4\sqrt{\frac{N_c}{2}} \int \frac{dX d^2 p_\perp}{2(2\pi)^3 \sqrt{X}} \Phi(X, p_\perp^2) \frac{1}{\sqrt{(X + m_q)^2 + p_\perp^2}} \left( \frac{m_q^2 + p_\perp^2}{X} + m_q \right),
\end{aligned} \tag{4.36}$$

where  $m_q = m_2$ ,  $X = m_Q x$  and use of Eq. (4.13) has been made. Since the wave function is even in  $p_z$ , a quantity defined in Eq. (2.2), it follows that

$$\begin{aligned}
&\int dx d^2 p_\perp \frac{\varphi(x, p_\perp)}{\sqrt{[m_Q x + m_q(1-x)]^2 + p_\perp^2}} p_z = 0 \\
&\rightarrow \int \frac{dX d^2 p_\perp}{\sqrt{X}} \frac{\Phi(X, p_\perp^2)}{\sqrt{(X + m_q)^2 + p_\perp^2}} \left( X - \frac{m_q^2 + p_\perp^2}{X} \right) = 0.
\end{aligned} \tag{4.37}$$

Therefore,  $f_V = f_P$  in the heavy quark limit. Moreover,  $\sqrt{m_Q}f_P$  is identical to  $F_P$  in Eq. (4.35) after applying the identity

$$\int \frac{dX d^2 p_\perp}{\sqrt{X}} \Phi(X, p_\perp^2) \frac{2(X + m_q)}{\sqrt{(X + m_q)^2 + p_\perp^2}} = \int \frac{dX d^2 p_\perp}{\sqrt{X}} \Phi(X, p_\perp^2) \frac{\sqrt{(X + m_q)^2 + p_\perp^2}}{X}, \quad (4.38)$$

following from Eq. (4.37).

Likewise, Eq. (2.23) for the decay constants of axial-vector mesons is reduced in the heavy quark limit to

$$\begin{aligned} \sqrt{m_Q}f_{1A} &\rightarrow 2\sqrt{\frac{N_c}{2}} \int \frac{dX d^2 p_\perp}{2(2\pi)^3 \sqrt{X}} \frac{\Phi_p(X, p_\perp^2)}{\sqrt{(X + m_q)^2 + p_\perp^2}} p_\perp^2, \\ \sqrt{m_Q}f_{3A} &\rightarrow \sqrt{N_c} \int \frac{dX d^2 p_\perp}{2(2\pi)^3 \sqrt{X}} \frac{\Phi_p(X, p_\perp^2)}{\sqrt{(X + m_q)^2 + p_\perp^2}} \left( \frac{(m_q^2 + p_\perp^2)^2}{X^2} - m_q^2 \right), \end{aligned} \quad (4.39)$$

where use of Eq. (4.37) has been applied for deriving the expression of  $f_{1A}$ . By virtue of the identities

$$\begin{aligned} \int \frac{dX d^2 p_\perp}{\sqrt{X}} \frac{\Phi_p(X, p_\perp^2)}{\sqrt{(X + m_q)^2 + p_\perp^2}} (p_z^2 - p_\perp^2/2) &= 0, \\ \int \frac{dX d^2 p_\perp}{\sqrt{X}} \frac{\Phi_p(X, p_\perp^2)}{\sqrt{(X + m_q)^2 + p_\perp^2}} (X^2 - m_q^2) &= 0, \end{aligned} \quad (4.40)$$

and

$$\begin{aligned} \frac{3}{\sqrt{2}} \int \frac{dX d^2 p_\perp}{\sqrt{X}} \frac{\Phi_p(X, p_\perp^2)}{\sqrt{(X + m_q)^2 + p_\perp^2}} p_\perp^2 \\ = \int \frac{dX d^2 p_\perp}{X} \Phi_p(X, p_\perp^2) \sqrt{\frac{p_\perp^2 + (m_q + X)^2}{2X}} \frac{p_\perp^2 + (m_q - X)^2}{2X}, \end{aligned} \quad (4.41)$$

following from the first equation of (4.40), one can show that  $f_{3A} = -\sqrt{2}f_{1A}$  and hence  $f_{A^{3/2}} = 0$  and  $\sqrt{m_Q}f_{A^{1/2}} = F_{A^{1/2}} = F_S$  in the  $m_Q \rightarrow \infty$  limit.

## D. Isgur-Wise functions

It is well known that the  $s$ -wave to  $s$ -wave meson transition in the heavy quark limit is governed by a single universal IW function  $\xi(\omega)$  [20]. Likewise, there exist two universal functions  $\tau_{1/2}(\omega)$  and  $\tau_{3/2}(\omega)$  describing ground-state  $s$ -wave to  $p$ -wave transitions [24]. Since the IW function  $\xi$  has been discussed in detail in [10], we will focus on the other two IW functions  $\tau_{1/2}$  and  $\tau_{3/2}$ .

Let us first consider the function  $\tau_{1/2}$ , which can be extracted from the  $B \rightarrow D_0^*$  or  $B \rightarrow D_1^{1/2}$  transition

$$\begin{aligned} \langle D_0^*(v') | \bar{h}_{v'}^c \Gamma h_v^b | B(v) \rangle &= -i \frac{1}{\sqrt{3}} \text{Tr} \left\{ \left( \frac{1+\not{v}'}{2} \right) \Gamma \left( \frac{1+\not{v}}{2} \right) \gamma_5 \mathcal{M}_3 \right\}, \\ \langle D_1^{1/2}(v', \varepsilon) | \bar{h}_{v'}^c \Gamma h_v^b | B(v) \rangle &= i \frac{1}{\sqrt{3}} \text{Tr} \left\{ \not{\varepsilon} \gamma_5 \left( \frac{1+\not{v}'}{2} \right) \Gamma \left( \frac{1+\not{v}}{2} \right) \gamma_5 \mathcal{M}_3 \right\}, \end{aligned} \quad (4.42)$$

where  $\mathcal{M}_3$  is the transition matrix element for the light antiquark:

$$\mathcal{M}_3 = \int [d^4 p_q] (m_q - \not{p}_q) (v' \cdot p_q + m_q), \quad (4.43)$$

and we have introduced the short-hand notation

$$[d^4 p_q] \equiv \frac{d^4 p_q}{(2\pi)^4} (2\pi) \delta(p_q^2 - m_q^2) \frac{\Phi_p^*(v' \cdot p_q) \Phi(v \cdot p_q)}{\sqrt{(v' \cdot p_q + m_q)(v \cdot p_q + m_q)}}. \quad (4.44)$$

The structure of  $\mathcal{M}_3$  dictated by Lorentz invariance has the form [57]

$$\mathcal{M}_3 = a_3 + b_3 \not{v} + c_3 \not{v}' + d_3 \not{v} \not{v}'. \quad (4.45)$$

This covariant decomposition allows us to easily determine the coefficients  $a_3, b_3, c_3, d_3$  with the results:

$$\begin{aligned} a_3 &= \int [d^4 p_q] m_q (v' \cdot p_q + m_q), \\ b_3 &= - \int [d^4 p_q] (v' \cdot p_q + m_q) \frac{1}{2} \left\{ \frac{(v + v') \cdot p_q}{1 + \omega} + \frac{(v - v') \cdot p_q}{1 - \omega} \right\}, \\ c_3 &= - \int [d^4 p_q] (v' \cdot p_q + m_q) \frac{1}{2} \left\{ \frac{(v + v') \cdot p_q}{1 + \omega} - \frac{(v - v') \cdot p_q}{1 - \omega} \right\}, \\ d_3 &= 0, \end{aligned} \quad (4.46)$$

where  $\omega \equiv v \cdot v'$ .

Then  $B \rightarrow D_0^*$  and  $B \rightarrow D_1^{1/2}$  transitions are simplified to

$$\begin{aligned} \langle D_0^*(v') | \bar{h}_v^c \Gamma h_v^b | B(v) \rangle &= -i 2\tau_{1/2}(\omega) \text{Tr} \left\{ \left( \frac{1 + \not{v}'}{2} \right) \Gamma \left( \frac{1 + \not{v}}{2} \right) \gamma_5 \right\}, \\ \langle D_1^{1/2}(v', \varepsilon) | \bar{h}_v^c \Gamma h_v^b | B(v) \rangle &= i 2\tau_{1/2}(\omega) \text{Tr} \left\{ \not{\varepsilon} \gamma_5 \left( \frac{1 + \not{v}'}{2} \right) \Gamma \left( \frac{1 + \not{v}}{2} \right) \gamma_5 \right\}, \end{aligned} \quad (4.47)$$

with

$$\begin{aligned} \tau_{1/2}(\omega) &= \frac{1}{2\sqrt{3}} (a_3 - b_3 + c_3 - d_3) \\ &= \frac{1}{2\sqrt{3}} \int [d^4 p_q] (v' \cdot p_q + m_q) \left( m_q + \frac{(v - v') \cdot p_q}{1 - \omega} \right). \end{aligned} \quad (4.48)$$

Since

$$v \cdot p_q = \frac{1}{2X} (p_\perp^2 + m_q^2 + X^2), \quad v' \cdot p_q = \frac{1}{2X'} (p_\perp^2 + m_q^2 + X'^2), \quad (4.49)$$

the IW function  $\tau_{1/2}$  can be explicitly expressed as

$$\begin{aligned} \tau_{1/2}(\omega) &= \frac{1}{2\sqrt{3}} \int \frac{dX d^2 p_\perp}{2(2\pi)^3 X^2} \frac{1}{\sqrt{z}(1-z)} \Phi_p^*(zX, p_\perp^2) \Phi(X, p_\perp^2) \\ &\times \sqrt{\frac{p_\perp^2 + (m_q + zX)^2}{p_\perp^2 + (m_q + X)^2}} \left[ p_\perp^2 + (m_q + X)(m_q - zX) \right], \end{aligned} \quad (4.50)$$

where  $z \equiv X'/X$  and it can be related to  $v \cdot v'$  by

$$z \rightarrow z_\pm = \omega \pm \sqrt{\omega^2 - 1}, \quad z_+ = \frac{1}{z_-}, \quad (4.51)$$

with the  $+$  ( $-$ ) sign corresponding to  $v^3$  greater (less) than  $v'^3$ . Note that  $v^3$  greater (less) than  $v'^3$  corresponds the daughter meson recoiling in the negative (positive)  $z$  direction in the rest frame of the parent meson. In other words, after setting  $v_\perp = v'_\perp = 0$ , the daughter meson recoiling in the positive and negative  $z$  directions are the only two possible choices of Lorentz frames. It is easily seen that  $\tau_{1/2}(\omega)$  remains the same under the replacement of  $z \rightarrow 1/z$ . This indicates that the Isgur-Wise function thus obtained is independent of the recoiling direction, namely, it is truly Lorentz invariant.

Next consider the  $B \rightarrow D_2^*$  or  $B \rightarrow D_1^{3/2}$  transition to extract the second universal function  $\tau_{3/2}$

$$\begin{aligned} \langle D_2^*(v', \varepsilon) | \bar{h}_{v'}^c \Gamma h_v^b | B(v) \rangle &= -i \text{Tr} \left\{ \varepsilon_{\alpha\beta} \gamma^\alpha \left( \frac{1+\not{v}'}{2} \right) \Gamma \left( \frac{1+\not{v}}{2} \right) \gamma_5 \mathcal{M}_4^\beta \right\}, \\ \langle D_1^{3/2}(v', \varepsilon) | \bar{h}_{v'}^c \Gamma h_v^b | B(v) \rangle &= -\frac{i}{\sqrt{6}} \text{Tr} \left\{ [(-\gamma_\alpha + v'_\alpha) \not{v} + 3\varepsilon_\alpha] \gamma_5 \left( \frac{1+\not{v}'}{2} \right) \Gamma \left( \frac{1+\not{v}}{2} \right) \gamma_5 \mathcal{M}_4^\alpha \right\}, \end{aligned} \quad (4.52)$$

where

$$\mathcal{M}_4^\alpha = \int [d^4 p_q] (m_q - \not{p}_q) p_q^\alpha. \quad (4.53)$$

Its most general expression is

$$\mathcal{M}_{4\alpha} = a_4 v_\alpha + b_4 v'_\alpha + c_4 \not{v} v_\alpha + d_4 \not{v}' v_\alpha + e_4 \not{v}' v'_\alpha + f_4 \not{v} v'_\alpha + g_4 \gamma_\alpha + h_4 \not{v} \gamma_\alpha + h'_4 \not{v}' \gamma_\alpha. \quad (4.54)$$

Although only terms proportional to  $a_4$ ,  $c_4$  and  $d_4$  will contribute to  $B \rightarrow D_2^*$  and  $B \rightarrow D_1^{3/2}$  transitions after contracting with the vertex of the spin 3/2 particles, all the terms in  $\mathcal{M}_{4\alpha}$  have to be retained in order to project out the coefficients. With  $\mathcal{M}_{4\alpha}$  contracting with  $v^\alpha$ ,  $v'^\alpha$  and  $\gamma^\alpha$  we find the following equations:

$$\begin{aligned} a_4 + b_4 \omega &= \int [d^4 p_q] m_q v \cdot p_q, \\ a_4 \omega + b_4 &= \int [d^4 p_q] m_q v' \cdot p_q, \\ c_4 + 2d_4 \omega + f_4 + 4g_4 &= - \int [d^4 p_q] m_q^2, \\ c_4 + d_4 \omega + g_4 &= - \int [d^4 p_q] \frac{v \cdot p_q}{2} \left( \frac{(v + v') \cdot p_q}{1 + \omega} + \frac{(v - v') \cdot p_q}{1 - \omega} \right), \\ d_4 + f_4 \omega &= - \int [d^4 p_q] \frac{v \cdot p_q}{2} \left( \frac{(v + v') \cdot p_q}{1 + \omega} - \frac{(v - v') \cdot p_q}{1 - \omega} \right), \\ c_4 \omega + d_4 &= - \int [d^4 p_q] \frac{v' \cdot p_q}{2} \left( \frac{(v + v') \cdot p_q}{1 + \omega} + \frac{(v - v') \cdot p_q}{1 - \omega} \right), \\ d_4 \omega + f_4 + g_4 &= - \int [d^4 p_q] \frac{v' \cdot p_q}{2} \left( \frac{(v + v') \cdot p_q}{1 + \omega} - \frac{(v - v') \cdot p_q}{1 - \omega} \right), \end{aligned} \quad (4.55)$$

and  $e_4 = d_4$ ,  $h_4 = h'_4 = 0$ . Solving the above equations yields

$$\begin{aligned} a_4 &= \frac{m_q}{2} \int [d^4 p_q] (\lambda_+ + \lambda_-), \\ b_4 &= \frac{m_q}{2} \int [d^4 p_q] (\lambda_+ - \lambda_-), \\ c_4 &= -\frac{1}{4} \int [d^4 p_q] \left( (\lambda_+ + \lambda_-)^2 - \frac{g_4}{(1 + \omega)(1 - \omega)} \right), \end{aligned} \quad (4.56)$$

$$\begin{aligned} d_4 &= -\frac{1}{4} \int [d^4 p_q] \left( (\lambda_+^2 - \lambda_-^2) + \frac{g_4 \omega}{(1+\omega)(1-\omega)} \right), \\ f_4 &= -\frac{1}{4} \int [d^4 p_q] \left( (\lambda_+ - \lambda_-)^2 - \frac{g_4}{(1+\omega)(1-\omega)} \right), \end{aligned}$$

and

$$g_4 = -\frac{1}{2} \int [d^4 p_q] \left( m_q^2 - \frac{1}{2}(1+\omega)\lambda_+^2 - \frac{1}{2}(1-\omega)\lambda_-^2 \right), \quad (4.57)$$

with

$$\lambda_+ \equiv \frac{(v+v') \cdot p_q}{1+\omega}, \quad \lambda_- \equiv \frac{(v-v') \cdot p_q}{1-\omega}. \quad (4.58)$$

Since only  $v_\alpha$ ,  $\not{v}v_\alpha$  and  $\not{v}'v_\alpha$  terms in  $M_{4\alpha}$  survive after contracting with the vertex of  $D_2^*$  and  $D_1^{3/2}$  particles, the matrix elements (4.52) are simplified to

$$\begin{aligned} \langle D_2^*(v', \varepsilon) | \bar{h}_{v'}^c \Gamma h_v^b | B(v) \rangle &= -i\sqrt{3} \tau_{3/2}(\omega) \varepsilon_{\alpha\beta} v^\beta \text{Tr} \left\{ \gamma^\alpha \left( \frac{1+\not{v}'}{2} \right) \Gamma \left( \frac{1+\not{v}}{2} \right) \gamma_5 \right\}, \\ \langle D_1^{3/2}(v', \varepsilon) | \bar{h}_{v'}^c \Gamma h_v^b | B(v) \rangle &= -\frac{i}{\sqrt{2}} \tau_{3/2}(\omega) \\ &\quad \times \text{Tr} \left\{ [\not{v}(1+\omega) + 3\varepsilon \cdot v] \gamma_5 \left( \frac{1+\not{v}'}{2} \right) \Gamma \left( \frac{1+\not{v}}{2} \right) \gamma_5 \right\}, \end{aligned} \quad (4.59)$$

with

$$\begin{aligned} \tau_{3/2}(\omega) &= \frac{1}{\sqrt{3}} (a_4 - c_4 - d_4) \\ &= \frac{1}{2\sqrt{3}} \int [d^4 p_q] \left[ (\lambda_+ + \lambda_-)(m_q + \lambda_+) + \frac{\lambda_+^2(1+\omega) + \lambda_-^2(1-\omega) - m_q^2}{2(1+\omega)} \right]. \end{aligned} \quad (4.60)$$

A more explicit expression of  $\tau_{3/2}$  reads

$$\begin{aligned} \tau_{3/2}(\omega) &= \frac{1}{\sqrt{3}} \int \frac{dX d^2 p_\perp}{2(2\pi)^3} \frac{2\sqrt{z} \Phi_p^*(zX, p_\perp^2) \Phi(X, p_\perp^2)}{\sqrt{[p_\perp^2 + (m_q + X)^2][p_\perp^2 + (m_q + zX)^2]}} \\ &\quad \times \left\{ \frac{1}{2(1-\omega)(1+\omega)^2} \left[ (1-2\omega)(v' \cdot p_q)(2v + v') \cdot p_q \right. \right. \\ &\quad \left. \left. + 3(v \cdot p_q)^2 - (1-\omega^2)m_q^2 \right] + \frac{1}{1-\omega^2} [v \cdot p_q - \omega(v' \cdot p_q)] m_q \right\}. \end{aligned} \quad (4.61)$$

After some manipulation, we obtain a simple relation between  $\tau_{3/2}$  and  $\tau_{1/2}$ :

$$\begin{aligned} \tau_{3/2}(\omega) &= \frac{2}{1+\omega} \tau_{1/2}(\omega) + \frac{\sqrt{3}}{1+\omega} \int \frac{dX d^2 p'_\perp}{2(2\pi)^3} \Phi_p^*(zX, p'_\perp^2) \Phi(X, p'_\perp^2) \\ &\quad \times \frac{\sqrt{z} p'_\perp^2}{\sqrt{[p'_\perp^2 + (m_q + X)^2][p'_\perp^2 + (m_q + zX)^2]}}. \end{aligned} \quad (4.62)$$

Finally we include the usual IW function  $\xi(\omega)$  for the sake of completeness [10]

$$\begin{aligned} \xi(\omega) &= \int \frac{dX d^2 p_\perp}{2(2\pi)^3 X} \frac{2\sqrt{z}}{1+z} \Phi^*(zX, p_\perp^2) \Phi(X, p_\perp^2) \\ &\quad \times \frac{p_\perp^2 + (m_q + X)(m_q + zX)}{\sqrt{[p_\perp^2 + (m_q + X)^2][p_\perp^2 + (m_q + zX)^2]}}. \end{aligned} \quad (4.63)$$

and the relevant matrix elements are given by

$$\begin{aligned}\langle D(v') | \bar{h}_{v'}^c \Gamma h_v^b | B(v) \rangle &= \xi(\omega) \text{Tr} \left\{ \gamma_5 \left( \frac{1+\not{v}'}{2} \right) \Gamma \left( \frac{1+\not{v}}{2} \right) \gamma_5 \right\}, \\ \langle D^*(v', \varepsilon) | \bar{h}_{v'}^c \Gamma h_v^b | B(v) \rangle &= \xi(\omega) \text{Tr} \left\{ \not{\varepsilon}^* \left( \frac{1+\not{v}'}{2} \right) \Gamma \left( \frac{1+\not{v}}{2} \right) i \gamma_5 \right\}.\end{aligned}\quad (4.64)$$

### E. Form factors in the heavy quark limit

From Eqs. (4.64), (4.47) and (4.59) we obtain the matrix elements of  $B \rightarrow D, D^*, D^{**}$  transitions in the heavy quark limit

$$\begin{aligned}\langle D(v') | V_\mu | B(v) \rangle &= \xi(\omega) (v + v')_\mu, \\ \langle D^*(v', \varepsilon) | V_\mu | B(v) \rangle &= -\xi(\omega) \epsilon_{\mu\nu\alpha\beta} \varepsilon^{*\nu} v'^\alpha v^\beta, \\ \langle D^*(v', \varepsilon) | A_\mu | B(v) \rangle &= i \xi(\omega) \left[ (1 + \omega) \varepsilon_\mu^* - (\varepsilon^* \cdot v) v'_\mu \right], \\ \langle D_0^*(v') | A_\mu | B(v) \rangle &= i 2\tau_{1/2}(\omega) (v - v')_\mu, \\ \langle D_1^{1/2}(v', \varepsilon) | V_\mu | B(v) \rangle &= -i 2\tau_{1/2}(\omega) \left[ (1 - \omega) \varepsilon_\mu^* + (\varepsilon^* \cdot v) v'_\mu \right], \\ \langle D_1^{1/2}(v', \varepsilon) | A_\mu | B(v) \rangle &= -2\tau_{1/2}(\omega) \epsilon_{\mu\nu\alpha\beta} \varepsilon^{*\nu} v'^\alpha v^\beta, \\ \langle D_1^{3/2}(v', \varepsilon) | V_\mu | B(v) \rangle &= i \frac{1}{\sqrt{2}} \tau_{3/2}(\omega) \left\{ (1 - \omega^2) \varepsilon_\mu^* - (\varepsilon^* \cdot v) [3v_\mu + (2 - \omega) v'_\mu] \right\}, \\ \langle D_1^{3/2}(v', \varepsilon) | A_\mu | B(v) \rangle &= \frac{1}{\sqrt{2}} \tau_{3/2}(\omega) (1 + \omega) \epsilon_{\mu\nu\alpha\beta} \varepsilon^{*\nu} v'^\alpha v^\beta, \\ \langle D_2^*(v', \varepsilon) | V_\mu | B(v) \rangle &= \sqrt{3} \tau_{3/2}(\omega) \epsilon_{\mu\nu\alpha\beta} \varepsilon^{*\nu\gamma} v_\gamma v'^\alpha v^\beta, \\ \langle D_2^*(v', \varepsilon) | A_\mu | B(v) \rangle &= -i \sqrt{3} \tau_{3/2}(\omega) \left\{ (1 + \omega) \varepsilon_{\mu\nu}^* v^\nu - \varepsilon_{\alpha\beta}^* v^\alpha v^\beta v'_\mu \right\}.\end{aligned}\quad (4.65)$$

It is easily seen that the  $B \rightarrow D^{**}$  matrix elements of weak currents vanish at the zero recoil point  $\omega = 1$  owing to the orthogonality of the wave functions of  $B$  and  $D^{**}$ . Setting  $p_B = m_B v$  and  $p_D = m_D v', \dots$ , etc. in Eqs. (3.1) and (3.5) and comparing with (4.65) yields all the form-factor HQS relations given in Sec. IV.A.

We are ready to check the heavy quark limit behavior of form factors to see if they satisfy the HQS constraints. Consider the form factor  $F_1^{BD_0^*}(q^2) = -u_+(q^2)$  first. Let  $x_2 = x, x_1 = 1 - x, m_2 = m_q, X = m_b x, X' = m_c x$ , it follows from Eq. (3.20) that

$$\begin{aligned}u_+(q^2) &= \frac{N_c}{16\pi^3} \int dx d^2 p'_\perp \frac{h'_P h''_S}{x^2 \hat{N}'_1 \hat{N}''_1} \left\{ 2(X + m_q) X' - 2m_q X - 2m_q^2 (1 - x)^2 - x^2 q^2 \right. \\ &\quad \left. + 2m_q x (X - X') - 2p'^2_\perp + 2x p'_\perp \cdot q_\perp \right\},\end{aligned}\quad (4.66)$$

where use of Eq. (2.2) and  $p''_\perp = p'_\perp - x q_\perp$  has been used. In the heavy quark limit  $x \sim \mathcal{O}(\Lambda_{\text{QCD}}/m_Q) \rightarrow 0$ , we have

$$u_+(q^2) \rightarrow -\frac{1}{2\sqrt{3}} \int \frac{dX d^2 p'_\perp}{2(2\pi)^3 X} \frac{\widetilde{M}_0''}{\widetilde{M}'_0 \widetilde{M}''_0} \varphi_p^*(x, p'^2_\perp) \varphi(x, p'^2_\perp) \left[ p'^2_\perp + (m_q + X)(m_q - X') \right]. \quad (4.67)$$

Substituting the replacements

$$\begin{aligned}\widetilde{M}'_0 &\rightarrow \sqrt{m_b [(X + m_q)^2 + p'^2_\perp] / X}, & \widetilde{M}''_0 &\rightarrow \sqrt{m_c [(X' + m_q)^2 + p'^2_\perp] / X'}, \\ \varphi(x, p'^2_\perp) &\rightarrow \sqrt{\frac{m_b}{X}} \Phi(X, p'^2_\perp), & \varphi_p(x, p'^2_\perp) &\rightarrow \sqrt{\frac{m_c}{X'}} \Phi_p(X', p'^2_\perp)\end{aligned}\quad (4.68)$$

valid in the infinite quark mass limit and noting that  $z = X'/X = m_c/m_b$ , we arrive at

$$\begin{aligned} u_+(q^2) &\rightarrow -\frac{1}{2\sqrt{3}} \int \frac{dX d^2 p'_\perp}{2(2\pi)^3 X^2} \frac{1}{z} \Phi_p^*(zX, p'^2_\perp) \Phi(X, p'^2_\perp) \\ &\times \sqrt{\frac{p'^2_\perp + (m_q + zX)^2}{p'^2_\perp + (m_q + X)^2}} \left[ p'^2_\perp + (m_q + X)(m_q - zX) \right], \end{aligned} \quad (4.69)$$

and hence

$$\frac{\sqrt{m_B m_{D_0^*}}}{m_B - m_{D_0^*}} F_1^{BD_0^*}(q^2) \rightarrow \tau_{1/2}(\omega). \quad (4.70)$$

Likewise, it is easily shown that

$$\frac{\sqrt{m_B m_D}}{m_B + m_D} F_1^{BD}(q^2) \rightarrow \xi(\omega). \quad (4.71)$$

In order to demonstrate that the  $B \rightarrow D^*$  form factors are related to the IW function  $\xi(\omega)$ , we need to apply the identity (3.35) which has the expression

$$\int dx d^2 p'_\perp \frac{2h'_P h''_V}{x \hat{N}'_1 \hat{N}''_1} \left( (q \cdot P) \frac{p'_\perp \cdot q_\perp}{q^2} - \frac{1}{x} (p'^2_\perp + m_q^2 - X^2) \right) = 0 \quad (4.72)$$

in the  $m_Q \rightarrow \infty$  limit. This identity allows us to integrate out the  $(p'_\perp \cdot q_\perp)/q^2$  term. Then the form factor  $g(q^2)$  that reads [see Eq. (B4)]

$$\begin{aligned} g(q^2) &= -\frac{1}{m_B + m_{D^*}} \frac{N_c}{16\pi^3} \int dx d^2 p'_\perp \frac{2h'_P h''_V}{x^2 \hat{N}'_1 \hat{N}''_1} \left\{ (X + X')(X + m_q) + x(q \cdot P) \frac{p'_\perp \cdot q_\perp}{q^2} \right. \\ &+ \left. 2 \frac{m_B + m_{D^*}}{w''_V} \left( x p'^2_\perp + x \frac{p'_\perp \cdot q_\perp}{q^2} \right) \right\} \end{aligned} \quad (4.73)$$

is reduced under the heavy quark limit to

$$-\frac{1}{m_B + m_{D^*}} \int \frac{dX d^2 p'_\perp}{2(2\pi)^3 X} \Phi^*(zX, p'^2_\perp) \Phi(X, p'^2_\perp) \frac{p'^2_\perp + (m_q + X)(m_q + zX)}{\sqrt{[p'^2_\perp + (m_q + X)^2][p'^2_\perp + (m_q + zX)^2]}}, \quad (4.74)$$

where use of Eqs. (2.11), (3.35) and (4.68) has been made. Comparing with Eq. (4.63) it is evident that the heavy quark limit of  $g(q^2)$  has the same expression as  $\xi(\omega)$  apart from a mass factor. Therefore, we arrive at<sup>7</sup>

$$\frac{2\sqrt{m_B m_{D^*}}}{m_B + m_{D^*}} V^{BD^*}(q^2) = -2\sqrt{m_B m_{D^*}} g(q^2) \rightarrow \xi(\omega). \quad (4.77)$$

---

<sup>7</sup> If the Taylor expansion of  $h''_V/\hat{N}''_1$  is performed to take care of the  $p'_\perp \cdot q_\perp$  term in the integrand of  $g(q^2)$ , it turns out that the heavy quark limit of the  $B \rightarrow D^*$  form factors will be related to the IW function

$$\zeta(\omega) = \int \frac{dX d^2 p'_\perp}{2(2\pi)^3} \Phi^*(X', p'^2_\perp) \Phi(X, p'^2_\perp) \frac{X'(X + m_q) + X'(X - X') p'^2_\perp \Theta_V}{\sqrt{[p'^2_\perp + (m_q + X)^2][p'^2_\perp + (m_q + X')^2]}}, \quad (4.75)$$

where

$$\Theta_V = \frac{\hat{N}''_1}{h''_V} \left( \frac{d}{dp'^2_\perp} \frac{h''_V}{\hat{N}''_1} \right)_{p'^2_\perp \rightarrow p'^2_\perp}. \quad (4.76)$$

This function  $\zeta(\omega)$  first obtained in [7] was found numerically identical to  $\xi(\omega)$ , as it should be. However, one has to appeal to the identity (4.72) in order to prove this equivalence analytically.

We next turn to the form factors  $q_{1/2}$  and  $q_{3/2}$  and see if they are related to the IW functions  $\tau_{1/2}$  and  $\tau_{3/2}$ , respectively. We first study the heavy quark limit behavior of  $q^{1A}$  and  $q^{3A}$ . It follows from Eq. (3.26) that

$$\begin{aligned} \sqrt{m_B m_{D_1^{1/2}}} q^{1A}(q^2) &= \sqrt{m_B m_{D_1^{1/2}}} \frac{N_c}{16\pi^3} \int dx d^2 p'_\perp \frac{2h'_P h''_{1A}}{x \hat{N}'_1 \hat{N}''_1} \left( p'^2_\perp + \frac{(p'_\perp \cdot q_\perp)^2}{q^2} \right) \\ &\rightarrow -\frac{1}{2} \int \frac{dX d^2 p'_\perp}{2(2\pi)^3} \Phi_p^*(zX, p'^2_\perp) \Phi(X, p'^2_\perp) \\ &\times \frac{\sqrt{z} p'^2_\perp}{\sqrt{[p'^2_\perp + (m_q + X)^2][p'^2_\perp + (m_q + zX)^2]}}, \end{aligned} \quad (4.78)$$

and

$$\begin{aligned} \sqrt{m_B m_{D_1^{3/2}}} q^{3A}(q^2) &\rightarrow -\frac{1}{2\sqrt{2}} \int \frac{dX d^2 p'_\perp}{2(2\pi)^3 X^2} \frac{\Phi_p^*(zX, p'^2_\perp) \Phi(X, p'^2_\perp)}{\sqrt{z}(1-z)} \\ &\times \sqrt{\frac{p'^2_\perp + (m_q + zX)^2}{p'^2_\perp + (m_q + X)^2}} \left[ p'^2_\perp + (m_q + X)(m_q - zX) \right] \\ &- \frac{1}{2\sqrt{2}} \int \frac{dX d^2 p'_\perp}{2(2\pi)^3} \Phi_p^*(zX, p'^2_\perp) \Phi(X, p'^2_\perp) \\ &\times \frac{\sqrt{z} p'^2_\perp}{\sqrt{[p'^2_\perp + (m_q + X)^2][p'^2_\perp + (m_q + zX)^2]}}. \end{aligned} \quad (4.79)$$

Since

$$q_{1/2}(q^2) = \frac{1}{\sqrt{3}} q^{1A}(q^2) - \sqrt{\frac{2}{3}} q^{3A}(q^2), \quad q_{3/2}(q^2) = \sqrt{\frac{2}{3}} q^{1A}(q^2) + \frac{1}{\sqrt{3}} q^{3A}(q^2), \quad (4.80)$$

following from Eq. (2.6), we obtain

$$\sqrt{m_B m_{D_1^{1/2}}} q_{1/2}(q^2) \rightarrow \tau_{1/2}(\omega) \quad (4.81)$$

and

$$-\frac{2\sqrt{2}}{1+\omega} \sqrt{m_B m_{D_1^{3/2}}} q_{3/2}(q^2) \rightarrow \tau_{3/2}(\omega), \quad (4.82)$$

as promised before.

All other HQS relations in Eqs. (4.1), (4.3) and (4.4) can be proved in the same manner except for the  $B \rightarrow D_2^*$  form factors  $h, k, b_+, b_-$  for which we are not able to show at present that they are related to  $\tau_{3/2}(\omega)$  in the heavy quark limit. Perhaps one needs some identities in [8] and those derived in Appendix B to verify the HQS relations between  $B \rightarrow D_2^*$  form factors and  $\tau_{3/2}(\omega)$ . This remains to be investigated.

## F. Numerical results for IW functions and discussion

Covariance requires that light-front wave functions be a function of  $v \cdot p_q$ . Currently, there exist several phenomenological light-front wave functions commonly utilized in the literature. There are several popular phenomenological light-front wave functions that have been employed to describe

various hadronic structures in the literature. Two of them, the Bauer-Stech-Wirbel (BSW) wave function  $\Phi_{\text{BSW}}(x, p_\perp^2)$  [46] and the Gaussian-type wave function  $\Phi_G(x, p_\perp^2)$  [26], have been widely used in the study of heavy mesons. In the heavy quark limit, we denote these wave functions as follows:

$$\begin{aligned}\Phi_{\text{BSW}}(X, p_\perp^2) &= 4\sqrt{2} \left(\frac{\pi}{\beta^2}\right) X \exp \left\{ -\frac{p_\perp^2 + X^2}{2\beta^2} \right\}, \\ \Phi_G(X, p_\perp^2) &= 4 \left(\frac{\pi}{\beta^2}\right)^{3/4} \sqrt{\frac{X^2 + m_q^2 + p_\perp^2}{2X}} \\ &\quad \times \exp \left\{ -\frac{1}{2\beta^2} \left[ p_\perp^2 + \left(\frac{X}{2} - \frac{m_q^2 + p_\perp^2}{2X}\right)^2 \right] \right\},\end{aligned}\quad (4.83)$$

where  $\Phi_G(X, p_\perp^2)$  is the heavy quark limit expression of the Gaussian-type wave function given in Eq. (2.12). For  $p$ -wave heavy mesons, the wave functions are

$$\Phi_p^{\text{BSW}}(X, p_\perp^2) = \sqrt{\frac{2}{\beta^2}} \Phi_{\text{BSW}}(X, p_\perp^2), \quad \Phi_p^G(X, p_\perp^2) = \sqrt{\frac{2}{\beta^2}} \Phi_G(X, p_\perp^2). \quad (4.84)$$

As pointed out in [10], not all the phenomenological light-front wave functions have the covariant property. We found that the Gaussian wave function and the invariant-mass wave function can be reexpressed as a pure function of  $v \cdot p_q$ . The wave function  $\Phi_G$  can be rewritten in terms of  $v \cdot p_q$ :

$$\begin{aligned}\Phi_G(X, p_\perp^2) &= 4 \left(\frac{\pi}{\beta^2}\right)^{3/4} \sqrt{\frac{X^2 + m_q^2 + p_\perp^2}{2X}} \\ &\quad \times \exp \left\{ -\frac{1}{2\beta^2} \left[ \left(\frac{X}{2} + \frac{m_q^2 + p_\perp^2}{2X}\right)^2 - m_q^2 \right] \right\} \\ &= 4 \left(\frac{\pi}{\beta^2}\right)^{3/4} \sqrt{v \cdot p_q} \exp \left\{ -\frac{1}{2\beta^2} \left[ (v \cdot p_q)^2 - m_q^2 \right] \right\}.\end{aligned}\quad (4.85)$$

Therefore this wave function preserves the Lorentz covariance of Eqs. (4.54), (4.45) and (4.28). This also can be examined by a numerical check of the covariant condition

$$\int \frac{dX d^2 p_\perp}{2(2\pi)^3 X} \Phi(X, p_\perp^2) X = \int \frac{dX d^2 p_\perp}{2(2\pi)^3 X} \Phi(X, p_\perp^2) \frac{m_q^2 + p_\perp^2}{X}, \quad (4.86)$$

which is satisfied if  $\Phi(X, p_\perp^2)$  is a function of  $v \cdot p_q$ . However, very surprisingly, the commonly used BSW wave function cannot be recast as a pure function of  $v \cdot p_q$ . Hence the BSW wave function breaks the Lorentz covariance. Indeed, we have already found previously [7] that there is some inconsistent problem by using the BSW wave function to calculate various transition form factors. Now we can understand why the BSW wave function gives such results inconsistent with HQS found in [7, 58]. Hence, by demanding relativistic covariance, we can rule out certain types of heavy meson light-front wave functions.

To perform numerical calculations of the decay constants and IW functions in the heavy quark limit, we follow [10] to use the input  $m_q = 250$  MeV and  $f_B = 180$  MeV to fix the parameter  $\beta_\infty$  to be 0.49. For decay constants we then obtain

$$F_P = F_V = 413 \text{ MeV}^{3/2}, \quad F_S = F_{A^{1/2}} = 399 \text{ MeV}^{3/2}. \quad (4.87)$$

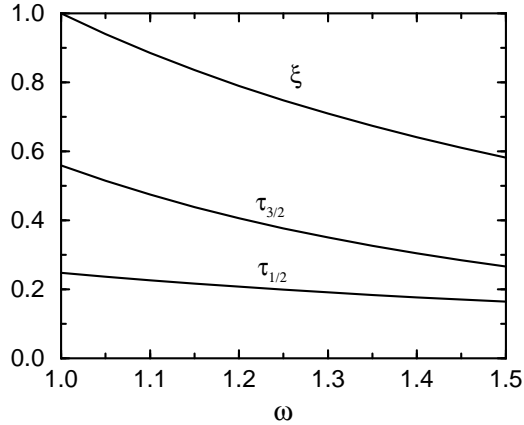


FIG. 6: The Isgur-Wise functions  $\xi$ ,  $\tau_{1/2}$  and  $\tau_{3/2}$  as a function of  $\omega$ .

The decay constant of the  $P_1^{3/2}$  heavy meson vanishes in the infinite quark mass limit. We see that the decay constants of ground-state  $s$ -wave mesons and low-lying  $p$ -wave mesons are similar in the heavy quark limit.

The IW functions (4.63), (4.50) and (4.62) can be fitted nicely to the form

$$f(\omega) = f(1)[1 - \rho^2(\omega - 1) + \frac{\sigma^2}{2}(\omega - 1)^2], \quad (4.88)$$

and it is found that (see Fig. 6)

$$\begin{aligned} \xi(\omega) &= 1 - 1.22(\omega - 1) + 0.85(\omega - 1)^2, \\ \tau_{1/2}(\omega) &= 0.31 \left(1 - 1.18(\omega - 1) + 0.87(\omega - 1)^2\right), \\ \tau_{3/2}(\omega) &= 0.61 \left(1 - 1.73(\omega - 1) + 1.46(\omega - 1)^2\right), \end{aligned} \quad (4.89)$$

where we have used the same  $\beta_\infty$  parameter for both wave functions  $\Phi$  and  $\Phi_p$ . It should be stressed that unlike  $\tau_{1/2}(1)$  and  $\tau_{3/2}(1)$ , the normalization  $\xi(1) = 1$  at the zero recoil point is a model-independent consequence; that is, it is independent of the structure of wave functions. In Table XV we have compared this work for the IW functions  $\tau_{1/2}(\omega)$  and  $\tau_{3/2}(\omega)$  with other model calculations. It turns out that our results are similar to that obtained in the ISGW model [17] (numerical results for the latter being quoted from [59]). Our result  $\rho^2 = 1.22$  for the slope parameter is consistent with the current world average of  $1.44 \pm 0.14$  extracted from exclusive semileptonic  $B$  decays [69].

It is interesting to notice that there is a sum rule derived by Uraltsev [22]

$$\sum_n |\tau_{3/2}^{(n)}(1)|^2 - \sum_n |\tau_{1/2}^{(n)}(1)|^2 = \frac{1}{4}, \quad (4.90)$$

where  $n$  stands for radial excitations. This sum rule clearly implies that  $|\tau_{3/2}(1)| \gg |\tau_{1/2}(1)|$ . Our results indicate that this sum rule is slightly over-saturated even by  $n = 0$   $p$ -wave states. Another sum rule due to Bjorken [21] reads

$$\rho^2 = \frac{1}{4} + \sum_n |\tau_{1/2}^{(n)}(1)|^2 + 2 \sum_n |\tau_{3/2}^{(n)}(1)|^2, \quad (4.91)$$

TABLE XV: The Isgur-Wise functions  $\tau_{1/2}$  and  $\tau_{3/2}$  at zero recoil and their slope parameters. The numerical results for [17, 60, 62, 63] denoted by “\*” are quoted from [59].

$\tau_{1/2}(1)$	$\rho_{1/2}^2$	$\tau_{3/2}(1)$	$\rho_{3/2}^2$	Ref.
0.31	1.18	0.61	1.73	This work
0.06	0.73	0.52	1.45	[60]*
0.09	1.1	0.28	0.9	[61]
0.13	0.57	0.43	1.39	[62]*
0.22	0.83	0.54	1.50	[63]*
0.34	1.08	0.59	1.76	[17]*
$0.35 \pm 0.08$	$2.5 \pm 1.0$	–	–	[64]
$0.41 \pm 0.04$	$1.30 \pm 0.23$	$0.66 \pm 0.02$	$1.93 \pm 0.16$	[65]
–	–	$0.74 \pm 0.15$	$0.90 \pm 0.05$	[66]

where  $\rho^2$  is the slope of the IW function  $\xi(\omega)$ . Combined with the Uraltsev sum rule (4.90) leads to

$$\rho^2 = \frac{3}{4} + 3 \sum_n |\tau_{1/2}^{(n)}(1)|^2. \quad (4.92)$$

Note that while the Bjorken sum rule receives perturbative corrections [70], the Uraltsev sum rule does not (for a recent study, see [71]).

## V. CONCLUSIONS

In this work we have studied the decay constants and form factors of the ground-state  $s$ -wave and low-lying  $p$ -wave mesons within a covariant light-front approach. This formalism that preserves the Lorentz covariance in the light-front framework has been developed and applied successfully to describe various properties of pseudoscalar and vector mesons. One of our main goals is to extend this approach to the  $p$ -wave meson case. Our main results are as follows:

- The main ingredients of the covariant light-front model, namely, the vertex functions, are explicitly worked out for both  $s$ -wave and  $p$ -wave mesons.
- The decay constant of light scalar mesons is largely suppressed relative to that of the pseudoscalar mesons and this suppression becomes less effective for heavy scalar resonances. The predicted decay constants  $|f_{D_{s0}^*}| = 71$  MeV and  $|f_{D_{s1}(2460)}| = 117$  MeV are consistent with the corresponding values of  $47 \sim 73$  MeV and  $110 \sim 190$  MeV inferred from the measurement of  $\overline{D}D_{s0}^*$  and  $\overline{D}D_{s1}$  productions in  $B$  decays.
- In the limit of SU(N)-flavor symmetry, the decay constants of the scalar meson and the  $^1P_1$  axial-vector meson are found to be vanished, as it should be.

- The analytic expressions for  $P \rightarrow S, A$  transition form factors can be obtained from that of  $P \rightarrow P, V$  ones by some simple replacements. We have also worked out the form factors in  $P \rightarrow T$  transitions.
- The momentum dependence of the physical form factors is determined by first fitting the form factors obtained in the spacelike region to a 3-parameter function in  $q^2$  and then analytically continuing them to the timelike region. Some of the  $V_2(q^2)$  form factors in  $P \rightarrow A$  transitions are fitted to a different 3-parameter form so that the fit parameters are stable within the chosen  $q^2$  range.
- Numerical results of the form factors for  $B(D) \rightarrow \pi, \rho, a_0(1450), a_1(1260), b_1(1235), a_2(1320)$ ,  $B(D) \rightarrow K, K^*, K^{**}$  and  $B \rightarrow D, D^*, D^{**}$  transitions are presented in detail, where  $K^{**}$  and  $D^{**}$  denote generically  $p$ -wave strange and charmed mesons, respectively.
- Comparison of this work with the ISGW2 model based on the nonrelativistic constituent quark picture is made for  $B \rightarrow D^{**}$  transition form factors. In general, the form factors at small  $q^2$  in both models agree within 40%. However,  $F_0^{BD_0^*}(q^2)$  and  $V_1^{BD_1^{1/2}}(q^2)$  have a very different  $q^2$  behavior in these two models as  $q^2$  increases. Relativistic effects are mild in  $B \rightarrow D^{**}$  transitions but can manifest in heavy-to-light transitions at maximum recoil. For example,  $V_0^{Ba_1}(0)$  is found to be 0.13 in the covariant LF model, while it is as big as 1.01 in the ISGW2 model.
- The decay amplitudes of  $B^- \rightarrow D^{**0}\pi^-$  involve the  $B \rightarrow D^{**}$  form factors and  $D^{**}$  decay constants. We have compared the model calculations with experiment and found a good agreement. In particular, the suppression of the  $D_0^{*0}\pi^-$  production relative to  $D^0\pi^-$  one clearly indicates a smaller  $B \rightarrow D_0^*$  form factor relative to the  $B \rightarrow D$  one.
- The heavy quark limit behavior of decay constants and form factors is examined and it is found that the requirement of heavy quark symmetry is satisfied.
- Decay constants and form factors are also evaluated independently in a covariant light-front formulism within the framework of heavy quark effective theory. The resultant decay constants and form factors agree with those obtained from the covariant light-front model and then extended to the heavy quark limit. The universal Isgur-Wise functions  $\xi(\omega), \tau_{1/2}(\omega)$  and  $\tau_{3/2}(\omega)$  are obtained and a relation between  $\tau_{1/2}$  and  $\tau_{3/2}$  is found. In the infinite quark mass limit, all the form factors are related to the Isgur-Wise functions. In addition to  $\xi(1) = 1$  at zero recoil  $\omega = 1$ , it is found that  $\tau_{1/2}(1) = 0.61$ ,  $\tau_{3/2}(1) = 0.31$  and  $\rho^2 = 1.22$  for the slope parameter of  $\xi(\omega)$ . The Bjorken and Uraltsev sum rules for the Isgur-Wise functions are fairly satisfied.

## Acknowledgments

We are grateful to Wolfgang Jaus for very helpful clarification and to Chuang-Hung Chen and Chao-Qiang Geng for valuable discussions. One of us (C.W.H.) wishes to thank the Institute of Physics, Academia Sinica for its hospitality during his summer visit where this work started. This research was supported in part by the National Science Council of R.O.C. under Grant Nos. NSC92-2112-M-001-016, NSC92-2811-M-001-054 and NSC92-2112-M-017-001.

## APPENDIX A: VERTEX FUNCTIONS IN THE CONVENTIONAL LIGHT-FRONT APPROACH

In the conventional light-front approach, a meson bound state consisting of a quark  $q_1$  and an antiquark  $\bar{q}_2$  with the total momentum  $P$  and spin  $J$  can be written as (see, for example [7])

$$\begin{aligned} |M(P, {}^{2S+1}L_J, J_z)\rangle &= \int \{d^3p_1\}\{d^3p_2\} 2(2\pi)^3\delta^3(\tilde{P} - \tilde{p}_1 - \tilde{p}_2) \\ &\quad \times \sum_{\lambda_1, \lambda_2} \Psi_{LS}^{JJ_z}(\tilde{p}_1, \tilde{p}_2, \lambda_1, \lambda_2) |q_1(p_1, \lambda_1)\bar{q}_2(p_2, \lambda_2)\rangle, \end{aligned} \quad (\text{A1})$$

where  $p_1$  and  $p_2$  are the on-mass-shell light-front momenta,

$$\tilde{p} = (p^+, p_\perp), \quad p_\perp = (p^1, p^2), \quad p^- = \frac{m^2 + p_\perp^2}{p^+}, \quad (\text{A2})$$

and

$$\begin{aligned} \{d^3p\} &\equiv \frac{dp^+ d^2p_\perp}{2(2\pi)^3}, \\ |q(p_1, \lambda_1)\bar{q}(p_2, \lambda_2)\rangle &= b_{\lambda_1}^\dagger(p_1) d_{\lambda_2}^\dagger(p_2) |0\rangle, \\ \{b_{\lambda'}(p'), b_\lambda^\dagger(p)\} &= \{d_{\lambda'}(p'), d_\lambda^\dagger(p)\} = 2(2\pi)^3 \delta^3(\tilde{p}' - \tilde{p}) \delta_{\lambda' \lambda}. \end{aligned} \quad (\text{A3})$$

In terms of the light-front relative momentum variables  $(x, p_\perp)$  defined by

$$\begin{aligned} p_1^+ &= x_1 P^+, \quad p_2^+ = x_2 P^+, \quad x_1 + x_2 = 1, \\ p_{1\perp} &= x_1 P_\perp + p_\perp, \quad p_{2\perp} = x_2 P_\perp - p_\perp, \end{aligned} \quad (\text{A4})$$

the momentum-space wave-function  $\Psi_{LS}^{JJ_z}$  for a  ${}^{2S+1}L_J$  meson can be expressed as

$$\Psi_{LS}^{JJ_z}(\tilde{p}_1, \tilde{p}_2, \lambda_1, \lambda_2) = \frac{1}{\sqrt{N_c}} \langle LS; L_z S_z | LS; JJ_z \rangle R_{\lambda_1 \lambda_2}^{SS_z}(x, p_\perp) \varphi_{LL_z}(x, p_\perp), \quad (\text{A5})$$

where  $\varphi_{LL_z}(x, p_\perp)$  describes the momentum distribution of the constituent quarks in the bound state with the orbital angular momentum  $L$ ,  $\langle LS; L_z S_z | LS; JJ_z \rangle$  is the corresponding Clebsch-Gordan coefficient and  $R_{\lambda_1 \lambda_2}^{SS_z}$  constructs a state of definite spin  $(S, S_z)$  out of light-front helicity  $(\lambda_1, \lambda_2)$  eigenstates. Explicitly,

$$R_{\lambda_1 \lambda_2}^{SS_z}(x, p_\perp) = \sum_{s_1, s_2} \langle \lambda_1 | \mathcal{R}_M^\dagger(1-x, p_\perp, m_1) | s_1 \rangle \langle \lambda_2 | \mathcal{R}_M^\dagger(x, -p_\perp, m_2) | s_2 \rangle \left\langle \frac{1}{2} \frac{1}{2}; s_1 s_2 | \frac{1}{2} \frac{1}{2}; SS_z \right\rangle, \quad (\text{A6})$$

where  $|s_i\rangle$  are the usual Pauli spinors, and  $\mathcal{R}_M$  is the Melosh transformation operator [3, 67]:

$$\begin{aligned} \langle s | \mathcal{R}_M(x, p_\perp, m_i) | \lambda \rangle &= \frac{\bar{u}_D(p_i, s) u(p_i, \lambda)}{2m_i} = -\frac{\bar{v}_D(p_i, s) v(p_i, \lambda)}{2m_i} \\ &= \frac{m_i + x_i M_0 + i \vec{\sigma}_{s\lambda} \cdot \vec{p}_\perp \times \vec{n}}{\sqrt{(m_i + x_i M_0)^2 + p_\perp^2}}, \end{aligned} \quad (\text{A7})$$

with  $u_{(D)}$ , a Dirac spinor in the light-front (instant) form,  $\vec{n} = (0, 0, 1)$ , a unit vector in the  $z$ -direction, and [cf. Eq. (2.2)]

$$M_0^2 = \frac{m_1^2 + p_\perp^2}{x_1} + \frac{m_2^2 + p_\perp^2}{x_2}. \quad (\text{A8})$$

Note that  $u_D(p, s) = u(p, \lambda) \langle \lambda | \mathcal{R}_M^\dagger | s \rangle$  and, consequently, the state  $|q(p, \lambda)\rangle \langle \lambda | \mathcal{R}_M^\dagger | s \rangle$  transforms like  $|q(p, s)\rangle$  under rotation, i.e. its transformation does not depend on its momentum.

In practice it is more convenient to use the covariant form for  $R_{\lambda_1 \lambda_2}^{SS_z}$  [4]:

$$R_{\lambda_1 \lambda_2}^{SS_z}(x, p_\perp) = \frac{1}{\sqrt{2} \widetilde{M}_0(M_0 + m_1 + m_2)} \bar{u}(p_1, \lambda_1)(\bar{P} + M_0)\Gamma v(p_2, \lambda_2), \quad (\text{A9})$$

with

$$\begin{aligned} \widetilde{M}_0 &\equiv \sqrt{M_0^2 - (m_1 - m_2)^2}, \\ \bar{P} &\equiv p_1 + p_2, \\ \hat{\varepsilon}^\mu(\pm 1) &= \left[ \frac{2}{P^+} \vec{\varepsilon}_\perp(\pm 1) \cdot \vec{P}_\perp, 0, \vec{\varepsilon}_\perp(\pm 1) \right], \quad \vec{\varepsilon}_\perp(\pm 1) = \mp(1, \pm i)/\sqrt{2}, \\ \hat{\varepsilon}^\mu(0) &= \frac{1}{M_0} \left( \frac{-M_0^2 + P_\perp^2}{P^+}, P^+, P_\perp \right). \end{aligned} \quad (\text{A10})$$

For the pseudoscalar and vector mesons, we have

$$\begin{aligned} \Gamma_P &= \gamma_5 \quad (\text{pseudoscalar}, S = 0), \\ \Gamma_V &= -\not{v}(S_z) \quad (\text{vector}, S = 1). \end{aligned} \quad (\text{A11})$$

It is instructive to derive the above expressions by using the relations

$$\begin{aligned} \bar{u}(p_1, \lambda_1) &= \bar{u}(p_1, \lambda_1) \frac{u_D(p_1, s_1)\bar{u}_D(p_1, s_1)}{2m_1}, \\ v(p_2, \lambda_2) &= \frac{-v_D(p_2, s_2)\bar{v}_D(p_2, s_2)}{2m_2} v(p_2, \lambda_2), \\ \bar{u}_D(p_1, s_1) \frac{\bar{P} + M_0}{2M_0} \gamma_5 v_D(p_2, s_2) &= \bar{u}_D((e_1, \vec{p}), s_1) \frac{\gamma_0 + 1}{2} \gamma_5 v_D((e_2, -\vec{p}), s_2) \\ &= \sqrt{(e_1 + m_1)(e_2 + m_2)} i\chi_{s_1}^\dagger \sigma_2 \chi_{s_2}^* \\ &= \sqrt{2(e_1 + m_1)(e_2 + m_2)} \left\langle \frac{1}{2} \frac{1}{2}; s_1 s_2 | \frac{1}{2} \frac{1}{2}; 00 \right\rangle, \\ \bar{u}_D(p_1, s_1) \frac{\bar{P} + M_0}{2M_0} (-\not{v}(S_z)) v_D(p_2, s_2) &= \bar{u}_D((e_1, \vec{p}), s_1) \frac{\gamma_0 + 1}{2} \bar{\varepsilon}(S_z) \cdot \vec{\gamma} v_D((e_2, -\vec{p}), s_2) \\ &= \sqrt{(e_1 + m_1)(e_2 + m_2)} i\chi_{s_1}^\dagger \bar{\varepsilon}(S_z) \cdot \vec{\sigma} \sigma_2 \chi_{s_2}^* \\ &= \sqrt{2(e_1 + m_1)(e_2 + m_2)} \left\langle \frac{1}{2} \frac{1}{2}; s_1 s_2 | \frac{1}{2} \frac{1}{2}; 1S_z \right\rangle, \\ \sqrt{2(e_1 + m_1)(e_2 + m_2)} &= \frac{\widetilde{M}_0(M_0 + m_1 + m_2)}{\sqrt{2}M_0}, \end{aligned} \quad (\text{A12})$$

where [cf. Eq. (2.2)]

$$M_0 = e_1 + e_2, \quad e_i = \sqrt{m_i^2 + p_\perp^2 + p_z^2}, \quad p_z = \frac{x_2 M_0}{2} - \frac{m_2^2 + p_\perp^2}{2x_2 M_0}, \quad (\text{A13})$$

$\chi_s$  is the usual Pauli spinor and we have used the usual properties, especially, the covariant one, of Dirac spinors. Applying equations of motion on spinors in Eq. (A9) leads to

$$\begin{aligned} \bar{u}(p_1)(\bar{P} + M_0)\gamma_5 v(p_2) &= (M_0 + m_1 + m_2)\bar{u}(p_1)\gamma_5 v(p_2), \\ \bar{u}(p_1)(\bar{P} + M_0)\not{v}(p_2) &= \bar{u}(p_1)[(M_0 + m_1 + m_2)\not{v} - \hat{\varepsilon} \cdot (p_1 - p_2)]v(p_2), \end{aligned} \quad (\text{A14})$$

and  $R_{\lambda_1\lambda_2}^{SS_z}$  is reduced to a more familiar form [4]. It is, however, more convenient to use the form shown in Eq. (A9) when extending to the  $p$ -wave meson case. Two remarks are in order. First,  $p_1 + p_2$  is not equal to the meson's four-momentum in the conventional LF approach as both the quark and antiquark are on-shell. On the contrary, the total four-momentum is conserved at each vertex in the covariant LF framework. Second, the longitudinal polarization 4-vector  $\hat{\varepsilon}^\mu(0)$  given above is not exactly the same as that of the vector meson and we have  $\hat{\varepsilon} \cdot \bar{P} = 0$ . We normalize the meson state as

$$\langle M(P', J', J'_z) | M(P, J, J_z) \rangle = 2(2\pi)^3 P^+ \delta^3(\tilde{P}' - \tilde{P}) \delta_{J'J} \delta_{J'_z J_z}, \quad (\text{A15})$$

so that

$$\int \frac{dx d^2 p_\perp}{2(2\pi)^3} \varphi_{L'L'_z}^*(x, p_\perp) \varphi_{LL_z}(x, p_\perp) = \delta_{L',L} \delta_{L'_z, L_z}. \quad (\text{A16})$$

Explicitly, we have

$$\varphi_{00} = \varphi, \quad \varphi_{1L_z} = p_{L_z} \varphi_p, \quad (\text{A17})$$

where  $p_{L_z=\pm 1} = \mp(p_{\perp x} \pm ip_{\perp y})/\sqrt{2}$ ,  $p_{L_z=0} = p_z$  are proportional to the spherical harmonics  $Y_{1L_z}$  in momentum space, and  $\varphi$ ,  $\varphi_p$  are the distribution amplitudes of  $s$ -wave and  $p$ -wave mesons, respectively. For a Gaussian-like wave function as shown in Eq. (2.12) [7], one has  $\varphi_p = \sqrt{2/\beta^2} \varphi$ .

For  $p$ -wave mesons, it is straightforward to obtain

$$\begin{aligned} \langle 1S; L_z S_z | 1S; J J_z \rangle p_{L_z} R_{\lambda_1 \lambda_2}^{SS_z}(x, p_\perp) &= \frac{1}{\sqrt{2} \widetilde{M}_0 (M_0 + m_1 + m_2)} \\ &\times \bar{u}(p_1, \lambda_1) (\bar{P} + M_0) \Gamma_{2s+1P_J} v(p_2, \lambda_2), \end{aligned} \quad (\text{A18})$$

with

$$\begin{aligned} \Gamma_{^3P_0} &= \frac{1}{\sqrt{3}} \left( \frac{K \cdot \bar{P}}{M_0} - K \right), \\ \Gamma_{^1P_1} &= \hat{\varepsilon} \cdot K \gamma_5, \\ \Gamma_{^3P_1} &= \frac{1}{\sqrt{2}} \left( \left( K - \frac{K \cdot \bar{P}}{M_0} \right) \hat{\varepsilon} - \hat{\varepsilon} \cdot K \right) \gamma_5, \\ \Gamma_{^3P_2} &= \hat{\varepsilon}_{\mu\nu} \gamma^\mu (-K^\nu), \end{aligned} \quad (\text{A19})$$

where  $K \equiv (p_2 - p_1)/2$ ,  $\hat{\varepsilon}_{\mu\nu}(m) = \langle 11; m'm'' | 11; 2m \rangle \hat{\varepsilon}_\mu(m') \hat{\varepsilon}_\nu(m'')$ . Note that the polarization tensor of a tensor meson satisfies the relations:  $\hat{\varepsilon}_{\mu\nu} = \hat{\varepsilon}_{\nu\mu}$  and  $\hat{\varepsilon}_{\mu\nu} \bar{P}^\mu = 0 = \hat{\varepsilon}_\mu^\mu$  and that  $\hat{\varepsilon}_\mu$ ,  $\hat{\varepsilon}_{\mu\nu}$  are identical to  $\varepsilon_\mu$ ,  $\varepsilon_{\mu\nu}$ , respectively, for maximal transverse polarized states ( $m = \pm J$ ). The above expressions for  $^3P_1$  and  $^3P_0$  states are consistent with [4, 5] and [68], respectively.

The vertex functions shown in Table 1 and Eq. (2.11) follow from the above explicit expressions for  $\Psi_{LS}^{JJ_z}$ . For example, by taking  $\hat{\varepsilon}_{\mu\nu}(-K^\nu)$  in place of  $\hat{\varepsilon}_\mu$  in Eq. (A14) we obtain the  $^3P_2$  vertex in the form shown in Table 1. Note that there are an overall factor and sign to be determined. The overall factor,  $(M^2 - M_0^2) \sqrt{x_1 x_2}$  [cf. Eq. (2.11)], is fixed by comparing the pseudoscalar decay constant  $f_P$  obtained in both covariant and conventional approaches [see Eqs. (2.16) and (2.17)], while the overall sign can be fixed by the HQS expectation for decay constants and form factors. For example, the sign of the  $P_1^{1/2}$  state relative to  $^3P_0$  is fixed by the HQS relation  $f_{P_1^{1/2}} = f_S$ .

An additional factor of  $i$  is assigned in Table 1 as in the usual Feynman rules to ensure that the corresponding operators are hermitian. For example, we have an  $i$  in front of  $\gamma_\mu$  but not  $\gamma_5$ , just like the usual QED and Yukawa vertices, respectively. Similarly, polarization vectors are decoupled from the vertex Feynman rules as usual.

## APPENDIX B: SOME USEFUL FORMULAS

In this Appendix we first collect some formulas in [8] relevant for the present work and then we proceed to summarize the formula for the product of four  $\hat{p}'_1$ 's needed for the calculation in Sec. III.

The explicit representation of the traces in Eqs. (3.11) and (3.22) can be found in [8]. For completeness we collect them in below:

$$\begin{aligned} S_{V\mu}^{PP} = & 2p'_{1\mu}[M'^2 + M''^2 - q^2 - 2N_2 - (m'_1 - m_2)^2 - (m''_1 - m_2)^2 + (m'_1 - m''_1)^2] \\ & + q_\mu[q^2 - 2M'^2 + N'_1 - N''_1 + 2N_2 + 2(m'_1 - m_2)^2 - (m'_1 - m''_1)^2] \\ & + P_\mu[q^2 - N'_1 - N''_1 - (m'_1 - m''_1)^2], \end{aligned} \quad (B1)$$

and

$$\begin{aligned} S_{\mu\nu}^{PV} = & (S_V^{PV} - S_A^{PV})_{\mu\nu} \\ = & -2i\epsilon_{\mu\nu\alpha\beta}\left\{p'_1{}^\alpha P^\beta(m''_1 - m'_1) + p'_1{}^\alpha q^\beta(m''_1 + m'_1 - 2m_2) + q^\alpha P^\beta m'_1\right\} \\ & + \frac{1}{W_V''}(4p'_{1\nu} - 3q_\nu - P_\nu)i\epsilon_{\mu\alpha\beta\rho}p'_1{}^\alpha q^\beta P^\rho \\ & + 2g_{\mu\nu}\left\{m_2(q^2 - N'_1 - N''_1 - m'^2_1 - m''^2_1) - m'_1(M''^2 - N''_1 - N_2 - m''^2_1 - m_2^2) \right. \\ & \left.- m''_1(M'^2 - N'_1 - N_2 - m'^2_1 - m_2^2) - 2m'_1 m''_1 m_2\right\} \\ & + 8p'_{1\mu}p'_{1\nu}(m_2 - m'_1) - 2(P_\mu q_\nu + q_\mu P_\nu + 2q_\mu q_\nu)m'_1 + 2p'_{1\mu}P_\nu(m'_1 - m''_1) \\ & + 2p'_{1\mu}q_\nu(3m'_1 - m''_1 - 2m_2) + 2P_\mu p'_{1\nu}(m'_1 + m''_1) + 2q_\mu p'_{1\nu}(3m'_1 + m''_1 - 2m_2) \\ & + \frac{1}{2W_V''}(4p'_\nu - 3q_\nu - P_\nu)\left\{2p'_{1\mu}[M'^2 + M''^2 - q^2 - 2N_2 + 2(m'_1 - m_2)(m''_1 + m_2)] \right. \\ & \left.+ q_\mu[q^2 - 2M'^2 + N'_1 - N''_1 + 2N_2 - (m_1 + m''_1)^2 + 2(m'_1 - m_2)^2] \right. \\ & \left.+ P_\mu[q^2 - N'_1 - N''_1 - (m'_1 + m''_1)^2]\right\}. \end{aligned} \quad (B2)$$

Note that our convention for  $\epsilon_{\mu\nu\alpha\beta}$ , namely,  $\epsilon_{0123} = 1$ , is different from that in [8].

The analytic expressions for  $P \rightarrow S, A$  transition form factors can be obtained from that of  $P \rightarrow P, V$  ones by some simple replacements. Hence, we list the explicit expressions for  $P \rightarrow P$  and  $P \rightarrow V$  transition form factors in [8]:

$$\begin{aligned} f_+(q^2) = & \frac{N_c}{16\pi^3} \int dx_2 d^2 p'_\perp \frac{h'_P h''_P}{x_2 \hat{N}'_1 \hat{N}''_1} \left[ x_1(M_0'^2 + M_0''^2) + x_2 q^2 \right. \\ & \left. - x_2(m'_1 - m''_1)^2 - x_1(m'_1 - m_2)^2 - x_1(m''_1 - m_2)^2 \right], \\ f_-(q^2) = & \frac{N_c}{16\pi^3} \int dx_2 d^2 p'_\perp \frac{2h'_P h''_P}{x_2 \hat{N}'_1 \hat{N}''_1} \left\{ -x_1 x_2 M'^2 - p'^2_\perp - m'_1 m_2 + (m''_1 - m_2)(x_2 m'_1 + x_1 m_2) \right. \end{aligned}$$

$$\begin{aligned}
& + 2 \frac{q \cdot P}{q^2} \left( p_{\perp}^{\prime 2} + 2 \frac{(p_{\perp}' \cdot q_{\perp})^2}{q^2} \right) + 2 \frac{(p_{\perp}' \cdot q_{\perp})^2}{q^2} - \frac{p_{\perp}' \cdot q_{\perp}}{q^2} \left[ M'^2 - x_2 (q^2 + q \cdot P) \right. \\
& \left. - (x_2 - x_1) M'^2 + 2x_1 M_0'^2 - 2(m_1' - m_2)(m_1' + m_1'') \right] \Big\}, \tag{B3}
\end{aligned}$$

and

$$\begin{aligned}
g(q^2) &= -\frac{N_c}{16\pi^3} \int dx_2 d^2 p_{\perp}' \frac{2h'_P h''_V}{x_2 \hat{N}'_1 \hat{N}''_1} \left\{ x_2 m_1' + x_1 m_2 + (m_1' - m_1'') \frac{p_{\perp}' \cdot q_{\perp}}{q^2} + \frac{2}{w''_V} \left[ p_{\perp}^{\prime 2} + \frac{(p_{\perp}' \cdot q_{\perp})^2}{q^2} \right] \right\}, \\
f(q^2) &= \frac{N_c}{16\pi^3} \int dx_2 d^2 p_{\perp}' \frac{h'_P h''_V}{x_2 \hat{N}'_1 \hat{N}''_1} \left\{ 2x_1(m_2 - m_1')(M_0'^2 + M_0''^2) - 4x_1 m_1'' M_0'^2 + 2x_2 m_1' q \cdot P \right. \\
& + 2m_2 q^2 - 2x_1 m_2 (M'^2 + M''^2) + 2(m_1' - m_2)(m_1' + m_1'')^2 + 8(m_1' - m_2) \left[ p_{\perp}^{\prime 2} + \frac{(p_{\perp}' \cdot q_{\perp})^2}{q^2} \right] \\
& + 2(m_1' + m_1'')(q^2 + q \cdot P) \frac{p_{\perp}' \cdot q_{\perp}}{q^2} - 4 \frac{q^2 p_{\perp}^{\prime 2} + (p_{\perp}' \cdot q_{\perp})^2}{q^2 w''_V} \left[ 2x_1 (M'^2 + M_0'^2) - q^2 - q \cdot P \right. \\
& \left. - 2(q^2 + q \cdot P) \frac{p_{\perp}' \cdot q_{\perp}}{q^2} - 2(m_1' - m_1'')(m_1' - m_2) \right] \Big\}, \\
a_+(q^2) &= \frac{N_c}{16\pi^3} \int dx_2 d^2 p_{\perp}' \frac{2h'_P h''_V}{x_2 \hat{N}'_1 \hat{N}''_1} \left\{ (x_1 - x_2)(x_2 m_1' + x_1 m_2) - [2x_1 m_2 + m_1'' + (x_2 - x_1)m_1'] \frac{p_{\perp}' \cdot q_{\perp}}{q^2} \right. \\
& - 2 \frac{x_2 q^2 + p_{\perp}' \cdot q_{\perp}}{x_2 q^2 w''_V} \left[ p_{\perp}' \cdot p_{\perp}'' + (x_1 m_2 + x_2 m_1')(x_1 m_2 - x_2 m_1'') \right] \Big\}, \\
a_-(q^2) &= \frac{N_c}{16\pi^3} \int dx_2 d^2 p_{\perp}' \frac{h'_P h''_V}{x_2 \hat{N}'_1 \hat{N}''_1} \left\{ 2(2x_1 - 3)(x_2 m_1' + x_1 m_2) - 8(m_1' - m_2) \left[ \frac{p_{\perp}^{\prime 2}}{q^2} + 2 \frac{(p_{\perp}' \cdot q_{\perp})^2}{q^4} \right] \right. \\
& - [(14 - 12x_1)m_1' - 2m_1'' - (8 - 12x_1)m_2] \frac{p_{\perp}' \cdot q_{\perp}}{q^2} \\
& + \frac{4}{w''_V} \left( [M'^2 + M''^2 - q^2 + 2(m_1' - m_2)(m_1'' + m_2)](A_3^{(2)} + A_4^{(2)} - A_2^{(1)}) \right. \\
& + Z_2(3A_2^{(1)} - 2A_4^{(2)} - 1) + \frac{1}{2}[x_1(q^2 + q \cdot P) - 2M'^2 - 2p_{\perp}' \cdot q_{\perp} \\
& - 2m_1'(m_1'' + m_2) - 2m_2(m_1' - m_2)](A_1^{(1)} + A_2^{(1)} - 1) \\
& \left. \left. + q \cdot P \left[ \frac{p_{\perp}^{\prime 2}}{q^2} + \frac{(p_{\perp}' \cdot q_{\perp})^2}{q^4} \right] (4A_2^{(1)} - 3) \right) \right\}. \tag{B4}
\end{aligned}$$

We next give the results for  $\hat{p}_1' \hat{p}_1' \hat{p}_1' \hat{p}_1'$  and  $\hat{p}_1' \hat{p}_1' \hat{p}_1' \hat{N}_2$ . In Eq. (3.12), under the typical integration

$$\frac{N_c}{16\pi^3} \int \frac{dx_2 d^2 p_{\perp}'}{x_2 \hat{N}'_1 \hat{N}''_1} h'_P h''_M \hat{S}^{PM}, \tag{B5}$$

in a  $P \rightarrow M$  transition matrix element,  $\hat{p}_1' \hat{p}_1' \hat{p}_1' \hat{p}_1'$  in  $\hat{S}^{PM}$  can be expressed in terms of three external momenta,  $P$ ,  $q$  and  $\tilde{\omega}$ . Up to the first order in  $\tilde{\omega}$ , we have

$$\hat{p}'_{1\mu} \hat{p}'_{1\nu} \hat{p}'_{1\alpha} \hat{p}'_{1\beta} \doteq \sum_{i=1}^9 I_{i\mu\nu\alpha\beta} A_i^{(4)} + \sum_{j=1}^4 J_{j\mu\nu\alpha\beta} B_j^{(4)} + \sum_{k=1}^2 K_{k\mu\nu\alpha\beta} C_k^{(4)} + O(\tilde{\omega}^2), \tag{B6}$$

where

$$\begin{aligned}
I_{1\mu\nu\alpha\beta} &= (gg)_{\mu\nu\alpha\beta} = g_{\mu\nu}g_{\alpha\beta} + g_{\mu\alpha}g_{\nu\beta} + g_{\mu\beta}g_{\nu\alpha}, \\
I_{2\mu\nu\alpha\beta} &= (gPP)_{\mu\nu\alpha\beta} = g_{\mu\nu}P_\alpha P_\beta + g_{\mu\alpha}P_\nu P_\beta + g_{\mu\beta}P_\nu P_\alpha + g_{\alpha\beta}P_\mu P_\nu + g_{\nu\beta}P_\mu P_\alpha + g_{\nu\alpha}P_\mu P_\beta, \\
I_{3\mu\nu\alpha\beta} &= (gPq)_{\mu\nu\alpha\beta} = g_{\mu\nu}(P_\alpha q_\beta + q_\alpha P_\beta) + \text{permutations}, \\
I_{4\mu\nu\alpha\beta} &= (gqq)_{\mu\nu\alpha\beta} = g_{\mu\nu}q_\alpha q_\beta + g_{\mu\alpha}q_\nu q_\beta + g_{\mu\beta}q_\nu q_\alpha + g_{\alpha\beta}q_\mu q_\nu + g_{\nu\beta}q_\mu q_\alpha + g_{\nu\alpha}q_\mu q_\beta, \\
I_{5\mu\nu\alpha\beta} &= (PPPP)_{\mu\nu\alpha\beta} = P_\mu P_\nu P_\alpha P_\beta, \\
I_{6\mu\nu\alpha\beta} &= (PPPq)_{\mu\nu\alpha\beta} = P_\mu P_\nu P_\alpha q_\beta + P_\mu P_\nu q_\alpha P_\beta + P_\mu q_\nu P_\alpha P_\beta + q_\mu P_\nu P_\alpha P_\beta, \\
I_{7\mu\nu\alpha\beta} &= (PPqq)_{\mu\nu\alpha\beta} = P_\mu P_\nu q_\alpha q_\beta + \text{permutations}, \\
I_{8\mu\nu\alpha\beta} &= (Pqqq)_{\mu\nu\alpha\beta} = P_\mu q_\nu q_\alpha q_\beta + q_\mu P_\nu q_\alpha q_\beta + q_\mu q_\nu P_\alpha q_\beta + q_\mu q_\nu q_\alpha P_\beta, \\
I_{9\mu\nu\alpha\beta} &= (qqq)_{\mu\nu\alpha\beta} = q_\mu q_\nu q_\alpha q_\beta, \\
J_{1\mu\nu\alpha\beta} &= (gP\tilde{\omega})_{\mu\nu\alpha\beta} = \frac{1}{\tilde{\omega} \cdot P} [g_{\mu\nu}(P_\alpha \tilde{\omega}_\beta + \tilde{\omega}_\alpha P_\beta) + \text{permutations}], \\
J_{2\mu\nu\alpha\beta} &= (PPP\tilde{\omega})_{\mu\nu\alpha\beta} = \frac{1}{\tilde{\omega} \cdot P} (P_\mu P_\nu P_\alpha \tilde{\omega}_\beta + P_\mu P_\nu \tilde{\omega}_\alpha P_\beta + P_\mu \tilde{\omega}_\nu P_\alpha P_\beta + \tilde{\omega}_\mu P_\nu P_\alpha P_\beta), \\
J_{3\mu\nu\alpha\beta} &= (PPq\tilde{\omega})_{\mu\nu\alpha\beta} = \frac{1}{\tilde{\omega} \cdot P} [(P_\mu P_\nu q_\alpha + P_\mu q_\nu P_\alpha + q_\mu P_\nu P_\alpha) \tilde{\omega}_\beta + \text{permutations}], \\
J_{43\mu\nu\alpha\beta} &= (Pqq\tilde{\omega})_{\mu\nu\alpha\beta} = \frac{1}{\tilde{\omega} \cdot P} [(P_\mu q_\nu q_\alpha + q_\mu P_\nu q_\alpha + q_\mu q_\nu P_\alpha) \tilde{\omega}_\beta + \text{permutations}], \\
K_{1\mu\nu\alpha\beta} &= (gq\tilde{\omega})_{\mu\nu\alpha\beta} = \frac{1}{\tilde{\omega} \cdot P} [g_{\mu\nu}(q_\alpha \tilde{\omega}_\beta + \tilde{\omega}_\alpha q_\beta) + \text{permutations}], \\
K_{2\mu\nu\alpha\beta} &= (qqq\tilde{\omega})_{\mu\nu\alpha\beta} = \frac{1}{\tilde{\omega} \cdot P} (q_\mu q_\nu q_\alpha \tilde{\omega}_\beta + q_\mu q_\nu \tilde{\omega}_\alpha q_\beta + q_\mu \tilde{\omega}_\nu q_\alpha q_\beta + \tilde{\omega}_\mu q_\nu q_\alpha q_\beta).
\end{aligned} \tag{B7}$$

By contracting  $\hat{p}'_{1\mu} \hat{p}'_{1\nu} \hat{p}'_{1\alpha} \hat{p}'_{1\beta}$  with  $\tilde{\omega}^\beta$ ,  $q^\beta$  and  $g^{\alpha\beta}$ , and comparing with the complete expressions of  $\hat{p}'_{1\mu} \hat{p}'_{1\nu} \hat{p}'_{1\alpha}$  and  $\hat{p}'_{1\mu} \hat{p}'_{1\nu}$  shown in [8], we obtain

$$\begin{aligned}
A_1^{(4)} &= \frac{1}{3}(A_1^{(2)})^2, \quad A_2^{(4)} = A_1^{(1)} A_1^{(3)}, \quad A_3^{(4)} = A_1^{(1)} A_2^{(3)}, \\
A_4^{(4)} &= A_2^{(1)} A_2^{(3)} - \frac{1}{q^2} A_1^{(4)}, \quad A_5^{(4)} = A_1^{(1)} A_3^{(3)}, \quad A_6^{(4)} = A_1^{(1)} A_4^{(3)}, \\
A_7^{(4)} &= A_1^{(1)} A_5^{(3)}, \quad A_8^{(4)} = A_1^{(1)} A_6^{(3)}, \quad A_9^{(4)} = A_1^{(1)} A_6^{(3)} - \frac{3}{q^2} A_4^{(4)}, \\
B_1^{(4)} &= A_1^{(1)} C_1^{(3)} - A_1^{(4)}, \quad B_2^{(4)} = A_1^{(1)} B_1^{(3)} - A_2^{(4)}, \quad B_3^{(4)} = A_1^{(1)} B_2^{(3)} - A_3^{(4)}, \\
B_4^{(4)} &= A_1^{(1)} C_2^{(3)} - A_4^{(4)}, \quad C_1^{(4)} = A_2^{(3)} C_1^{(1)} + \frac{q \cdot P}{q^2} A_1^{(4)}, \quad C_2^{(4)} = A_6^{(3)} C_1^{(1)} + 3 \frac{q \cdot P}{q^2} A_4^{(4)},
\end{aligned} \tag{B8}$$

where [8]

$$\begin{aligned}
A_1^{(1)} &= \frac{x_1}{2}, \quad A_2^{(1)} = A_1^{(1)} - \frac{p'_\perp \cdot q_\perp}{q^2}, \quad C_1^{(1)} = -\hat{N}_2 + Z_2, \\
Z_2 &= \hat{N}_1' + m_1'^2 - m_2^2 + (1 - 2x_1)M'^2 + (q^2 + q \cdot P) \frac{p'_\perp \cdot q_\perp}{q^2}, \\
A_1^{(2)} &= -p_\perp'^2 - \frac{(p'_\perp \cdot q_\perp)^2}{q^2}, \quad A_2^{(2)} = (A_1^{(1)})^2, \quad A_3^{(2)} = A_1^{(1)} A_2^{(1)}, \\
A_4^{(2)} &= (A_2^{(1)})^2 - \frac{1}{q^2} A_1^{(2)}, \quad A_1^{(3)} = A_1^{(1)} A_1^{(2)}, \quad A_2^{(3)} = A_2^{(1)} A_1^{(2)},
\end{aligned} \tag{B9}$$

$$\begin{aligned}
A_3^{(3)} &= A_1^{(1)} A_2^{(2)}, \quad A_4^{(3)} = A_2^{(1)} A_2^{(2)}, \quad A_5^{(3)} = A_1^{(1)} A_4^{(2)}, \\
A_6^{(3)} &= A_2^{(1)} A_4^{(2)} - \frac{2}{q^2} A_2^{(1)} A_1^{(2)}, \\
B_1^{(2)} &= A_1^{(1)} Z_2 - A_1^{(2)}, \quad B_1^{(3)} = A_1^{(1)} (B_1^{(2)} - A_1^{(2)}), \quad B_2^{(3)} = A_2^{(1)} B_1^{(2)} + \frac{q \cdot P}{q^2} A_1^{(2)}.
\end{aligned}$$

Following the prescription in [8], the spurious contributions  $C_{1,2}^{(4)}$  should be vanished by including the zero mode contribution and we have

$$A_2^{(3)} \hat{N}_2 \rightarrow A_2^{(3)} Z_2 + \frac{q \cdot P}{q^2} A_1^{(4)}, \quad A_6^{(3)} \hat{N}_2 \rightarrow A_6^{(3)} Z_2 + 3 \frac{q \cdot P}{q^2} A_4^{(4)}, \quad (\text{B10})$$

which lead to the  $\hat{p}'_\mu \hat{p}'_\nu \hat{p}'_\alpha \hat{N}_2$  formula shown in Eq. (3.14). Note that in general  $B_j^{(i)}$  are non-vanishing by themselves, but they do vanish under integration in some choice of vertex function [8]. There are some attempts to include these effects for generic vertex functions [27]. The important of these effects can be checked numerically. For example, we have checked numerically that the integral of Eq. (B5) with  $\hat{S}^{PM}$  replaced by  $B_i^{(j)}$  are vanishingly small. In practice, one only needs  $A_j^{(i)}$  terms for  $\hat{p}'_1 \dots \hat{p}'_1$  formulas.

- [1] M.V. Terent'ev, Sov. J. Phys. **24**, 106 (1976); V.B. Berestetsky and M.V. Terent'ev, *ibid.* **24**, 547 (1976); **25**, 347 (1977).
- [2] P.L. Chung, F. Coester, and W.N. Polyzou, Phys. Lett. B **205**, 545 (1988).
- [3] W. Jaus, Phys. Rev. D **41**, 3394 (1990).
- [4] W. Jaus, Phys. Rev. D **44**, 2851 (1991).
- [5] C. R. Ji, P. L. Chung, and S. R. Cotanch, Phys. Rev. D **45**, 4214 (1992).
- [6] W. Jaus, Phys. Rev. D **53**, 1349 (1996) [Erratum-*ibid.* D **54**, 5904 (1996)].
- [7] H. Y. Cheng, C. Y. Cheung, and C. W. Hwang, Phys. Rev. D **55**, 1559 (1997).
- [8] W. Jaus, Phys. Rev. D **60**, 054026 (1999).
- [9] B. L. Bakker, H. M. Choi, and C. R. Ji, Phys. Rev. D **65**, 116001 (2002).
- [10] H.Y. Cheng, C.Y. Cheung, C.W. Hwang, and W.M. Zhang, Phys. Rev. D **57**, 5598 (1998).
- [11] S. J. Chang and S. K. Ma, Phys. Rev. **180**, 1506 (1969).
- [12] S. J. Chang, R. G. Root, and T. M. Yan, Phys. Rev. D **7**, 1133 (1973); T. M. Yan, *ibid.* **7**, 1780 (1973).
- [13] BaBar Collaboration, B. Aubert *et al.*, Phys. Rev. Lett. **90**, 242001 (2003).
- [14] CLEO Collaboration, D. Besson *et al.*, Phys. Rev. D **68**, 032002 (2003).
- [15] Belle Collaboration, K. Abe *et al.*, hep-ex/0307021.
- [16] Particle Data Group, K. Hagiwara *et al.*, Phys. Rev. D **66**, 010001 (2002).
- [17] N. Isgur, D. Scora, B. Grinstein, and M.B. Wise, Phys. Rev. D **39**, 799 (1989).
- [18] J. P. de Melo, J. H. Sales, T. Frederico, and P. U. Sauer, Nucl. Phys. A **631**, 574C (1998) [arXiv:hep-ph/9802325].
- [50] B. L. Bakker, H. M. Choi, and C. R. Ji, Phys. Rev. D **67**, 113007 (2003) [arXiv:hep-ph/0303002].

[20] N. Isgur and M. B. Wise, Phys. Lett. B **232**, 113 (1989); **237**, 527 (1990).

[21] J.D. Bjorken, SLAC-PUB-5278 (1990); J.D. Bjorken, J. Dunietz, and J. Taron, Nucl. Phys. B **371**, 111 (1992).

[22] N. Uraltsev, Phys. Lett. B **501**, 86 (2001).

[23] M. Suzuki, Phys. Rev. D **47**, 1252 (1993).

[24] N. Isgur and M. B. Wise, Phys. Rev. D **43**, 819 (1991).

[25] A. Le Yaouanc, L. Oliver, O. Pene, and J. C. Raynal, Phys. Lett. B **387**, 582 (1996) [arXiv:hep-ph/9607300]; S. Veseli and I. Dunietz, Phys. Rev. D **54**, 6803 (1996) [arXiv:hep-ph/9607293].

[26] P. L. Chung, F. Coester, and W. N. Polyzou, Phys. Lett. B **205**, 545 (1988).

[27] W. Jaus, Phys. Rev. D **67**, 094010 (2003) [arXiv:hep-ph/0212098].

[28] J. Carbonell, B. Desplanques, V.A. Karmanon, and J.F. Mathiot, Phys. Rep. **300**, 215 (1998).

[29] C. W. Hwang, Eur. Phys. J. C **23**, 585 (2002) [arXiv:hep-ph/0112237].

[30] D. Scora and N. Isgur, Phys. Rev. D **52**, 2783 (1995).

[31] J.C.R. Bloch, Yu.L. Kalinovsky, C.D. Roberts, and S.M. Schmidt, Phys. Rev. D **60**, 111502 (1999).

[32] BaBar Collaboration, B. Aubert *et al.*, Phys. Rev. D **67**, 092003 (2003).

[33] C. Bernard *et al.*, Phys. Rev. D **65**, 014510 (2002).

[34] F.E. Close and N.A. Törnqvist, J. Phys. G **28**, R249 (2002) [hep-ph/0204205].

[35] K. Maltman, Phys. Lett. B **462**, 14 (1999).

[36] V. Chernyak, Phys. Lett. B **509**, 273 (2001).

[37] Belle Collaboration, P. Krokovny *et al.*, hep-ex/0308019.

[38] H. Y. Cheng, Phys. Rev. D **68**, 094005 (2003).

[39] Belle Collaboration, Y. Mikami *et al.*, KEK Preprint 2003-69.

[40] BaBar Collaboration, B. Aubert *et al.*, hep-ex/0310050.

[41] S. Godfrey, Phys. Lett. B **568**, 254 (2003).

[42] BaBar Collaboration, B. Aubert *et al.*, hep-ex/0308026.

[43] CELO Collaboration, R.S. Galik, Nucl. Phys. **A663**, 647 (2000); S. Anderson *et al.*, CLEO-CONF-99-6 (1999).

[44] M. Neubert, Phys. Lett. **B418**, 173 (1998).

[45] H. Y. Cheng, Phys. Rev. D **67**, 094007 (2003).

[46] M. Wirbel, S. Stech, and M. Bauer, Z. Phys. C **29**, 637 (1985); M. Bauer, B. Stech, and M. Wirbel, *ibid.* **34**, 103 (1987); M. Bauer, B. Stech, and M. Wirbel, *ibid.* **42**, 671 (1989).

[47] P.J. O'Donnell, Q.P. Xu, and H.K.K. Tung, Phys. Rev. D **52**, 3966 (1995).

[48] D. Melikhov, Phys. Rev. D **53**, 2460 (1996); Phys. Lett. B **380**, 363 (1996).

[49] FOCUS Collaboration, Phys. Lett. B **544**, 89 (2002).

[50] B. L. Bakker, H. M. Choi, and C. R. Ji, Phys. Rev. D **67**, 113007 (2003).

[51] D. Melikhov and B. Stech, Phys. Rev. D **62**, 014006 (2000).

[52] P. Ball and V.M. Braun, Phys. Rev. D **58**, 094016 (1998); P. Ball, J. High Energy Phys. **9809**, 005 (1998) [hep-ph/9802394].

[53] P. Ball, V.M. Braun, and H. Dosch, Phys. Rev. D **44**, 3567 (1991); P. Ball, Phys. Rev. D **48**,

3190 (1993) [arXiv:hep-ph/9305267].

[54] A. Deandrea, R. Gatto, G. Nardulli, and A.D. Polosa, Phys. Rev. D **59**, 074012 (1999).

[55] T.M. Aliev and M. Savci, Phys. Lett. B **456**, 256 (1999).

[56] H. Georgi, Phys. Lett. B **240**, 447 (1990); E. Eichten and B. Hill, Phys. Lett. B **234**, 511 (1990); **243**, 427 (1990).

[57] T. M. Yan, H. Y. Cheng, C. Y. Cheung, G. L. Lin, Y. C. Lin, and H. L. Yu, Phys. Rev. D **46**, 1148 (1992); H. Y. Cheng, C. Y. Cheung, G. L. Lin, Y. C. Lin, T. M. Yan, and H. L. Yu, *ibid.* D **46**, 5060 (1992); *ibid.* D **47**, 1030 (1993); M. B. Wise, Phys. Rev. D **45**, R2188 (1992); G. Burdman and J. Donoghue, Phys. Lett. B **280**, 287 (1992).

[58] N. B. Demchuk, P. Yu. Kulikov, I. M. Narodetskii, and P. J. O'Donnell, Phys. Atom. Nucl. **60**, 1292 (1997).

[59] V. Morenas, A. Le Yaouanc, L. Oliver, O Péne, and J.C. Raynal, Phys. Rev. D **56**, 5668 (1997).

[60] P. Cea, P. Colangelo, L. Cosmai, and G. Nardulli, Phys. Lett. B **206**, 691 (1988).

[61] A. Deandrea, N. Di Bartolomeo, R. Gatto, G. Nardulli, and A.D. Polosa, Phys. Rev. D **58**, 034004 (1998).

[62] S. Veseli and I. Dunietz, Phys. Rev. D **54**, 6803 (1996).

[63] S. Godfrey and N. Isgur, Phys. Rev. D **32**, 189 (1985).

[64] P. Colangelo, F. De Fazio, and N. Paver, Phys. Rev. D **58**, 116005 (1998).

[65] A. Wambach, Nucl. Phys. B **343**, 647 (1995).

[66] M.Q. Huang and Y.B. Dai, Phys. Rev. D **59**, 034018 (1999).

[67] W. R. de Araujo, M. Beyer, T. Frederico, and H. J. Weber, J. Phys. G **25**, 1589 (1999) [arXiv:hep-ph/9904307].

[68] M. A. DeWitt, H. M. Choi, and C. R. Ji, Phys. Rev. D **68**, 054026 (2003).

[69] Heavy Flavor Averaging Group, <http://www.slac.stanford.edu/xorg/hfag/semi/summer03-eps/summer03.shtml>

[70] C.G. Boyd, Z. Ligeti, I.Z. Rothstein, and M.B. Wise, Phys. Rev. D **55**, 3027 (1997).

[71] M.P. Dorsten, hep-ph/0310025.